Characterizing the Role of RNA-Binding Protein Human Antigen R in the Neuromuscular Junction in Duchenne Muscular Dystrophy

By: Gurleen Bhaura

A thesis submitted to the University of Ottawa in partial fulfillment of the requirements for the degree of Master of Science in Cellular and Molecular medicine

Department of Cellular and Molecular Medicine
Faculty of Medicine
University of Ottawa

© Gurleen Bhaura, Ottawa, Canada, 2026

Abstract

Duchenne muscular dystrophy (DMD) is a progressive X-linked disorder caused by mutations in the dystrophin gene, leading to severe skeletal muscle fibre degeneration and neuromuscular junction (NMJ) abnormalities, including fragmentation and disorganization of the post-synaptic apparatus. Human Antigen R (HuR) is an RNA-binding protein involved in post-transcriptional regulation of transcripts associated with muscle differentiation and endplate function. However, its role in maintaining the structure of the post-synaptic apparatus at the NMJ remains unclear. This project investigated HuR's contribution to dystrophic endplate organization in the *mdx* mouse model of DMD. First, we confirmed significant post-synaptic disorganization in the *mdx* muscle relative to wild-type (WT) controls. Additionally, HuR protein expression was elevated (~3-fold) across multiple fast- and slow-twitch *mdx* muscles from 4-12 weeks, with smaller, non-significant increases observed at 24+ weeks. To further characterize HuR localization, subcellular fractionation was performed in the tibialis anterior (TA) muscle at 11 weeks, a time point representative of the increased HuR expression observed across the multiple muscles and ages we examined. Subcellular fractionation demonstrated significantly increased nuclear HuR protein levels in *mdx* muscle compared to WT controls ($p<0.001$). Consistent with these findings, immunofluorescence analyses also revealed a strong trend towards increased nuclear HuR abundance in *mdx* muscle fibres relative to WT controls in the TA when all ages were combined ($p=0.054$). Given these findings, we knocked down HuR expression in vivo using recombinant adeno-associated virus-mediated short hairpin RNA delivery through intramuscular injections in the TA muscles of *mdx* mice. HuR protein expression was reduced by approximately 60% relative to shLuc-treated controls, restoring HuR levels to those observed in WT muscle ($p<0.01$). This led to a partial improvement in post-synaptic organization, as evidenced by

increased acetylcholine receptor compactness compared with shLuc-treated *mdx* muscle ($p<0.05$) and untreated *mdx* muscle ($p<0.0001$). Finally, the pan-histone deacetylase inhibitor Vorinostat was evaluated as a pharmacological approach to assess changes in HuR expression, localization, and potential effects on post-synaptic morphology. However, Vorinostat did not significantly increase acetylated tubulin levels, suggesting that adequate HDAC inhibition may not have been achieved, which limited our ability to assess its effects on HuR expression and post-synaptic organization. Overall, HuR protein expression is dysregulated in dystrophic muscle across multiple ages and muscle types, while reducing HuR expression partially improved post-synaptic membrane organization, supporting a role for HuR in the molecular mechanisms underlying endplate abnormalities in DMD.

Table of Contents

Abstract ..... ii-iii

Dedication and Acknowledgements vii

Funding and Statement of Authorship viii

List of Figures ..... viii-x

List of Tables x

List of Abbreviations ..... x-xiv

CHAPTER 1 – INTRODUCTION 1-36

1.1 Duchenne Muscular Dystrophy (DMD): Clinical Features and Pathogenesis 1

1.2 Current and Emerging Therapies for DMD 1

1.3 The Dystrophin Gene: Structure, Mutations, and Isoforms 4

1.4 Structure and Function of the Neuromuscular Junction (NMJ) 8

1.5 Signalling Pathways Regulating NMJ Development and Maintenance 10

1.5.1 *Development of the Post-synaptic Apparatus* 10

1.5.2 *Maintenance of the Post-synaptic Apparatus Through Localized Transcriptional Control*..... 11

1.5.3 *Additional Regulators of NMJ Organization.*..... 14

1.6 Differences in NMJ Morphology Between WT and *mdx* Mice..... 15

1.7 RNA-Binding Proteins as Post-Transcriptional Regulators of Gene Expression 19

1.8 The ELAVL/Hu Protein Family 20

1.9 HuR as a Post-Transcriptional Regulator of Disease-Related mRNAs 23

1.10 HuR and Its Stabilization of DMD-Related Transcripts 24

1.11 The Critical Role of Post-Transcriptional Regulators Such as HuR at the NMJ 25

1.12 HuR as a Regulator of Myogenesis..... 28

1.13 Insights into HuR Function from Constitutive & Skeletal Muscle-Specific Knockout Models..... 30

1.14 Rationale 31

1.15 Hypotheses and Research Objectives for the Project 32

CHAPTER 2 – MATERIALS AND METHODS 33–42

2.1 Descriptive/Phenotypic Phase - Characterization of HuR Expression and Subcellular Localization in Dystrophic Skeletal Muscle 33

2.1.1 *Endplate Staining and Imaging*..... 34

2.1.2 *HuR Protein Isolation and Quantification* 34

2.1.3 *HuR Western Blots* 35

2.1.4 *Subcellular Fractionation of HuR* 36

2.1.5 *HuR Immunofluorescence Staining and Imaging* 36

2.1.6 *Macrophage Staining and Imaging* 37

2.2 Mechanistic Phase - The Effects of HuR Knockdown in *mdx* Skeletal Muscle 38

2.3 Therapeutic Phase - Pharmacological Modulation of HuR Using Vorinostat in *mdx* Mice 40

2.3.1 Animal Grip Strength Testing 41

2.4 Statistical Analyses 42

CHAPTER 3 – RESULTS 43-70

3.1 Analyses of Post-synaptic Membrane Structure and HuR Expression in WT & *mdx* Muscle.... 43

3.1.1 *mdx Mice Exhibit Disorganized Morphology of the Post-synaptic Apparatus* 43

3.1.2 *HuR Protein Levels Are Upregulated in mdx Mice Across Different Ages and Muscles* 44

3.1.3 *Elevated Nuclear HuR Protein with Limited Cytoplasmic Redistribution in mdx Muscle* 48

3.1.4 *HuR Localization in WT and mdx TA Muscle Across Disease Progression as Revealed by Immunofluorescence* 50

3.1.5 *Minimal HuR–Macrophage Co-localization by Immunofluorescence* 53

3.2 The Impact of HuR Knockdown on the Organization of the Post-synaptic Membrane in *mdx* Muscle 57

3.2.1 *HuR Knockdown Normalizes Elevated HuR Protein Levels in mdx Muscle* 57

3.2.2 *HuR Knockdown Partially Improved Endplate Morphology in mdx Muscle* 58

3.2.3 *Blinded NMJ Scoring Reveals Fewer Severely Disorganized Endplates Following HuR Knockdown*.. 60

3.3 The Pharmacological Treatment of *mdx* Mice to Modulate the Expression and Localization of HuR in Muscle 62

3.3.1 *Grip Strength Following Vorinostat-Treated mdx Mice*..... 63

3.3.2 *Post-Synaptic Organization Following Vorinostat Treatment in mdx Mice*..... 64

3.3.3 *HuR Protein Expression and Localization Following Vorinostat Treatment* 66

3.3.4 *No Significant Effects on Tubulin Acetylation Following Vorinostat Treatment in mdx Muscle*..... 69

CHAPTER 4 – DISCUSSION 71-83

4.1 NMJ Disorganization as a Central Pathological Feature in DMD..... 71

4.2 Elevated HuR Protein Expression in Dystrophic Muscle 72

4.3 HuR Localization Remains Largely Nuclear in Dystrophic Skeletal Muscle 73

4.4 Contribution of Immune Cells to Elevated HuR Expression 75

4.5 Genetic & Pharmacological Modulation of HuR Expression and Localization and Their Effects on Post-synaptic Morphology 76

4.6 Limitations 78

4.7 Future Directions 80

4.8 Conclusion 82

Works Cited 84-128

Dedication

This thesis is dedicated to my brother, Ivraj Bhaura.

Acknowledgments

I would like to express my sincere gratitude to both Dr. Bernard Jasmin and Dr. Aymeric Ravel-Chapuis for their instrumental guidance, mentorship, and support throughout this project. The opportunity to join your lab has been incredibly meaningful to me and invaluable to my growth as both a researcher and an individual. I am forever grateful – thank you.

I am also deeply thankful to my thesis committee members, Dr. Jocelyn Côté and Dr. Mireille Khacho, for their constructive feedback and insightful discussions regarding my research. Special thanks to Dr. Khacho and her lab for generously providing the *mdx* mice required for the in vivo Vorinostat experiments. I would also like to acknowledge my thesis defence committee members: Dr. Rashmi Kothary and Dr. Jocelyn Côté. Thank you for your time in evaluating my thesis and for your suggestions for improvement.

I am especially grateful to our lab manager, Jonathan Gobin, for his training and mentorship in the experimental techniques used throughout this thesis, and to Dr. Lola Lessard for her NMJ analyses following the in vivo Vorinostat experiments. Many thanks to past and present members of the Jasmin lab, including Chimène Fahmi, Shatha Atieh, Dhrashti Patel, Marc Charron, Leanne Dawe, Anubhuti Sarkar, Rashida Rajgara, as well as to the Ravel-Chapuis lab, for their friendship, support, and advice.

I would also like to thank Dr. Chloë van Oostende-Triplet and Liyuan Wang from the Cell Biology & Image Acquisition Core, Dr. Kerstin Ure from the Animal Behaviour & Physiology Core, the Louise Pelletier Histology Core, and Geneviève Paris from the Common Equipment and Technical Services (CETS) team for their technical assistance and training. I also express my appreciation to the Animal Care and Veterinary Services (ACVS) department, the Graduate Office, Marie Florence, and all administrative/support staff at Roger Guindon Hall.

To my family - Gurcharan, Davinder, Ivraj, and Kirpa Bhaura - thank you for your endless love, encouragement, and support. Your sacrifices and unwavering faith in me have been a constant source of strength. To AD, MG, the extended Bhaura & Bola families, and my dear friends - thank you for standing by me throughout this journey. I feel incredibly fortunate to have you all in my life, and I carry your love with me in everything I do.

I acknowledge that this research was conducted on the unceded and unsurrendered territory of the Anishinaabe Algonquin Nation, stewards of the Ottawa River Watershed. I respect and honour their sovereignty and support ongoing efforts toward decolonization.

Lastly, I would also like to recognize the laboratory mice whose sacrifice made this research possible. Their contributions to advancing scientific knowledge are sincerely appreciated.

Funding

This project was supported by grants awarded to Dr. Bernard Jasmin by the Muscular Dystrophy Association and the Association Française contre les Myopathies. Thank you for your support.

Statement of Authorship

Dr. Bernard Jasmin served as the principal investigator and was responsible for the project's design, supervision, and funding. Dr. Aymeric Ravel-Chapuis contributed to the conception of this project and designed the AAV constructs used in the HuR knockdown experiments. Jonathan Gobin bred most of the C57 and *mdx* mice used in this study, with additional mice provided by Dr. Mireille Khacho. Gurleen Bhaura conducted all experiments and analyses, except the Vorinostat-treated NMJ analyses, which Dr. Lola Lessard completed. Gurleen Bhaura wrote this manuscript, and Dr. Bernard Jasmin revised it.

List of Figures

Figure 1 - Clinical Manifestations and Skeletal Muscle Pathology Associated with Duchenne Muscular Dystrophy (DMD) 4

Figure 2 - Dystrophin Glycoprotein Complex and Dystrophin Isoforms 7

Figure 3 - Key Signalling Pathways Involved in NMJ Formation and Maintenance 15

Figure 4 - NMJs in *mdx* mice and DMD Patients Exhibit Fragmented and Disorganized Post-Synaptic Endplate Morphology Compared to Healthy WT Mice 17

Figure 5 – The Structural Organization and Functional Characteristics of the Hu/ELAVL Family of RNA-Binding Proteins 22

Figure 6 - Post-Transcriptional Regulation of NMJ-Associated Transcripts by HuR and Related Pathways in Mouse Skeletal Muscle 28

Figure 7 - Mechanism of HuR-Mediated mRNA Stabilization and Nucleocytoplasmic Shuttling in Muscle Fibres of Mice 30

Figure 8 - Experimental Overview of the Descriptive/Phenotypic Phase 38

Figure 9 - Experimental Plan Used to Investigate the Role of HuR in Dystrophic Skeletal Muscle 40

Figure 10 - Experimental Design Used to Evaluate the Therapeutic Effects of HuR Modulation in Dystrophic Skeletal Muscle 42

Figure 11 - *mdx* Mice Exhibit Fragmented and Disorganized Post-synaptic Endplate Morphology Compared to WT Controls 44

Figure 12 - HuR Protein Levels are Elevated in *mdx* TA Muscle From 4-12 Weeks 45

Figure 13 - HuR Protein Levels are Increased in *mdx* DIA Muscle at 4-8 Weeks 46

Figure 14 - HuR Protein Levels are Elevated in *mdx* EDL Muscle with Significance at 4-8 Weeks 46

Figure 15 - HuR Protein Levels are Increased in *mdx* SOL Muscle at 4-8 Weeks 47

Figure 16 - Subcellular Fractionation Reveals Increased Nuclear HuR Protein in *mdx* TA Muscle at 11 Weeks 50

Figure 17 - HuR Immunofluorescence in WT and *mdx* TA Muscle at 4 Weeks 51

Figure 18 - HuR Immunofluorescence in WT and *mdx* TA Muscle at 8 Weeks 52

Figure 19 - HuR Immunofluorescence in WT and *mdx* TA Muscle at 24+ Weeks 52

Figure 20 - HuR Localization Exhibits a Strong Trend Toward Increased Nuclear Abundance in *mdx* TA Muscle 53

Figure 21 - HuR Signal Shows Limited Co-Localization with Macrophages at 4 Weeks in *mdx* TA Muscle 54

Figure 22 - HuR Signal Shows Limited Co-Localization with Macrophages at 8 Weeks in *mdx* TA Muscle 55

Figure 23 - HuR Signal Shows Limited Co-Localization with Macrophages at 24+ Weeks in *mdx* TA Muscle 55

Figure 24 - Macrophages Contribute Minimally to Total Nuc^{HuR} Despite Increased Infiltration in *mdx* TA Muscle 56

Figure 25 - AAV-Mediated HuR Knockdown Significantly Reduces HuR Protein Expression in *mdx* TA Muscle 58

Figure 26 - Representative Images of Post-synaptic Endplates in Non-Injected or shLuc-injected WT Mice and *mdx* Mice Injected with Either shLuc or shHuR 59

Figure 27 - HuR Knockdown Partially Improves Endplate Organization in *mdx* TA Muscle 61

Figure 28 - Quantification of AChR Compactness Following HuR Knockdown in *mdx* TA Muscle at 10 Weeks 62

Figure 29 - Body Weight and Grip Strength in Vehicle- and Vorinostat-injected *mdx* Mice 64

Figure 30 - Organization of the Post-Synaptic Apparatus in *mdx* TA Muscle Following Vorinostat Treatment 65

Figure 31 - Endplate Organization in *mdx* Muscle Following Vorinostat Treatment 66

Figure 32 - HuR Protein Levels in Vehicle- Injected and Vorinostat-Treated *mdx* EDL Muscle 67

Figure 33 - HuR Protein Expression in Vehicle-Injected and Vorinostat-Treated *mdx* SOL Muscle 67

Figure 34 - HuR Localization Following Vorinostat Treatment in *mdx* TA Muscle Fibre Cross-Sections 68

Figure 35 - Quantification of Nuclear and Cytoplasmic HuR Abundance following Vorinostat Treatment in *mdx* TA Muscle 69

Figure 36 - Acetylated Tubulin Levels in EDL Muscles of Vehicle- and Vorinostat-injected *mdx* Mice 70

Figure 37 - Acetylated Tubulin Levels in SOL Muscles of Vehicle- and Vorinostat-injected *mdx* Mice 70

List of Tables

Table 1 - Summary of Statistical Analyses of Elevated HuR Protein Levels in *mdx* Mice Across Muscles and Ages 48

List of Abbreviations

AAV	Adeno-Associated Virus
ACh	Acetylcholine
AChE	Acetylcholinesterase
AChR	Acetylcholine Receptor
AChR-β	Acetylcholine Receptor Beta Subunit
ALS	Amyotrophic Lateral Sclerosis
AMPK	AMP-Activated Protein Kinase
ARE or AUR	AU-Rich Element
BSA	Bovine Serum Albumin
β-Actin	Beta Actin
β2-Adrenergic	Beta 2-Adrenergic

β-Tubulin	Beta Tubulin
Ca^{2+}	Calcium
Ca^{2+}/CaMKII	Ca^{2+}/Calmodulin Dependent Kinase II
CCND1	Cyclin D1
CDK1,5	Cyclin-Dependent Kinase 1 and 5
ChAT	Choline Acetyltransferase
cDNA	Complementary DNA
CHK2	Checkpoint Kinase 2
COLQ	Collagen Q
COX-2	Cyclooxygenase-2
CSA	Cross-Sectional Area
DAMPs	Damage Associated Molecular Patterns
DAPC	Dystrophin-Associated Protein Complex
DGC	Dystrophin Glycoprotein Complex
DIA	Diaphragm
Dvl	Dishevelled
DM1	Myotonic Dystrophy Type 1
DMD	Duchenne Muscular Dystrophy
DMSO	Dimethyl Sulfoxide
DNA	Deoxyribonucleic Acid
DOK7	Docking Protein 7 or Downstream of Kinase 7
EB1	End-Binding protein 1 (EB1)
ECM	Extra-Cellular Matrix
EDL	Extensor Digitorum Longus
ELAVL1	Embryonic Lethal Abnormal Vision-Like Protein 1
EMG	Electromyographic
FTD	Frontotemporal Dementia
Fzd	Frizzled
FUS	Fused in Sarcoma
GABP or NRF-2	GA-Binding Protein or Nuclear Respiratory Factor 2
GF	Grams of Force

GFP	Green Fluorescent Protein
HDAC	Histone Deacetylase
HDACi	HDAC inhibitor
HNS	HuR Nucleocytoplasmic Shuttling Sequence
HPβCD	Hydroxypropyl-β-Cyclodextrin
HRP	Horseradish Peroxidase
HuR	Human Antigen R
HuR-CP1	HuR Cleavage Product 1
HuR-CP2	HuR Cleavage Product 2
IF	Immunofluorescence
IL-6,8	Interleukin-6, 8
iNOS	Inducible Nitric Oxide Synthase
IP	Intraperitoneal Injection
kDa	Kilodalton
KSRP	KH-Type Splicing Regulatory Protein
LRP4	Low-Density Lipoprotein Receptor-Related Protein 4
Luc	Luciferase
MACF1	Microtubule Actin Cross-linking Factor 1
MAP1B	Microtubule-Associated Protein 1B
Mac^{HuR}	Macrophages Expressing HuR
mEPPs	Miniature End-Plate Potentials
MEU	Protein Extraction Buffer
MKP-1	Mitogen Activated Protein Kinase Phosphatase-1
MOM	Mouse On Mouse
mRNA	Messenger RNA
Munc13	Mammalian Uncoordinated-13
MuSK	Muscle Specific Kinase
MyoD	Myogenic Differentiation Factor D
MyoG	Myogenin
Na^+	Sodium
NCAM	Neuronal Cell Adhesion Molecule

NF-κB	Nuclear Factor Kappa-Light-Chain-Enhancer of Activated B Cells
NF1	Neurofibromatosis Type-1
NMJ	Neuromuscular Junction
NRG/ErbB	Neuregulin/Erythroblastic Leukemia Viral Oncogene Homolog Receptors
Nuc^{HuR}	Nuclei Expressing HuR
OCT	Optimal Cutting Temperature
PBS	Phosphate-Buffered Saline
PFA	Paraformaldehyde
PGC-1α	Peroxisome Proliferator-Activated Receptor Gamma Coactivator 1-Alpha
p21	Cyclin-Dependent Kinase Inhibitor
p38 MAPK	P38 Mitogen-Activated Protein Kinase
p53	Tumour Protein 53
PKC	Protein Kinase C
PSCs	Peri-synaptic Schwann Cells
Rapsyn	Receptor-Associated Protein of the Synapse
RBP	RNA-Binding Protein
RFU	Relative Fluorescence Units
RIM	Rab-3 Interacting Molecule
RNA	Ribonucleic Acid
rAAV	Recombinant Adeno-Associated Virus
RRM	RNA Recognition Motif
SAHA	Suberoylanilide Hydroxamic Acid
SDS	Sodium Dodecyl Sulphate
shRNA	Short Hairpin RNA
SFK	Src Family of Kinases
SMA	Spinal Muscular Atrophy
SMN	Survival of Motor Neuron Protein

SMAD	Suppressor of Mothers against Decapentaplegic Protein
SNARE	Soluble N-ethylmaleimide-sensitive factor Attachment Protein Receptor
SOL	Soleus
SV	Synaptic Vesicles
SV2	Synaptic Vesicle Glycoprotein 2
TA	Tibialis Anterior
TBS-T	Tris Buffered Saline with Tween 20
TDP-43	TAR-DNA Binding Protein 43
TGF-β	Transforming Growth Factor-Beta
TNF-α	Tumour Necrosis Factor-Alpha
TRN2	Nuclear Import Receptor Transportin-2
TubA	Tubastatin A
UTR	Untranslated Region
UTRN	Utrophin Gene
V	Volts
VEGF	Vascular Endothelial Growth Factor
Wnt/β-catenin	Wingless Related Integrated Site/Catenin Beta-1
WT	Wild Type

Chapter 1 – Introduction

1.1 Duchenne Muscular Dystrophy (DMD) - Clinical Features & Pathogenesis

Duchenne muscular dystrophy (DMD) is a progressive and fatal muscle-wasting disease (Bez Batti Angulski et al., 2023; Mercuri et al., 2023). It follows an X-linked recessive inheritance pattern, caused by inherited or de novo alterations in the dystrophin gene, and results in the absence of dystrophin protein or the production of a nonfunctional form (Cohn et al., 2000; Duan et al., 2021; Hoffman et al., 1987). Affecting approximately 1 in every 3,500-5,000 live male births worldwide, DMD presents in childhood and is characterized as one of the most severe forms of muscular dystrophy (Bez Batti Angulski et al., 2023; Mercuri et al., 2023). Muscle weakness and wasting develop gradually, initially affecting the proximal muscles of the limbs and later spreading to more distal muscle groups (Duan et al., 2021; Patterson et al., 2023). Early symptoms typically appear by 2-3 years of age and include frequent falls, difficulty rising from a seated position (Gowers' sign), a waddling gait, and difficulty climbing stairs. Affected individuals may also exhibit delayed gross motor development and lose the ability to walk independently by ages 10-12 (Birnkrant et al., 2018). As the disease progresses, respiratory support is often required in adolescence, and other symptoms such as scoliosis, cognitive impairments, behavioural issues, dysphagia, constipation, diarrhea, and contractures also occur (Figure 1) (Patterson et al., 2023; Ricotti et al., 2016). Life expectancy remains limited, with most individuals succumbing to cardiac or respiratory complications between the ages of 20 and 40 years (Bez Batti Angulski et al., 2023; Mercuri et al., 2023).

1.2 Current and Emerging Therapies for DMD

Current therapeutic approaches for DMD primarily aim to slow disease progression and preserve functional capacity rather than to correct the underlying genetic defect (Guiraud et al.,

2019). Multidisciplinary care, including physiotherapy and respiratory support, remains an essential component of disease management, while glucocorticoids continue to represent the standard pharmacological treatment (Birnkrant et al., 2018; Montagna et al., 2025). Although glucocorticoid therapy can prolong ambulation and preserve respiratory and upper-limb function, its long-term use is associated with significant adverse effects, including weight gain, growth suppression, and reduced bone mineral density (Montagna et al., 2025; Yao et al., 2021). Advances in molecular medicine have led to therapies designed to restore dystrophin expression by addressing the underlying genetic cause of DMD (Chamberlain et al., 2017). These include exon-skipping therapies such as Eteplirsen, Golodirsen, and Viltolarsen, gene replacement and gene-editing approaches utilizing adeno-associated viral (AAV) vectors and CRISPR/Cas9 technology, stop-codon readthrough therapies such as Gentamicin, and stem cell-based strategies aimed at restoring dystrophin expression through the transplantation of healthy myogenic cells (Dzierlega et al., 2020; Namgoong et al., 2016; Nudelman et al., 2010; Potter et al., 2021; Sun et al., 2020; Zhang et al., 2020). In parallel, upregulation of utrophin, a structurally and functionally similar protein to dystrophin, has also been investigated as a complementary therapeutic strategy, with compounds such as Ezutromid or Celecoxib used to partially compensate for the dystrophin deficiency in DMD (Péladeau et al., 2018, 2020; Tinsley et al., 2011). While these approaches have demonstrated considerable promise, challenges related to delivery efficiency, widespread skeletal muscle targeting, and long-term safety continue to limit their therapeutic efficacy (Verhaart et al., 2019).

Despite these advances, current therapies do not fully prevent the progressive degeneration of dystrophic muscle (Verhaart et al., 2019; Yao et al., 2021). Consequently, attention has increasingly focused on pharmacological approaches that target secondary pathological processes

associated with disease progression, including chronic inflammation, fibrosis, oxidative stress, impaired regeneration, muscle ischemia, calcium dysregulation, and muscle wasting (Verhaart et al., 2019; Yao et al., 2021). Therapeutic approaches currently under investigation include anti-inflammatory agents (e.g., Vamorolone and corticosteroids), antifibrotic therapies (e.g. Losartan), antioxidant compounds (e.g. Coenzyme Q10), sodium–hydrogen exchanger inhibitors (e.g. Rimeporide), phosphodiesterase inhibitors (e.g. Sildenafil), and Follistatin-based therapies designed to enhance muscle growth and regenerative capacity (Yao et al., 2021). Among these approaches, Histone Deacetylase (HDAC) inhibitors, including Givinostat and Vorinostat (Suberoylanilide Hydroxamic Acid or SAHA), have attracted particular interest for their ability to modulate multiple pathways implicated in dystrophic pathology, with the former being FDA-approved for use in DMD patients over 6 years (Mozzetta et al., 2024). HDAC inhibitors have been shown to enhance muscle regeneration, reduce fibrosis, and improve muscle function in preclinical models of DMD, making them a promising therapeutic strategy to slow disease progression and improve muscle health (Consalvi et al., 2013; Osseni et al., 2022).

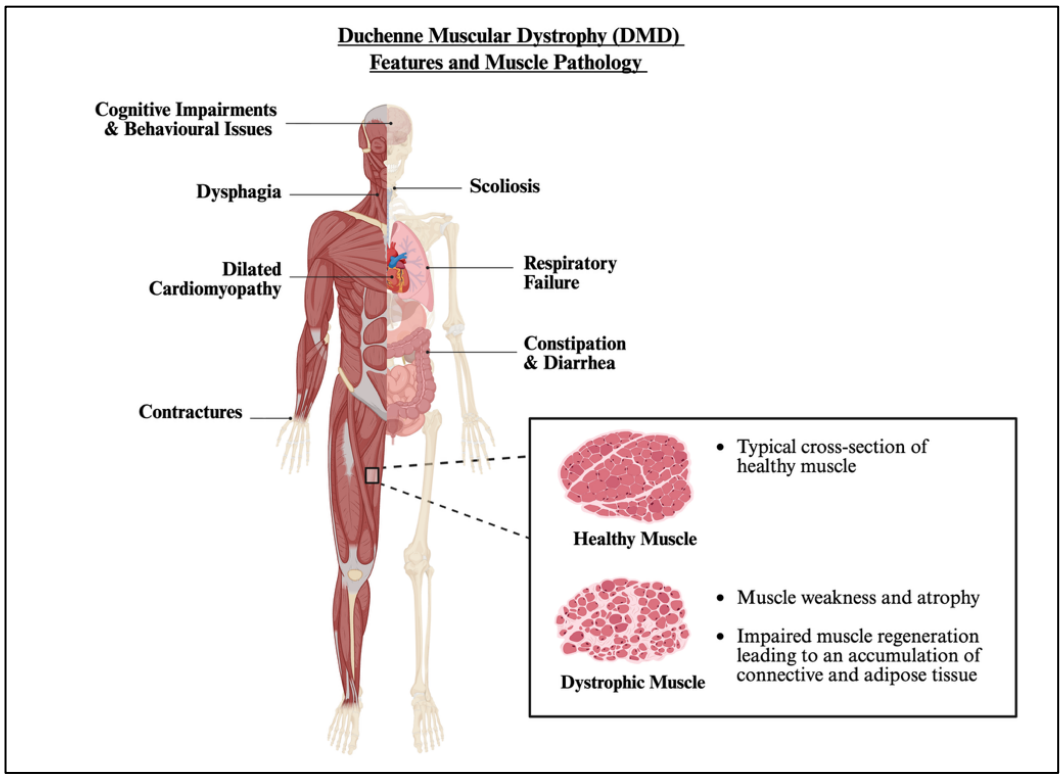


Figure 1. Clinical Manifestations and Skeletal Muscle Pathology Associated with Duchenne Muscular Dystrophy (DMD). DMD is a progressive neuromuscular disorder characterized by widespread systemic complications, including skeletal muscle weakness, contractures, scoliosis, respiratory insufficiency, dilated cardiomyopathy, gastrointestinal dysfunction, dysphagia, and cognitive or behavioural impairments. Histologically, healthy skeletal muscle displays tightly organized muscle fibres with minimal connective tissue, whereas dystrophic muscle exhibits muscle fibre degeneration, impaired regeneration, variable fibre size, and progressive accumulation of adipose and fibrotic connective tissue, ultimately contributing to muscle atrophy and functional decline. This figure was created using BioRender.

1.3 The Dystrophin Gene - Structure, Mutations, and Isoforms

Dystrophin is a key cytoskeletal protein encoded by the DMD gene and is found at the plasma membrane of muscle and non-muscle tissue (Venugopal et al., 2025). It functions as a mechanical and signalling link between the sarcolemma (muscle cell membrane), the cytoskeleton, and the extracellular matrix (Houang et al., 2018). Together with its associated proteins, dystrophin is an integral component of the dystrophin-associated protein complex (DAPC or DPC), otherwise known as the dystrophin-glycoprotein complex (DGC), which is a group of transmembrane proteins that work together to stabilize the muscle sarcolemma (Darras et al., 1993; Morales et al., 2023). This allows the myofiber to be structurally supported and protected from injury during

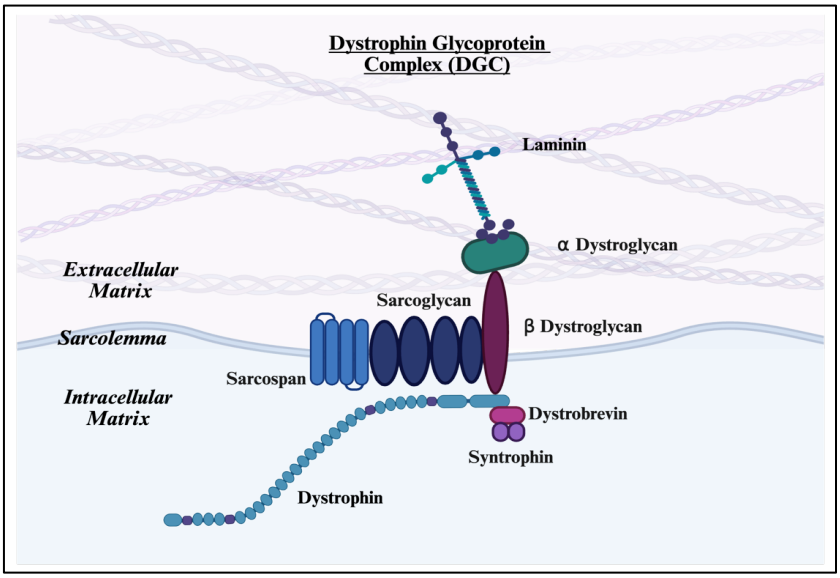
muscle contraction and relaxation (Darras et al., 1993; Morales et al., 2023). However, in DMD, loss of dystrophin and other DGC components compromises sarcolemmal stability, predisposing muscle fibres to injury, disrupting calcium regulation, and promoting oxidative stress and inflammation (Duan et al., 2021; Houang et al., 2018; Venugopal et al., 2025). Over time, muscle fibres undergo continuous cycles of degeneration and regeneration that eventually overwhelm the tissue's regenerative capacity and contribute to progressive disease (Abdel-Salam et al., 2009; Cardone et al., 2023). In *mdx* mice, the mouse model for DMD, this regenerative decline in muscle has been associated with disrupted satellite cell polarity (Dumont et al., 2016, 2015). This disrupts asymmetric satellite cell division and impairs the maintenance of the progenitor cell population and the generation of myogenic cells needed to support ongoing muscle fibre repair (Dumont et al., 2016, 2015). As regeneration becomes increasingly ineffective, chronic inflammation persists, and muscle tissue is progressively replaced by adipose and fibrotic connective tissue, ultimately reducing muscle mass and functional capacity (Cardone et al., 2023; Feige et al., 2018; Molina et al., 2021).

The dystrophin gene is the largest in the human genome and shows substantial transcriptional complexity, producing multiple isoforms through distinct promoters and alternative splicing (García-Cruz et al., 2020; Miro et al., 2020). It encodes the full-length 427-kDa dystrophin protein (Dp427) from a 14-kb mRNA transcript composed of 79 exons, including an N-terminal, central rod, cysteine-rich, and C-terminal domain (García-Cruz et al., 2020; Miro et al., 2020). Due to its large size, the dystrophin gene is highly vulnerable to mutation, with roughly one-third of DMD mutations occurring spontaneously, in part due to germline mosaicism (Nallamilli et al., 2021). Among affected individuals, 60-70% of disease-causing mutations are deletions, 10-15% are duplications, and the remaining ~20% consist of point mutations, small insertions or deletions,

splice-site mutations, and related sequence changes (Bladen et al., 2015). Deletion and duplication events cluster in two primary regions of the gene, between exons 3-9 and 45-55, with approximately 7% and 47% of patients exhibiting mutations in these hotspots, respectively (Min et al., 2019). Disease severity and functional consequences are strongly influenced by whether the mutation alters the translational reading frame (Hanson et al., 2021). Out-of-frame mutations generally eliminate functional dystrophin production and are associated with DMD, while in-frame mutations often permit the synthesis of a shortened dystrophin protein that retains partial function, resulting in the milder Becker muscular dystrophy phenotype (Hanson et al., 2021).

Expression of dystrophin isoforms is further regulated in a tissue-specific manner by at least seven independent promoters (Muntoni et al., 2003; Tyers et al., 2018). Three of these drive the production of full-length isoforms (Dp427p, Dp427m, and Dp427c), with Dp427m representing the primary form expressed in skeletal and cardiac muscle (Tetorou et al., 2024). In addition, several shorter dystrophin variants are produced, including Dp260, Dp140, Dp116, and Dp71, each showing distinct expression patterns across different tissues (Figure 2) (Muntoni et al., 2003; Tyers et al., 2018). Notably, the central nervous system exhibits greater diversity in dystrophin isoforms due to extensive alternative splicing, whereas splicing of the muscle-specific Dp427m isoform is comparatively limited (Barbosa-Morais et al., 2012; Raj et al., 2015).

A)



B)

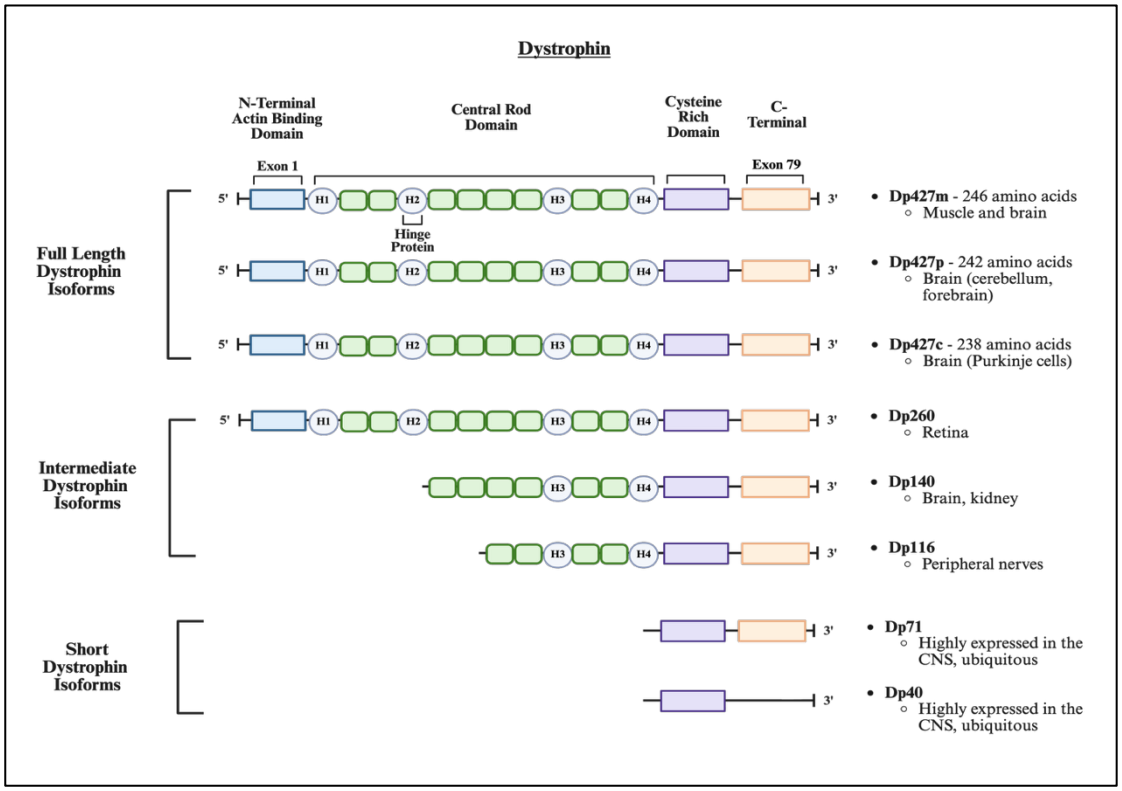


Figure 2. Dystrophin Glycoprotein Complex and Dystrophin Isoforms. Panel A illustrates the dystrophin glycoprotein complex (DGC), which links the intracellular cytoskeleton to the extracellular matrix through interactions between dystrophin and other components of the DGC, including dystroglycans, sarcoglycans, sarcospan, dystrobrevin, syntrophin, and laminin. Panel B depicts the major dystrophin isoforms generated from the DMD gene through alternative promoter usage. Full-length (Dp427) and shorter (Dp260, Dp140, Dp116, Dp71, and Dp40) isoforms are shown alongside their structural domains and principal sites of expression. The figures in both panels were created using BioRender, with the figure in panel A adapted from Valera, I.C. et al., 2021 and Wilson, D.G.S. et al., 2022, while the figure in panel B was adapted from Florczyk-Soluch, U. et al., 2021 and Vaillend, C. et al., 2025.

1.4 Structure & Function of the Neuromuscular Junction (NMJ)

In addition to its well-established role in maintaining muscle fibre stability, dystrophin is also an important component of the neuromuscular junction (NMJ), a highly specialized area of the sarcolemma, where an action potential or synapse is transmitted between motor neurons and their corresponding muscle fibres (Davis et al., 2022; Iyer et al., 2021). The NMJ can be divided into three sections: the pre-synaptic portion (nerve terminal or terminal boutons), the synaptic (junctional) cleft, and the post-synaptic portion, often referred to as the motor end plate (Khalil et al., 2026). At the pre-synaptic region of the NMJ, motor neurons originating from the spinal cord branch into terminal axons that form synaptic boutons at the muscle surface (Rodríguez Cruz et al., 2020). These nerve terminals contain components essential for neurotransmission, including synaptic vesicles (SVs), voltage-gated calcium (Ca^{2+}) channels, endoplasmic reticulum, and mitochondria (Slater, 2017). The pre-synaptic neurotransmitter Acetylcholine (ACh) is synthesized by Choline Acetyltransferase (ChAT), which catalyzes the conversion of choline and acetyl coenzyme A into ACh (Sam et al., 2026). ACh is subsequently stored within SVs and released into the synaptic cleft through calcium-dependent exocytosis (Khalil et al., 2026). This process is coordinated by proteins involved in synaptic vesicle docking and membrane fusion, including components of the Soluble N-ethylmaleimide-sensitive factor Attachment Protein Receptor (SNARE) complex, Synaptic Vesicle glycoprotein 2 (SV2), Rab-3 Interacting Molecule (RIM), and Mammalian Uncoordinated-13 (Munc13), which act together to allow efficient ACh release (Baker et al., 2016; Lai et al., 2017). Following synaptic transmission, acetylcholinesterase (AChE), which is highly concentrated within the synaptic cleft, rapidly hydrolyzes ACh to terminate neurotransmission and maintain cholinergic homeostasis at the NMJ (Khalil et al., 2026; Ohno et al., 1998). Peri-synaptic Schwann cells (PSCs), or terminal Schwann cells, are another

important component of the NMJ, functioning as non-myelinating glial cells that cover the NMJ and contribute to synaptic formation, maturation, and maintenance (Alvarez-Suarez et al., 2020; Slater, 2017).

Likewise, the synaptic cleft is the space between the motor nerve terminal and the post-synaptic sarcolemma of the muscle fibre (Rodríguez Cruz et al., 2020). It contains the synaptic basal lamina and a specialized extracellular matrix (ECM) layer composed of several proteins essential for NMJ development, maturation, and stability, including laminins, collagens, heparan sulphate proteoglycans (such as agrin), and nidogens (Sanes, 2003; Singhal, 2011). In addition to agrin-mediated Acetylcholine Receptor (AChR) clustering, these proteins regulate both pre- and post-synaptic structures (Singhal, 2011). Synaptic laminins regulate pre-synaptic active zones, synaptic vesicle positioning, junctional fold formation, and the maturation of AChR clusters into their characteristic "pretzel-like" morphology (Patton et al., 1997). Laminins additionally restrict excessive terminal nerve sprouting and help maintain precise alignment between pre-synaptic release sites and post-synaptic junctional folds, which is critical for efficient neuromuscular transmission (Sanes, 2003; Singhal, 2011). Consistent with this, the loss of laminin β2 disrupts NMJ structure by reducing junctional folding and causing scattered synaptic vesicles, ultimately impairing synaptic transmission (Noakes et al., 1995). Likewise, collagens within the synaptic basal lamina also play important roles in NMJ maintenance and signalling (Latvanlehto et al., 2010). Collagen IV contributes to the stabilization of mature motor nerve terminals, whereas Collagen XIII supports the proper organization of AChR clusters and alignment of synaptic structures (Latvanlehto et al., 2010). Collagen Q (ColQ) anchors AChE at the NMJ to regulate ACh turnover within the synaptic cleft and also interacts with Muscle-Specific Kinase (MuSK) to support post-synaptic differentiation (Cartaud et al., 2004; Sigoillot et al., 2010). Likewise,

nidogen-2 further contributes to post-synaptic AChR cluster maturation and long-term maintenance of the NMJ (Shi et al., 2012).

Moreover, the motor endplate or post-synaptic apparatus, is the thickened portion of the muscle sarcolemma that can fold onto itself to form junctional folds that nerve terminals can then fit into (Khalil et al., 2026). Junctional folds increase the surface area of the post-synaptic membrane and contain specialized components required for efficient neuromuscular transmission, including nicotinic acetylcholine receptors (nAChRs or AChRs) and voltage-gated sodium (Na^+) channels (Davis et al., 2022; Iyer et al., 2021). AChRs are concentrated at the crests of the folds, while Na^+ channels are primarily localized within the depths of the folds to facilitate post-synaptic membrane excitability (Rodríguez Cruz et al., 2020). Upon ACh binding, AChRs allow sodium influx into the sarcolemma, generating an end-plate potential (EPP) that depolarizes the membrane and triggers propagation of an action potential along the muscle fibre, leading to muscle contraction (Slater, 2017). Synaptic nuclei, a specialized group of 3-6 nuclei positioned beneath the post-synaptic membrane, also help regulate the expression of proteins (such as AChR subunits) required for NMJ structure and function (Belotti et al., 2020; Ferraro et al., 2012). Together, these components coordinate NMJ structural development and functional integrity.

1.5 Signalling Pathways Regulating NMJ Development & Maintenance

1.5.1 *Development of the Post-synaptic Apparatus*

The NMJ involves many regulatory pathways that underlie its formation and maintenance (Figure 3) (Iyer et al., 2021; Li et al., 2018; Ng et al., 2020; Rodríguez Cruz et al., 2020; Tintignac et al., 2015; Wu et al., 2010). Among these, the Agrin-LRP4-MuSK signalling axis plays a central role in post-synaptic organization (Barik et al., 2014; Eguchi et al., 2016; Tezuka et al., 2014). Agrin is a proteoglycan signalling factor released by motor neurons to induce synaptic

differentiation and organize the NMJ (Daniels, 2012). Here, it binds to Low-Density Lipoprotein Receptor Related Protein 4 (LRP4) on the post-synaptic muscle membrane, leading to activation of MuSK, a transmembrane receptor tyrosine kinase required for post-synaptic differentiation (Zong et al., 2012). Activated MuSK initiates the clustering and stabilization of AChRs by recruiting the scaffolding protein Receptor-Associated Protein of the Synapse (Rapsyn) (Gautam et al., 1995). Rapsyn is essential for post-synaptic specialization, as it anchors AChRs to the post-synaptic actin cytoskeleton through its interactions with the DGC (Moransard et al., 2003). Following this, MuSK undergoes phosphorylation, generating a binding site for Downstream of Kinase-7 or Docking Protein 7 (DOK7), a cytoplasmic adaptor protein required for full MuSK activation (Bergamin et al., 2010). By modulating MuSK signalling, DOK7 plays a critical role in both synapse formation and NMJ maintenance (Iyer et al., 2021; Li et al., 2018; Ng et al., 2020; Rodríguez Cruz et al., 2020; Tintignac et al., 2015; Wu et al., 2010). Similarly, agrin-mediated phosphorylation of the AChR-β subunit has been shown by previous studies to support the clustering and anchoring of AChRs at higher densities in the post-synaptic membrane (Borges et al., 2008, 2001). Although NMJs can still form in mice lacking this AChR-β subunit phosphorylation, these animals develop structurally simple synapses, indicating that this modification contributes to post-synaptic maturation as opposed to initial synapse formation (Friese et al., 2007).

1.5.2 *Maintenance of the Post-synaptic Apparatus Through Localized Transcriptional Control*

Following formation of the post-synaptic apparatus, maintenance of the mature NMJ requires continued expression of synaptic proteins at the motor endplate while simultaneously repressing their expression in extra-synaptic regions of the muscle fibre (Figure 3). This spatially restricted pattern of gene expression is regulated by several signalling pathways that coordinate

synaptic transcription, receptor stability, and post-synaptic organization. Among these, ACh contributes not only to promoting neurotransmission, but also to the spatial organization and maturation of the NMJ by restricting extra-synaptic AChR distribution in the post-synaptic membrane (An et al., 2010). ACh-induced muscle depolarization suppresses AChR clustering outside the synapse by altering receptor stability and localization while simultaneously repressing AChR transcription throughout the muscle fibre (An et al., 2010). Evidence for this role is provided by mice lacking Choline Acetyltransferase (ChAT), which exhibit widened endplate regions and excessive motor nerve branching, indicating that ACh normally promotes the dispersal of aneural AChR clusters not stabilized by agrin signalling (Misgeld et al., 2002). This process also involves Cyclin-Dependent Kinase 5 (Cdk5), which acts through interactions between rapsyn and the calcium-dependent protease, calpain (Chen et al., 2007; Lin et al., 2005). During NMJ development, Cdk5 contributes to the spatial restriction and organization of AChR clusters, as Cdk5-null mice exhibit broader AChR-rich regions, whereas Cdk5 inhibition enhances agrin-induced AChR clustering (Fu et al., 2005). AChR activation increases calcium influx across the post-synaptic membrane, stimulating calpain/Cdk5 signalling that promotes cytoskeletal remodelling and disperses AChR clusters (Patrick et al., 1999; Xie et al., 2006). In contrast, agrin stabilizes AChR clusters by suppressing calpain activity and counteracting cluster dispersal (Chen et al., 2007). Calcium-dependent signalling also contributes to NMJ organization, as inhibition of voltage-gated L-type Ca^{2+} channels increases MuSK expression and disrupts normal AChR distribution (Chen et al., 2011). In addition, ACh suppresses extra-synaptic AChR transcription through Protein Kinase C (PKC)- and Ca^{2+}/Calmodulin Dependent Kinase II (CaMKII)-dependent signals that reduce Myogenin (MyoG) expression, a transcription factor that regulates AChR-associated genes (Eftimie et al., 1991; Li et al., 1992; Macpherson et al., 2002). In summary, these

opposing mechanisms refine the spatial distribution of AChRs and promote maturation of the post-synaptic apparatus.

Neuregulins (NRGs) are a family of growth factors that signal through ErbB receptor tyrosine kinases expressed at the NMJ (Mei et al., 2014). At the post-synaptic membrane, NRG-1 and NRG-2 activate ErbB2, ErbB3, and ErbB4 receptors, initiating intracellular signalling cascades that regulate the transcription of AChR subunit genes from subsynaptic myonuclei (Meier et al., 1998; Moscoso et al., 1995; Rimer et al., 2004; Schmidt et al., 2011). A major downstream effector of this pathway is the transcription factor GA-binding protein (GABP), which binds N-box elements within the promoters of synaptic genes and promotes localized expression of AChR subunits, rapsyn, utrophin, and AChE at the motor endplate (Angus et al., 2005; Briguet et al., 2000; Fromm et al., 2001; Handschin et al., 2007; Herndon et al., 2008). GABP activity is further enhanced by the transcriptional coactivator PGC-1α, which facilitates synaptic gene expression and enhances AChR clustering (Angus et al., 2005; Briguet et al., 2000; Fromm et al., 2001; Handschin et al., 2007; Herndon, 2008; Lin et al., 2004; Wu et al., 2002). In addition to regulating synaptic transcription, NRG/ErbB signalling contributes directly to post-synaptic stability by phosphorylating α-dystrobrevin, a component of the DGC, thereby supporting AChR stabilization (Schmidt et al., 2011). More broadly, several DGC-associated proteins, including α-dystroglycan, α-dystrobrevin, and syntrophin, contribute to the organization and maintenance of the post-synaptic membrane through supporting junctional fold development, AChR density, AChR-associated transcript stability, and receptor recycling (Akaaboune et al., 1999; Gehle et al., 1997; Goddeeris et al., 2013; Grady et al., 2000, 2003; Hara et al., 2011). Proper glycosylation is required for the DGC proteins, as well as numerous other NMJ-associated proteins, for their proper formation and stabilization, including agrin, LRP4, MuSK, and AChR subunits (Belaya et al.,

2012; Gehle et al., 1997; Martin, 2007; Martin et al., 1999; Zoltowska et al., 2013). As such, abnormalities in glycosylation-related pathways can reduce NMJ density, impairing neuromuscular transmission and post-synaptic organization (Gehle et al., 1997; Martin, 2007; Martin et al., 1999; Nguyen et al., 2002; Rodríguez Cruz et al., 2020).

1.5.3 *Additional Regulators of NMJ Organization*

Several additional signalling pathways and structural proteins contribute to NMJ development and maintenance (Figure 3). Wnt signalling interacts closely with the MuSK/LRP4 pathway during synaptic development, with Wnt4 and Wnt11 promoting aneural AChR clustering and early synaptic patterning prior to innervation (Boëx et al., 2018; Messéant et al., 2017; Rodríguez Cruz et al., 2020; Wu et al., 2010). Src-family kinases function downstream of MuSK activation and contribute to the stabilization of AChR clusters by strengthening interactions between AChRs and rapsyn (Sadasivam et al., 2005; Smith et al., 2001). Additional structural regulators include Neuronal Cell Adhesion Molecule (NCAM) and Microtubule Actin Cross-linking Factor 1 (MACF1). NCAM facilitates the establishment and maturation of neuromuscular contacts during development, while MACF1 coordinates interactions between microtubules and actin filaments to support post-synaptic stability (Ghasemizadeh et al., 2021; Hata et al., 2018; Oury et al., 2019; Ryan, 2001). Deficiencies in either protein have been associated with impaired endplate maturation, synaptic organization, and neuromuscular transmission (Covault et al., 1986; Ghasemizadeh et al., 2021; Moscoso et al., 1995; Oury et al., 2019). Overall, these interconnected signalling and structural pathways are essential for NMJ development and maintenance, with impairments in these regulatory mechanisms contributing to NMJ abnormalities.

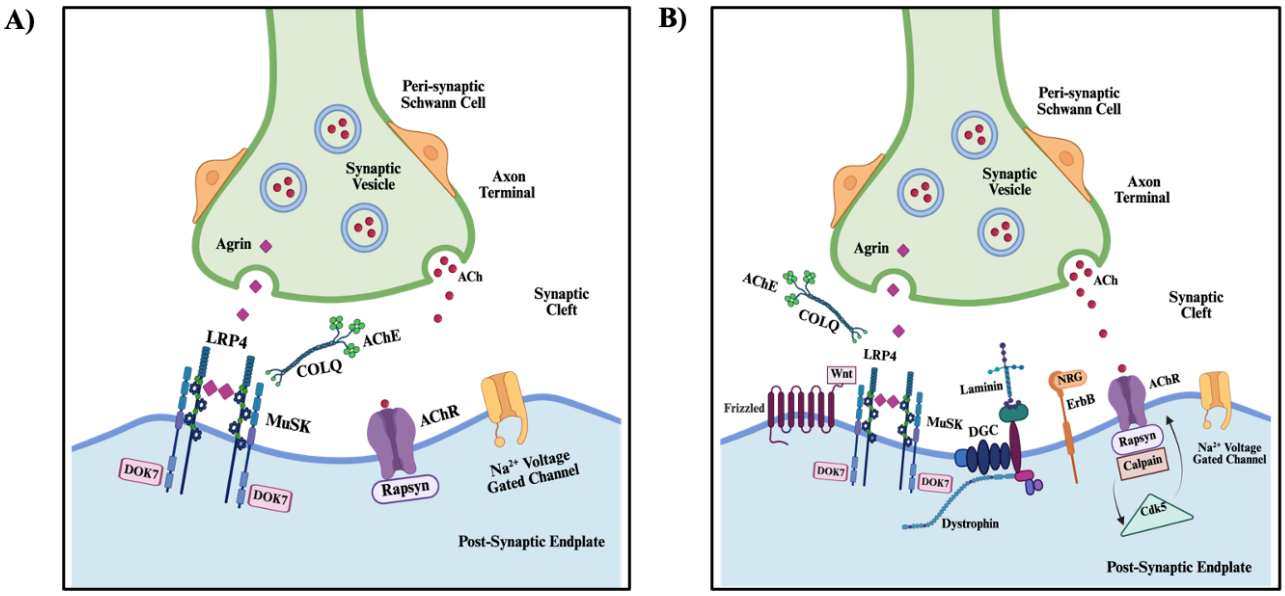


Figure 3. Key Signalling Pathways Involved in NMJ Formation and Maintenance. Panel A depicts the molecular mechanisms underlying NMJ formation. Agrin released from the motor axon terminal activates the LRP4-MuSK signalling pathway, promoting acetylcholine receptor (AChR) clustering and stabilization through DOK7 and Rapsyn. Acetylcholinesterase (AChE), anchored by collagen Q (COLQ), hydrolyzes acetylcholine (ACh) within the synaptic cleft to terminate synaptic signalling. Panel B illustrates signalling pathways involved in NMJ maintenance. Wnt/Frizzled signalling contributes to post-synaptic organization and receptor stability, while laminin and the dystrophin-glycoprotein complex (DGC) help preserve the structural integrity of the post-synaptic apparatus. Neuregulin (NRG) signalling through ErbB receptors supports the maintenance of AChR expression and post-synaptic function. Peri-synaptic Schwann cells, synaptic vesicles, and voltage-gated sodium (Na^+) channels further contribute to efficient neuromuscular transmission and long-term synaptic stability. The figures in both panels were created using BioRender and adapted from Rodríguez Cruz et al., 2020 and Liang et al., 2026.

1.6 Differences in NMJ Morphology in WT and *mdx* mice

Healthy NMJs in mice exhibit a complex, branched morphology often described as "pretzel-like" (Davis et al., 2022). In mature skeletal muscle, the NMJ undergoes continuous remodelling and reflects a high degree of functional plasticity (Davis et al., 2022; Iyer et al., 2021; Rodríguez Cruz et al., 2020). NMJ morphology can be influenced by a range of physiological and pathological factors, including aging, altered muscle activity, exercise, denervation, and the loss of crucial structural or signalling proteins (Iyer et al., 2021; Lovering et al., 2020; Ng et al., 2020).

Importantly, the morphology of the human NMJ differs substantially from that of mice (Slater, 2017). NMJs in humans are generally smaller and characterized by thinner motor axons,

less elaborate pre-synaptic nerve terminals, and more fragmented post-synaptic endplates, with "coin-shaped" or nummular morphology (Slater, 2017; Zhang et al., 2021). Despite these structural differences, human NMJs innervate muscle fibres that are considerably larger than those in mice, often reaching approximately twice the diameter of those fibres (Jones et al., 2017; Slater, 2017). Furthermore, unlike murine NMJs, which undergo age-associated remodelling and degeneration, the overall structure of human NMJs remains remarkably stable throughout adulthood (Jones et al., 2017; Valdez et al., 2010). At the post-synaptic membrane of the NMJ, the DGC plays a critical role in maintaining synaptic structure and stability (Belhasan et al., 2020). In DMD, the absence of dystrophin and associated proteins such as syntrophin, α-dystrobrevin, and dystroglycan leads to perturbations in NMJ organization and function (Belhasan et al., 2020; Grady et al., 2000; Lovering et al., 2020). Although dystrophin is not required for NMJ formation, it remains essential for synaptic maintenance, remodelling, and long-term homeostasis (Kong, 1999; Pilgram et al., 2010).

NMJs in both patients with DMD and *mdx* mice exhibit extensive structural, neurophysiological, and molecular abnormalities, some of which include: fragmentation, denervation, pre- and post-synaptic alterations, reduced safety factor, elevated quantal content, reduced MuSK expression, and impaired AChR organization and recycling (Figure 4) (Banks et al., 2009; Iyer et al., 2021; Ng et al., 2020; Pilgram et al., 2010; Theroux et al., 2008). These pathological changes compromise neuromuscular transmission and overall NMJ function, contributing to reduced muscle force following injury, lower electromyographic (EMG) amplitudes, diminished miniature end-plate potentials (mEPPs), and increased neuromuscular transmission failure in dystrophic muscle (Pratt et al., 2015a). In parallel, post-synaptic responsiveness to ACh decreases, while pre-synaptic terminals exhibit excessive branching and

undergo premature neurotransmitter depletion during sustained activity (van der Pijl et al., 2016). Additional cellular abnormalities promote further NMJ dysfunction in DMD. Peri-synaptic Schwann Cells (PSCs) show impaired coverage of pre-synaptic terminals and disrupted organization of their cellular processes or extensions, alongside an increased number of synaptic nuclei associated with ongoing neuromuscular remodelling (Pratt et al., 2015b). In general, these findings highlight the multifaceted disruption of NMJ organization and signalling in dystrophic muscle (Figure 4). These abnormalities impair efficient, coordinated muscle contraction, thereby increasing mechanical stress on already fragile dystrophin-deficient muscle fibres (Lovering et al., 2020; Ng et al., 2020; Rodríguez Cruz et al., 2020). Over time, repeated cycles of impaired excitation and contraction further exacerbate membrane instability, fibre degeneration, and progressive muscle wasting and weakness characteristic of DMD, underscoring the central role of NMJ dysfunction in disease pathophysiology (Lovering et al., 2020; Ng et al., 2020; Rodríguez Cruz et al., 2020).

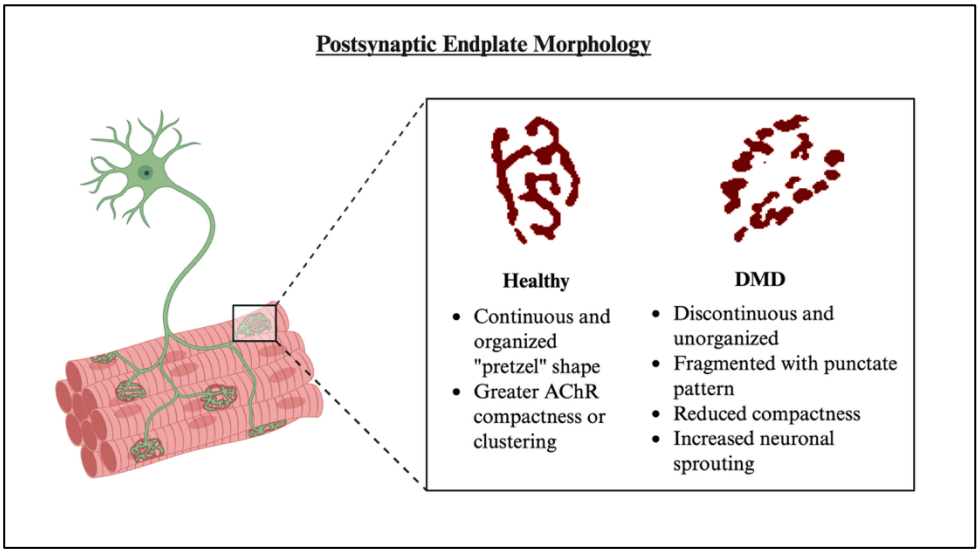


Figure 4. NMJs in *mdx* mice and DMD Patients Exhibit Fragmented and Disorganized Post-Synaptic Endplate Morphology Compared to Healthy WT Mice. Illustration of wild-type (WT) and *mdx* neuromuscular junction (NMJ) post-synaptic acetylcholine receptor (AChR) morphology, highlighting the continuous "pretzel-like" organization in WT muscle and the fragmented, discontinuous morphology observed in *mdx* muscle. This pattern of endplate disorganization and fragmentation is also observed in the NMJs of patients with Duchenne muscular dystrophy (DMD). This figure was created using BioRender.

Studies investigating NMJ structure and function in *mdx* mice have demonstrated that manipulating various synaptic regulators can reduce disease severity and enhance functional outcomes (Lovering et al., 2020; Ng et al., 2020). Notable examples include the upregulation of Utrophin, PGC-1α, LRP4, and MuSK/Rapsyn (Chan et al., 2014; Handschin et al., 2007; Hollinger et al., 2013; Hui et al., 2021; Pisani et al., 2018; Trajanovska, 2019). These findings underscore the potential of NMJ-targeted interventions as a therapeutic strategy for DMD. Utrophin upregulation has been shown to partially compensate for the absence of dystrophin by reinforcing the linkage between the cytoskeleton and extracellular matrix at the sarcolemma and NMJ, leading to improved functional recovery in *mdx* mice, enhanced AChR cluster formation, and improved synaptic morphology (Pisani et al., 2018). Similarly, PGC-1α overexpression in transgenic *mdx* mice was shown to promote transcription of genes involved in oxidative metabolism and NMJ maintenance (including utrophin, rapsyn, and AChR subunits), leading to increased AChR clustering and improved muscle function in dystrophic muscle (Handschin et al., 2007). Enhanced LRP4 expression has also been associated with enhanced agrin-mediated MuSK signalling, which increases AChR clustering, reduces denervation and fragmentation, and improves neuromuscular transmission and muscle strength in *mdx* mice (Hui et al., 2021). In addition, increasing MuSK and/or rapsyn expression protected dystrophic muscle from contraction-induced injury and improved overall functional performance (Trajanovska et al., 2019). Collectively, these findings demonstrate that preserving NMJ stability and synaptic organization can mitigate key pathological features of DMD, supporting the NMJ as both an important contributor to disease progression and a promising therapeutic target in dystrophic muscle (Ng et al., 2020). As such, understanding the molecular mechanisms that regulate synaptic maintenance may provide further insight into the

pathways contributing to NMJ defects in DMD (Deschênes-Furry et al., 2005; Joassard et al., 2015; Karmouch et al., 2020).

1.7 RNA-Binding Proteins as Post-Transcriptional Regulators of Gene Expression

Precise regulation of post-transcriptional gene expression is essential for coordinating skeletal muscle and synaptic function (Apponi et al., 2011; Shi, 2021; Van Pelt et al., 2019). RNA-binding proteins (RBPs) are crucial post-transcriptional regulators that coordinate multiple stages of RNA metabolism, including mRNA polyadenylation, transport, localization, stability, and nucleocytoplasmic trafficking (Glisovic et al., 2008). A primary mechanism by which RBPs influence protein expression is by modulating mRNA stability and transcript half-life, often via interactions with AU-rich elements (AREs) in the 3' untranslated regions (UTRs) of target transcripts (Sephton et al., 2015). Through these mechanisms, RBPs allow cells to rapidly modify protein synthesis in response to developmental and environmental signals, without requiring changes in transcription (Apponi et al., 2011; Shi et al., 2021; Van Pelt et al., 2019).

Beyond their established roles in RNA metabolism, RBPs are increasingly recognized as critical regulators of NMJ development, maturation, and maintenance by coordinating the spatiotemporal expression of genes required for synaptic structure and function (Hörnberg et al., 2013; Swanger et al., 2011). The importance of RBP-mediated post-transcriptional regulation is underscored by the involvement of several RBPs in neurological and neuromuscular disorders characterized by synaptic dysfunction (Thelen et al., 2020). For example, Spinal Muscular Atrophy (SMA) is caused by insufficient levels of Survival Motor Neuron (SMN) protein, which interacts with many RBPs and facilitates the assembly of ribonucleoprotein complexes involved in RNA processing, transport, and translation (Fallini et al., 2014; Goulet et al., 2013; Lefebvre et al., 1995; Li et al., 2014). Similarly, mutations in TAR DNA-binding protein 43 (TDP-43) and Fused in

Sarcoma (FUS), two RBPs that regulate RNA processing, transport, and local translation, are associated with Amyotrophic Lateral Sclerosis (ALS) and Frontotemporal Dementia (FTD) (Chia et al., 2018; Lee et al., 2012; Polymenidou et al., 2011; Thelen et al., 2020). Notably, FUS has been detected at both central synapses and the NMJ, where it contributes to local RNA regulation required for synaptic function (Efimova et al., 2017; So et al., 2018). Collectively, these findings highlight the importance of RBPs in maintaining neuronal and neuromuscular homeostasis and demonstrate how disruption of post-transcriptional regulatory networks can contribute to synaptic dysfunction and disease (Thelen et al., 2020). Among the numerous RBP families identified to date, the Hu/ELAV family has attracted particular attention due to its involvement in regulating gene expression programs associated with inflammation, tissue remodelling, and regeneration - processes that contribute significantly to the pathogenesis of DMD (Colombrita, 2013; Shi et al., 2021).

1.8 The ELAVL/Hu Protein Family

The Hu family of RNA-binding proteins consists of four members encoded by the ELAV-like gene, the mammalian homolog of the Drosophila ELAV family (Figure 5) (Colombrita, 2013; Shi et al., 2021). Three of these - HuB, HuC, and HuD - are primarily associated with neuronal differentiation and are localized in the cytoplasm (Apponi et al., 2011; Van Pelt et al., 2019). In contrast, the fourth member of this family, HuR, is mainly nuclear and broadly expressed in tissues such as the intestines, adipose tissue, and spleen (Hinman et al., 2008; Simone et al., 2013; Wutikeli et al., 2025). Although Hu proteins influence multiple stages of RNA metabolism, including transcription, alternative splicing, polyadenylation, nuclear export, translation, and mRNA localization, they are best characterized for their role in stabilizing target transcripts in the cytoplasm through binding AREs located in the 3’ UTRs of these mRNAs (Pascale et al., 2008;

Van Pelt et al., 2019; Wutikeli et al., 2025). This interaction enhances transcript stability by protecting transcripts from ribonuclease-mediated degradation, displacing destabilizing RNA-binding factors, and facilitating the recruitment of additional stabilizing proteins (Pascale et al., 2008; Van Pelt et al., 2019; Wutikeli et al., 2025). In addition to these cytoplasmic functions, Hu proteins participate in several nuclear regulatory processes, including transcription, alternative splicing, and polyadenylation (Pascale et al., 2008; Simone et al., 2013; Wutikeli et al., 2025). Structurally, all Hu proteins contain three highly conserved RNA recognition motifs (RRMs), a flexible hinge region, and an N-terminal domain (Apponi et al., 2011; Van Pelt et al., 2019). The hinge region contains a sequence that enables nucleocytoplasmic shuttling, and in HuR, this region is referred to as the HuR nucleocytoplasmic shuttling (HNS) sequence (Clark et al., 2025; Fan et al., 1998). The HNS sequence comprises nuclear localization and nuclear export signals, which allow HuR to translocate to the cytoplasm in response to physiological or pathological stimuli and stabilize target mRNA (Brennan et al., 2001; Hinman et al., 2008; Simone et al., 2013).

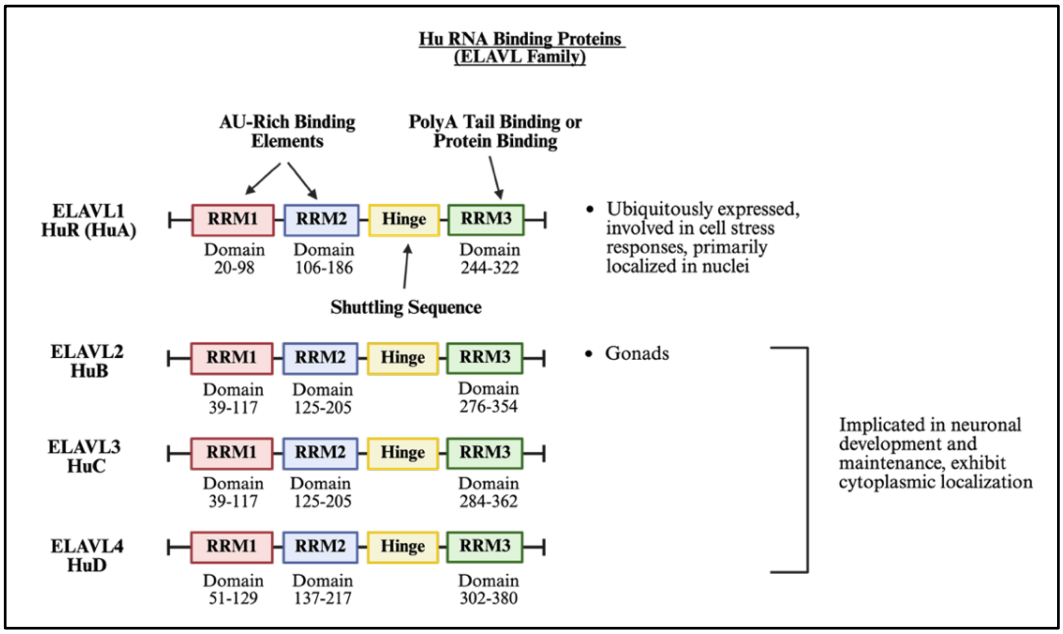


Figure 5. The Structural Organization and Functional Characteristics of the Hu/ELAVL Family of RNA-Binding Proteins. This figure illustrates the four members of the Hu/ELAVL (embryonic lethal abnormal vision like) family of RNA-binding proteins: ELAVL1 (HuR/HuA), ELAVL2 (HuB), ELAVL3 (HuC), and ELAVL4 (HuD). All family members contain three conserved RNA recognition motifs (RRMs 1-3) separated by a hinge region containing a nucleocytoplasmic shuttling sequence. RRM1 and RRM2 primarily mediate binding to adenylate-uridylate-rich elements (AREs) within the 3′ untranslated regions (UTRs) of target mRNAs, whereas RRM3 contributes to poly(A) tail binding and protein-protein interactions involved in post-transcriptional regulation. HuR is ubiquitously expressed and primarily localized to the nucleus, where it regulates transcripts involved in cellular stress responses. In contrast, HuB, HuC, and HuD are predominantly localized to the cytoplasm and are enriched in neuronal tissue development and maintenance. This figure was created using BioRender and adapted from Hinman et al., 2008 and Wutikeli, H. et al., 2025.

The selective recognition of AREs by Hu proteins is influenced by competition with other ARE-binding proteins that promote mRNA decay (Dassi, 2017; Simone et al., 2013). By displacing or blocking these destabilizing factors, Hu proteins can enhance mRNA stability (Shi et al., 2021). This stabilization may occur through mechanisms such as oligomerization on target mRNAs or interference with the recruitment of the degradation machinery (Dassi, 2017; Shi et al., 2021). Additionally, post-translational modifications of Hu proteins modulate their activity and influence the stability of multiple mRNA targets (Grammatikakis et al., 2017). Beyond mRNA stability, Hu proteins can also regulate gene expression at the translational level, either increasing or inhibiting protein synthesis by interacting with the 3’ or 5’ UTRs of target transcripts (Hinman et al., 2008; Simone et al., 2013).

1.9 HuR as a Post-Transcriptional Regulator of Disease-Related mRNAs

Human antigen R (HuR) is an RBP encoded by the ELAV-like gene that binds to and stabilizes the AREs in the 3' and, in some cases, the 5' UTRs of target mRNAs (Abdelmohsen et al., 2008; Srikantan et al., 2012a). Through these interactions, HuR generally enhances mRNA stability and/or translation in processes such as cell proliferation, differentiation, senescence, stress response, angiogenesis, inflammation, and apoptosis (Srikantan et al., 2012a). As such, HuR has been widely implicated in the pathophysiology of many disease states, including cancer and inflammatory, cardiovascular, neurodegenerative, and neuromuscular diseases (Beauchamp et al., 2010; Figueroa et al., 2003; Grammatikakis et al., 2017; Srikantan et al., 2012a; von Roretz et al., 2011).

In cancer, HuR is often overexpressed and/or redistributed to the cytoplasm, where it promotes the stability or enhances the translation of transcripts associated with increased cell survival and proliferation (e.g., cyclins, cyclin-dependent kinase inhibitor p21, and tumour protein p53), angiogenesis and inflammation (e.g., Vascular Endothelial Growth Factor or VEGF and Cyclooxygenase-2 or COX-2), as well as evasion of immune recognition and metastatic progression (e.g., Transforming Growth Factor-β or TGF-β, and mitogen-activated protein kinase phosphatase or MKP-1) (Abdelmohsen, 2010; Srikantan et al., 2012a; Wang et al., 2013). Beyond its role in cancer-associated pathways, HuR also functions as an important post-transcriptional regulator of inflammation, stabilizing the expression of several pro-inflammatory cytokines such as Tumour Necrosis Factor-α (TNF-α), Interleukin-6 (IL-6), Interleukin-8 (IL-8), and TGF-β, which stimulate immune cell recruitment, fibrosis, and tissue remodelling (Nabors et al., 2001; Zhou et al., 2007). Similarly, HuR enhances the expression of transcripts encoding COX-2 and inducible Nitric Oxide Synthase (iNOS), which act together to sustain prolonged immune

responses (Di Marco et al., 2005; Sengupta et al., 2003; Srikantan et al., 2012a). Moreover, in cardiovascular disease, HuR regulates transcripts involved in vascular signalling and smooth muscle function, including TGF-β, COX-2, iNOS, angiotensin receptors, and β2-adrenergic receptors, which are typically associated with hypertension, ischemia, and vascular remodelling (Klöss et al., 2005; Misquitta et al., 2001). HuR has also been implicated in neurological and neuromuscular diseases through its post-transcriptional regulation of Neurofibromatosis type-1 (NF1) and SMN mRNA (Schultz et al., 2020). HuR interacts with the 3' UTRs of both transcripts and, in the case of SMN, promotes mRNA stability and increases SMN protein expression, linking HuR to pathways relevant to motor neuron function and maintenance (Farooq et al., 2009; Haeussler et al., 2000; Perera et al., 2016; Schultz et al., 2020). Thus, by regulating the stability and translation of numerous disease-relevant transcripts, HuR has emerged as a key mediator of cellular responses to stress, injury, inflammation, and tissue remodelling.

1.10 HuR and Its Stabilization of DMD-Related Transcripts

HuR-mediated stabilization of target transcripts, as observed in other disease states, may also contribute to the persistent pathological signalling pathways associated with DMD, including chronic inflammation, cellular stress, impaired muscle regeneration, and fibrosis (Bez Batti Angulski et al., 2023; Bhatnagar, 2010). Targets regulated by HuR, including p21 and p53, which are involved in cellular stress responses and cell-cycle progression, may be relevant within the chronic regenerative environment and oxidative stress environment characteristic of dystrophic muscle (Englund et al., 2022; Grammatikakis et al., 2017; Lafarga et al., 2009; Memme et al., 2021). Similarly, pro-inflammatory transcripts regulated by HuR, such as TNF-α, IL-6, IL-8, COX-2, and iNOS, may contribute to the sustained inflammatory response observed in dystrophic muscle resulting from repeated contraction-induced injury as the disease progresses (Di Marco et

al., 2005; J. Zhang et al., 2025). In addition, other targets regulated by HuR, such as TGF-β, VEGF, and MKP-1, have been associated with fibrosis, angiogenesis, oxidative stress adaptation, tissue remodelling, and cell survival pathways (Srikantan et al., 2012a). In the context of DMD, dysregulation of these processes may participate in the accumulation of connective tissue, persistent oxidative stress, impaired angiogenesis and defective regenerative signalling observed in dystrophic muscle (Deasy et al., 2009; Grammatikakis et al., 2017; Ismaeel et al., 2019; Kuwano et al., 2008; Podkalicka et al., 2019; Shi et al., 2010; Srikantan et al., 2012a). Overall, these observations suggest that HuR may contribute to pathological processes in DMD by stabilizing transcripts involved in inflammation, regeneration, fibrosis, and stress adaptation.

1.11 The Critical Role of Post-Transcriptional Regulators such as HuR in the NMJ

At the NMJ, HuR regulates transcripts encoding proteins critical for post-synaptic structure and function, including AChR-β and AChE, particularly under denervation and pathological conditions (Figure 6) (Deschênes-Furry et al., 2005; Joassard et al., 2015; Karmouch et al., 2020). Together, these findings position HuR as an important post-transcriptional regulator of gene expression programs that support NMJ morphology and provide a rationale for investigating whether its dysregulation contributes to post-synaptic abnormalities in dystrophic skeletal muscle.

In 2015, Joassard et al. demonstrated that denervation induces HuR expression and promotes its cytoplasmic accumulation, leading to enhanced stability of AChR β-subunit mRNAs. AChRs are transmembrane proteins localized to the post-synaptic membrane that transduce acetylcholine signals at the NMJ to initiate muscle contraction (Joassard et al., 2015). HuR binds directly to AREs within the 3'UTR of AChR β-subunit transcripts, protecting them from decay and increasing steady-state mRNA levels (Joassard et al., 2015). This process is regulated by p38 MAPK signalling, which activates HuR and drives its cytoplasmic localization following

denervation (Joassard et al., 2015). Pharmacological inhibition of p38 MAPK using SB203580 accelerated AChR β-subunit mRNA degradation by approximately 1.6-fold, whereas activation of p38 MAPK with Anisomycin extended transcript half-life by approximately 1.4-fold (Joassard et al., 2015).

In addition, during skeletal muscle differentiation, HuR binds directly to an ARE within the 3'UTR of the AChE transcript, resulting in increased AChE expression (Deschênes-Furry et al., 2005). Since AChE is highly enriched in the synaptic basal lamina of the NMJ and is essential for skeletal muscle contraction by terminating neurotransmission in both the central and peripheral nervous systems, it is essential in preventing prolonged muscle stimulation and fatigue (Deschênes-Furry et al., 2005). Overexpression of HuR slows the decay of AChE mRNA in vitro, whereas HuR downregulation diminishes steady-state AChE transcript abundance (Deschênes-Furry et al., 2005). This work provided early evidence for HuR's involvement in the post-transcriptional regulation of synaptic gene expression (Deschênes-Furry et al., 2005).

Similarly, recent work using a mouse model of congenital myasthenic syndrome caused by acetylcholinesterase deficiency due to COLQ loss further supports a role for HuR in stabilizing synaptic mRNAs at the NMJ (Karmouch et al., 2020). COLQ is required for anchoring and concentrating AChE within the synaptic basal lamina, and its absence resulted in elevated HuR protein levels and increased cytoplasmic redistribution (Karmouch et al., 2020). These changes correlated with enhanced stability and increased steady-state levels of AChR β-subunit mRNAs (Karmouch et al., 2020). HuR was shown to bind specifically to AREs within the AChR β-subunit 3'UTR, directly promoting transcript stabilization in a p38 MAPK-dependent manner (Karmouch et al., 2020). Pharmacological manipulation of p38 signalling altered both HuR abundance and

AChR subunit mRNA levels, further linking this pathway to synaptic mRNA regulation (Karmouch et al., 2020).

Beyond transcripts directly regulated by HuR, post-transcriptional mechanisms have also been implicated in regulating genes involved in NMJ structure and function, including utrophin A and α-dystrobrevin-1 (Figure 6). Notably, utrophin A expression is subject to post-transcriptional control that contributes to its enrichment at the post-synaptic membrane and preferential expression in slow, oxidative skeletal muscle fibres (Gramolini et al., 2001a, 2001b; Chakkalakal et al., 2003a). This process is mediated by cis-acting elements within the 3'UTR of the utrophin transcript, including a conserved ARE that influences mRNA turnover and responsiveness to signalling pathways associated with the slow-muscle phenotype, such as calcineurin signalling (Chakkalakal et al., 2003b, 2008). Furthermore, the RNA-binding protein KH-Type Splicing Regulatory Protein (KSRP) binds this ARE and promotes utrophin mRNA decay, providing direct evidence that RBPs contribute to the regulation of NMJ-associated transcripts (Amirouche et al., 2013; Chakkalakal et al., 2003; Gramolini et al., 2001). Furthermore, α-dystrobrevin-1 is a component of the dystrophin-glycoprotein complex that contributes to the structural organization and stability of the post-synaptic apparatus at the NMJ (Grady et al., 2000, 2003). Although α-dystrobrevin-1 isoforms are transcribed from a common promoter, transcripts encoding α-dystrobrevin-1 preferentially accumulate at synaptic sites, indicating that post-transcriptional mechanisms contribute to its localized expression (Newey et al., 2001). These findings provide additional evidence that transcript-specific regulatory processes help coordinate the spatial expression of proteins required for NMJ structure and function (Newey et al., 2001). Collectively, these findings highlight the importance of post-transcriptional regulation, including RBP-mediated mechanisms, in controlling the expression of genes required for synaptic organization and

maintenance. Given its established role in regulating transcripts involved in cholinergic signalling and post-synaptic function, HuR may represent an important mediator of gene expression programs that contribute to NMJ structure (Joassard et al., 2015; Karmouch et al., 2020). Defining HuR's role within the post-synaptic apparatus may therefore provide valuable insight into the mechanisms underlying endplate abnormalities in dystrophic skeletal muscle.

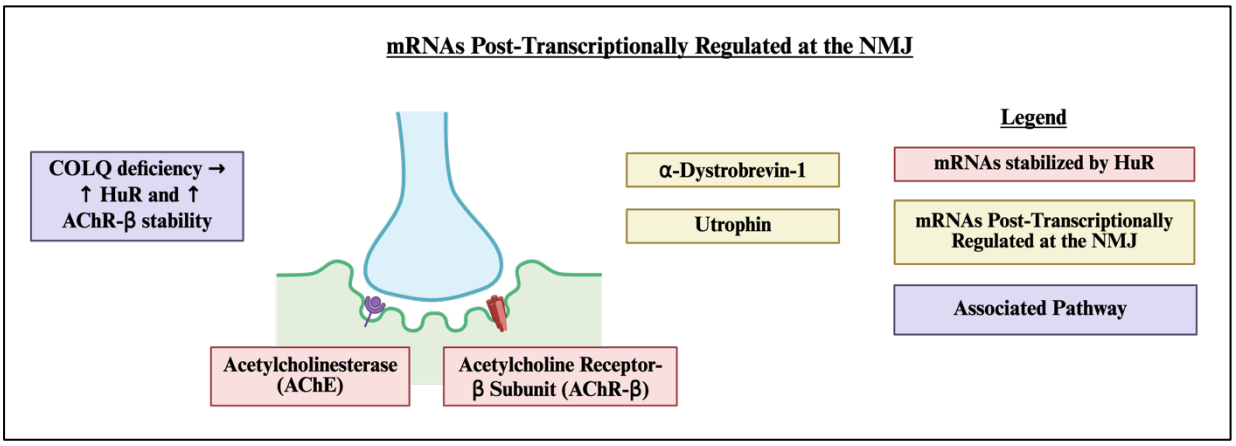


Figure 6. Post-Transcriptional Regulation of NMJ-Associated Transcripts by HuR and Related Pathways in Mouse Skeletal Muscle. HuR stabilizes AChE and AChR-β transcripts through interactions with AU-rich elements (AREs) located within their 3′ untranslated regions (3′UTRs). Other NMJ-associated transcripts, utrophin A and α-dystrobrevin-1, are also regulated post-transcriptionally and contribute to the organization of the post-synaptic apparatus. In COLQ-deficient muscle, p38 MAPK-dependent cytoplasmic accumulation of HuR further enhances AChR-β mRNA stabilization. This figure was created in BioRender.

1.12 HuR as a Regulator of Myogenesis

Beyond regulating transcripts at the NMJ, HuR is a well-established mediator of skeletal muscle differentiation and regeneration, coordinating the expression of numerous myogenesis-related mRNAs. HuR has previously been shown to stabilize p21 mRNA, promoting irreversible cell-cycle withdrawal and initiating the myogenic differentiation program (Apponi et al., 2011; Figueroa et al., 2003; Giessen et al., 2003; von Roretz et al., 2011). Additionally, HuR stabilizes the transcripts of Myogenic Differentiation 1 (MyoD) and Myogenin (MyoG), both fundamental regulators of myogenic differentiation, to promote the fusion of myoblasts into myotubes (Figueroa et al., 2003; Giessen et al., 2003; von Roretz et al., 2011). The ability of HuR to regulate

these processes is closely linked to its nucleocytoplasmic shuttling; although HuR is predominantly localized within the nucleus under normal conditions, many of its mRNA-stabilizing and translational functions require its translocation and accumulation in the cytoplasm, where it stabilizes its target transcripts involved in muscle development and regeneration (Beauchamp et al., 2010; Figueroa et al., 2003; Giessen et al., 2003; von Roretz et al., 2011). HuR's translocation is regulated by its cleavage, which occurs through a caspase-dependent process (Figure 7). Both in vivo and in vitro, inhibition of caspase activity in myoblasts or genetic deletion of caspase-3 in mice markedly reduced HuR cleavage and significantly diminished its cytoplasmic localization in muscle fibres (Beauchamp et al., 2010; Figueroa et al., 2003; Giessen et al., 2003; von Roretz et al., 2011). Caspase-mediated processing of HuR generates two fragments, HuR cleavage product 1 (HuR-CP1) and HuR cleavage product 2 (HuR-CP2) (Beauchamp et al., 2010; Figueroa et al., 2003; Giessen et al., 2003; von Roretz et al., 2011). HuR-CP1 interacts with the HuR nuclear import receptor transportin-2 (TRN2), promoting the accumulation of HuR in the cytoplasm. When TRN2-mediated nuclear import is disrupted, HuR-CP1 facilitates the cytoplasmic retention of full-length HuR, thereby stabilizing MyoD and MyoG mRNAs and supporting myogenic differentiation (Beauchamp et al., 2010). Following differentiation, HuR returns to the nucleus, completing a dynamic pattern of subcellular localization observed during adult muscle regeneration and embryonic myogenesis, characterized by cytoplasmic HuR levels increasing during periods of active differentiation and declining as regeneration progresses (Beauchamp et al., 2010; Figueroa et al., 2003; Giessen et al., 2003; von Roretz et al., 2011).

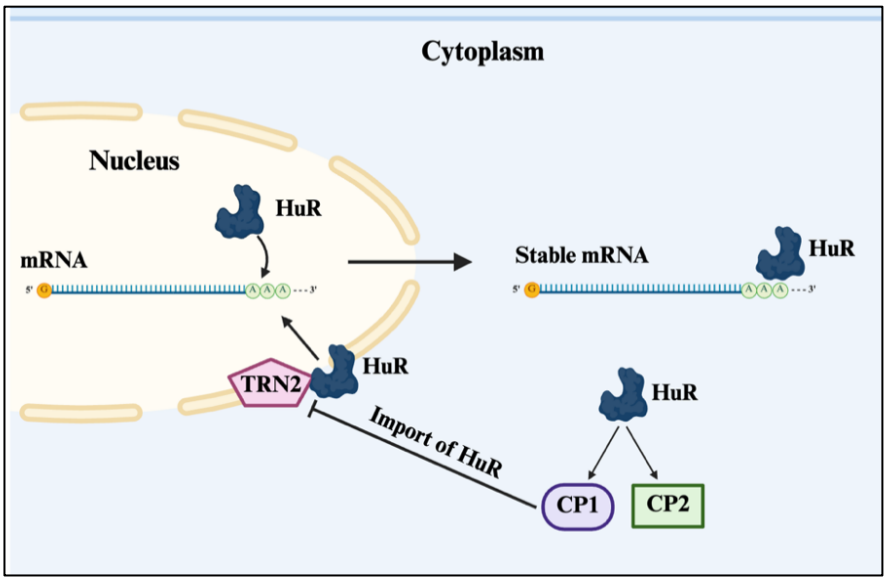


Figure 7. **Mechanism of HuR-Mediated mRNA Stabilization and Nucleocytoplasmic Shuttling in Muscle Fibres of Mice.** HuR binds adenylate-uridylate-rich elements (AREs) located within target mRNA transcripts and promotes transcript stabilization following export from the nucleus to the cytoplasm. HuR localization and transport are regulated through interactions with transport proteins, including Transportin 2 (TRN2) and import/export complexes, which control the nucleocytoplasmic shuttling required for its post-transcriptional regulatory activity. Through these mechanisms, HuR modulates the stability and translation of transcripts involved in cellular stress responses, inflammation, proliferation, and differentiation. This figure was created using BioRender and adapted from Wang et al., 2013.

1.13 Insights into HuR Function from Constitutive and Skeletal Muscle-Specific Knockout Models

Genetic studies in mice have further underscored the context-specific functions of HuR. Complete loss of HuR resulted in embryonic lethality, with severe developmental defects including decreased limb size, asplenia, and impaired skeletal patterning of digits and long bones (Katsanou et al., 2009; Shi et al., 2021). Analyses of embryonic fibroblasts derived from these models revealed shortened half-lives of transcripts encoding transcription factors critical for limb patterning and skeletal outgrowth (e.g., Hoxd13, Tbx4, Ets2), signifying the contribution of HuR to the regulation of gene expression programs required for skeletal patterning (Katsanou et al., 2009; Shi et al., 2021). In contrast, within a conditional, muscle-specific HuR knockout mouse model, an increase in the amount of oxidative type I fibres was observed, which helped protect against muscle wasting due to cancer cachexia (Janice Sánchez et al., 2019). This fibre-type shift

was accompanied by enhanced exercise endurance, suggesting that HuR normally restricts the formation of oxidative fibres in adult muscle (Janice Sánchez et al., 2019). Mechanistically, this effect has been linked to HuR's cooperation with KSRP to destabilize PGC-1α mRNA, a regulator of energy metabolism, highlighting HuR's role in maintaining fibre-type balance in mature skeletal muscle (Janice Sánchez et al., 2019).

1.14 Rationale

The rationale for this project is supported by previous findings reported by Deschênes-Furry et al. (2005), Joassard et al. (2015), and Karmouch et al. (2020), which collectively identify HuR as an important post-transcriptional regulator of synaptic development, maintenance, and adaptation in skeletal muscle. These studies demonstrate that HuR binds AREs located within the 3'UTRs of synaptic mRNAs, including AChE and AChR β-subunit, to promote their stability and enhance their expression (Deschênes-Furry et al., 2005; Joassard et al., 2015; Karmouch et al., 2020). Through this mechanism, HuR helps regulate genes essential for endplate organization and structure.

Importantly, HuR activity is enhanced under conditions of denervation and cellular stress, which promote both its expression and translocation to the cytoplasm, where it can exert its mRNA-stabilizing functions (Mazroui et al., 2008). Given that dystrophic skeletal muscle is characterized by chronic degeneration, impaired regeneration, and NMJ defects, dysregulated HuR expression or localization may contribute to pathological alterations at the NMJ endplate in DMD (Massopust et al., 2020; van der Pijl et al., 2016). However, despite the role of HuR in post-synaptic mRNA regulation, its contribution to organization at the endplate in dystrophic skeletal muscle remains largely unexplored.

Previous studies have shown that *mdx* mice exhibit pronounced NMJ abnormalities, including increased fragmentation, reduced compactness, altered post-synaptic morphology, and impaired synaptic transmission (Lovering et al., 2020; Pratt et al., 2015b). As several HuR-regulated transcripts are essential for synaptic development and maintenance (Deschênes-Furry et al., 2005; Joassard et al., 2015; Karmouch et al., 2020), perturbations in HuR expression or subcellular localization may contribute to these structural abnormalities. Therefore, this project aimed to investigate the role of HuR in regulating post-synaptic membrane organization in *mdx* skeletal muscle by characterizing its expression, localization, and modulation relative to WT controls. By doing so, this work seeks to further elucidate the contribution of post-transcriptional regulatory mechanisms to post-synaptic membrane defects in DMD.

1.15 Hypotheses & Research Objectives for the Project

The central hypothesis of this project is that HuR is overexpressed in skeletal muscle fibres of *mdx* mice compared to WT mice, negatively impacting post-synaptic membrane structure; accordingly, reducing HuR expression may improve endplate defects. The main research question of this project is how HuR and its modulation affect NMJ structure in *mdx* mice compared to WT mice. This project aims to (1) build upon known qualitative disruptions of the NMJ endplates in *mdx* mice versus their control, WT counterparts, (2) examine the role of HuR in the post-synaptic apparatus in the DMD context, and (3) modulate HuR expression to assess potential effects on endplate structure. This work will improve understanding of HuR's role in regulating post-synaptic membrane structure and provide insight into whether modulating it represents a potential therapeutic strategy to improve synaptic organization in DMD.

Chapter 2 - Materials and Methods

This project follows a three-phase framework: (i) a descriptive/phenotypic phase that builds upon established findings of endplate disruption in *mdx* mice; (ii) a mechanistic phase in which HuR expression is genetically downregulated to evaluate its effects on post-synaptic membrane morphology; and (iii) a therapeutic phase that assesses the impact of pharmacological HuR downregulation on endplate organization.

All mice were euthanized by intraperitoneal (IP) injection of sodium pentobarbital (100 mg/kg), followed by cervical dislocation. Subsequently, the required muscles were dissected and processed according to downstream applications: (i) flash-frozen in liquid nitrogen for protein and RNA extraction; (ii) fixed in 4% paraformaldehyde (PFA) for NMJ imaging; or (iii) embedded in Tissue-Tek OCT Compound (Fisher Healthcare - Ottawa, Ontario, Canada) and frozen in isopentane previously cooled with liquid nitrogen. All tissue samples were stored at -80°C until further analysis.

2.1 Descriptive/Phenotypic Phase - Characterization of HuR Expression and Subcellular Localization in Dystrophic Skeletal Muscle

The descriptive/phenotypic phase involved WT and *mdx* endplate analysis, quantification of HuR protein abundance by Western blot, and assessment of HuR distribution by immunofluorescence (Figure 8). HuR protein expression was measured in the following muscles: tibialis anterior (TA), diaphragm (DIA), extensor digitorum longus (EDL), and soleus (SOL). These muscles were harvested from 3-4 *mdx* and WT mice at various ages (4, 8, 12, and 24+ weeks old) to reflect the progressive nature of DMD and the different skeletal muscle fibre types present in the body. The EDL, SOL, and DIA muscles at 12 weeks, and the DIA muscle at 24+ weeks, were not collected due to limited availability, as noted in Table 1.

2.1.1 *Endplate Staining and Imaging*

Following dissection, TA muscles from WT and *mdx* mice were immediately fixed in 4% paraformaldehyde (PFA) in 1× phosphate-buffered saline (PBS) for 1 hour to ensure adequate fixation, then transferred to 1% PFA in 1× PBS and stored at -20°C. The muscle was then subdivided into three regions by gently separating fibres along their longitudinal axis, with each region then being dissected further under a stereomicroscope (1.6× magnification) by progressively isolating smaller fibre bundles until single muscle fibres were obtained. Approximately 50–60 isolated fibres were collected per sample, after which they were blocked in 1% bovine serum albumin (BSA) in PBS and then incubated with Alexa Fluor 488-conjugated α-BTX (1:500) for one hour. After additional PBS washes, fibres were mounted on glass slides using Vectashield mounting medium containing DAPI (MJS BioLynx - Brockville, Ontario, Canada). Slides were imaged using a Leica Thunder Imager equipped with a 10×/0.32 dry objective. Images were processed using small-volume computational clearing at 60% strength. Exposure times and imaging parameters were kept constant across all samples to allow accurate comparisons. Following image acquisition, 40–60 images of the post-synaptic apparatus per group were selected for analysis. A blinded scoring approach was employed using the SIAL plug-in within ImageJ/FIJI, in which images were randomized and independently rated on a scale from 1 (normal and well-organized endplate) to 3 (highly disorganized and fragmented endplate), thereby minimizing potential bias between WT and *mdx* samples (Tyrpak et al., 2020).

2.1.2 *HuR Protein Isolation and Quantification*

Protein extraction was performed using MEU buffer prepared from a 1.25× urea-thiourea stock. Protein cleanup and quantification were performed using the CB-X Protein Assay kit (G Biosciences - Ottawa, Ontario, Canada) in 96-well plates. Absorbance was measured at 595 nm on

a BioTek Synergy H1 microplate reader (Agilent Technologies – Santa Clara, California, USA), and the concentrations of the protein samples were calculated using the standard curve formula.

2.1.3 *HuR Western Blots*

Protein samples (15–30 µg) were mixed with 4× loading buffer (Bio-Rad - Mississauga, Ontario, Canada) containing β-mercaptoethanol and heated at 70°C for 10 minutes before gel loading. Gels were prepared by assembling either large or mini cassettes with gaskets and spacers, inserting combs, and casting resolving (10%) and stacking gels (5%) according to standard acrylamide formulations. Electrophoresis was then performed in 1× Tris-Glycine running buffer, with samples loaded alongside the Page Ruler pre-stained protein ladder (Thermofisher Scientific - Mississauga, Ontario, Canada) at 80-100 V until all proteins were fully resolved. Proteins were transferred to nitrocellulose membranes at 0.45 µm (Millipore Sigma/Cytiva - Oakville, Ontario, Canada) using a transfer sandwich consisting of sponges, thin filter paper (Bio-Rad - Mississauga, Ontario, Canada), gel, and membrane, with transfer occurring under constant current (0.17 A, ~40 Volts or V) at 4 °C for 16–18 hours. Membranes were rinsed, stained with 1x Ponceau S to verify successful protein transfer, and destained with Tris-Buffered Saline with Tween (TBS-T, 1% w/v). Non-specific binding was blocked with 5% Bovine Serum Albumin (BSA) in TBS-T for 1 hour at room temperature. Membranes were incubated overnight at 4°C with primary antibodies, rinsed with TBS-T, and incubated with secondary antibodies. Primary antibodies included HuR 3A2 HRP (Santa Cruz Biotechnology - Dallas, Texas, USA) at 1:1000 and β-actin HRP (Santa Cruz Biotechnology - Dallas, Texas, USA) at 1:10,000. Proteins were then detected using chemiluminescent ECL substrate (Bio-Rad - Mississauga, Ontario, Canada) and imaged on a ChemiDoc system (Bio-Rad – Mississauga, Ontario, Canada) at varying exposure times, along

with colorimetric imaging for ladders. Data analysis was performed using Bio-Rad ImageLab version 6.1.

2.1.4 *Subcellular Fractionation of HuR*

Nuclear and cytoplasmic protein fractions were isolated from the TA muscle of WT and *mdx* mice at 11 weeks using the NE-PER Nuclear and Cytoplasmic Extraction Reagents kit (Thermofisher Fisher Scientific, Mississauga, Ontario, Canada) according to the manufacturer's instructions. Briefly, freshly harvested muscle tissue was homogenized in Cytoplasmic Extraction Reagent I (CER I) supplemented with protease inhibitors, followed by the addition of Cytoplasmic Extraction Reagent II (CER II) to disrupt the plasma membrane while maintaining nuclear integrity. Following centrifugation, the supernatant containing the cytoplasmic protein fraction was collected. The remaining nuclear pellet was subsequently resuspended in Nuclear Extraction Reagent (NER) and subjected to intermittent vortexing to solubilize nuclear proteins. Following centrifugation, the supernatant containing the nuclear protein fraction was collected. Protein extracts were stored at -80°C until further analysis by western blotting. Fractionation efficiency was verified by immunoblotting with Histone H3 (Cell Signalling Technology, 1:1000 dilution) and α-tubulin (Sigma-Aldrich, 1:5000 dilution) as nuclear and cytoplasmic markers, respectively.

2.1.5 *HuR Immunofluorescence Staining and Imaging*

TA muscles from WT and *mdx* mice were embedded in optimal cutting temperature (OCT) compound, flash-frozen, and cryo-sectioned into 10 μm-thick cross-sections. For each sample, 3-6 sections were collected across 3-4 slides. Immunofluorescence staining was performed using the mouse-on-mouse (MOM) immunodetection kit (Vector Laboratories, MJS BioLynx, Brockville, ON, Canada). Sections were fixed in 4% PFA in 1× PBS and quenched with 0.1 M glycine in PBS. To reduce nonspecific binding of mouse-derived primary antibodies, sections were blocked for 1

hour in MOM blocking reagent, then incubated in MOM diluent. Primary antibodies were diluted in MOM diluent and applied for 30 minutes at room temperature. After PBS washes, sections were incubated with MOM biotinylated anti-mouse IgG for 10 minutes, followed by a 15-minute incubation with a streptavidin-based detection system and appropriate secondary antibodies. Sections were then mounted with Vectashield containing DAPI and stored at -20°C until imaging was completed using the Leica Thunder microscope. Primary antibodies included mouse anti-HuR (clone 3A2; 1:50 dilution, Santa Cruz) and rabbit anti-laminin (1:100 dilution, Sigma Aldrich). Secondary reagents consisted of biotinylated anti-mouse IgG (1:250), Streptavidin-TR (1:500, Invitrogen), and donkey anti-rabbit Alexa Fluor 488 (1:200, Invitrogen). HuR immunofluorescence images were quantified using image segmentation and machine learning-based classification with the Labkit plugin in ImageJ/Fiji. Nuclear and cytoplasmic regions were identified based on DAPI and laminin staining, respectively. Measurements from 2-3 cross-sectional images per mouse were averaged before statistical analysis, so each data point represented a single animal (n = 7-8 mice across all ages). Measurements included mean integrated density (abundance = mean gray intensity × area), enabling assessment of HuR localization within each cellular compartment (Kelley, 2019).

2.1.6 *Macrophage Staining and Imaging*

Macrophage immunofluorescence staining was performed using the same MOM protocol described above; however, F4/80 (Rat anti-mouse, monoclonal antibody, Bio-Rad) was used as the primary antibody in place of laminin. Laminin and F4/80 were not co-stained due to potential spectral overlap between fluorophores. Quantitative analysis involved manually counting and recording the total number of macrophages, macrophages expressing HuR (Mac^{HuR}), and nuclei expressing HuR (Nuc^{HuR}). Macrophage infiltration was quantified as the percentage of F4/80-

positive macrophages relative to the total number of nuclei within each muscle cross-section. Similarly, the contribution of macrophages to total HuR expression was calculated as the percentage of HuR-positive macrophages (Mac^{HuR}) relative to the total number of HuR-positive nuclei (Nuc^{HuR}).

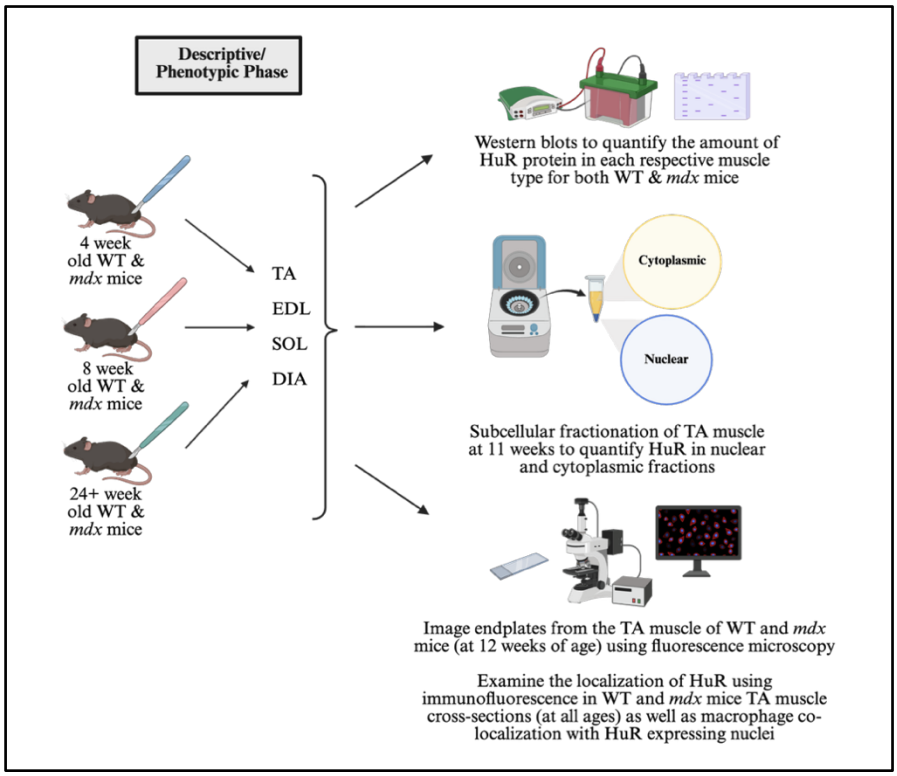


Figure 8. **Experimental Overview of the Descriptive/Phenotypic Phase.** Skeletal muscles from Wild-type (WT) and *mdx* mice at multiple ages (4-24+ weeks) were collected from the Tibialis Anterior (TA), Extensor Digitorum Longus (EDL), Soleus (SOL), and Diaphragm (DIA) muscles to characterize HuR expression and localization during disease progression. HuR protein expression was assessed by western blot analysis, while subcellular fractionation was performed to determine the distribution of HuR between nuclear and cytoplasmic compartments. HuR abundance and localization within muscle fibres were further examined by immunofluorescence staining at all ages in TA muscle cross-sections, while fluorescence microscopy was conducted to examine endplates from the TA muscle at 12 weeks. This figure was created using BioRender.

2.2 Mechanistic Phase –The Effects of HuR Knockdown in *mdx* Skeletal Muscle

Genetic downregulation of HuR was achieved using an AAV-mediated shRNA approach to investigate whether reducing HuR expression could improve post-synaptic endplate organization in dystrophic skeletal muscle (Figure 9). Multiple shRNA sequences targeting HuR were initially evaluated in the pLKO lentiviral vector system for their ability to reduce HuR

expression. The sequence exhibiting the greatest knockdown efficiency was subsequently subcloned into an AAV expression vector. Recombinant AAV2/9 particles encoding the HuR-targeting shRNA (AAV2/9-shHuR) were produced by the Canadian Neurophotonics Platform Viral Vector Core Facility. AAV2/9 particles expressing a luciferase-targeting shRNA (AAV2/9-shLuc) were obtained from the same facility and served as the control vector. Intramuscular injections were subsequently performed in 3-4 *mdx* mice, with AAV2/9-shHuR administered to the TA muscle of one hindlimb and AAV2/9-shLuc administered to the contralateral TA muscle, serving as an internal control. Before injections, mice were anesthetized with 4% isoflurane and oxygen until loss of movement and reduced respiration were observed. Injection sites were shaved and disinfected before administration, and each TA muscle received a single injection containing 1×10^{11} AAV vector genomes in 30 µL of saline, calculated based on the average body weight of *mdx* mice. Following injections, the animals were monitored during recovery for 3-5 hours post-procedure and again the following day. Muscles were harvested four weeks post-injection to allow sufficient time for HuR knockdown, as confirmed by western blot analysis. As expected, higher HuR expression was observed in shLuc-injected control muscles compared to shHuR-treated muscles. In a subsequent experiment, the same protocol was applied to 3-4 additional *mdx* mice, in which TA muscles were collected for post-synaptic membrane analysis to investigate the effects of HuR gene expression downregulation on the structure of the post-synaptic apparatus; these muscles were later subjected to blinded endplate analysis using the SIAL plug-in on FIJI/ImageJ (Tyrpak et al., 2020). Subsequently, quantification of endplate morphometric parameters, including area, perimeter, and compactness, was then performed using the NMJ-Morph plug-in on FIJI/ImageJ and compared to non-injected *mdx* endplates (Landini, 2008; Minty et al., 2020).

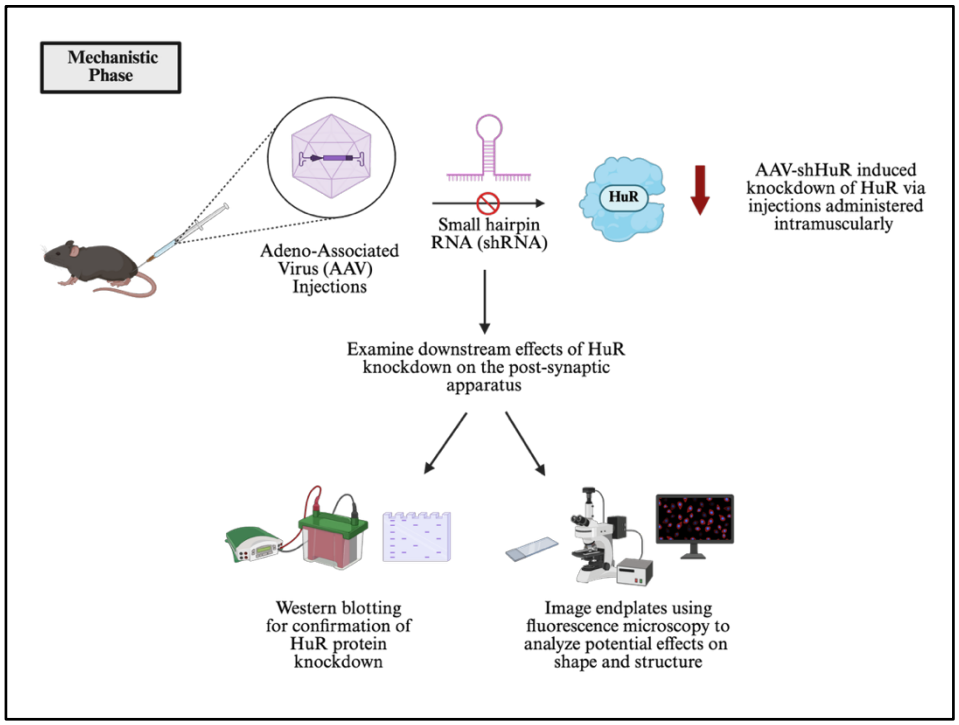


Figure 9. **Experimental Plan Used to Investigate the Role of HuR in Dystrophic Skeletal Muscle.** In the mechanistic phase of the study, *mdx* mice received intramuscular injections of rAAV2/9 vectors expressing either shHuR or a control shRNA (shLuc) to reduce HuR expression in skeletal muscle. Successful HuR knockdown was validated by Western blot analysis. The effects of HuR downregulation on the post-synaptic apparatus were subsequently assessed by analyzing endplate morphology with α-bungarotoxin staining and fluorescence microscopy. This figure was created using BioRender.

2.3 Therapeutic Phase - Pharmacological Modulation of HuR Using Vorinostat in *mdx* Mice

In the therapeutic phase, the pan-HDAC inhibitor Vorinostat was administered to *mdx* mice to assess its effects on HuR expression, localization, and overall endplate organization and structure (Figure 10). Vorinostat stock solutions were prepared at a maximum concentration of 7.5 mg/mL in a vehicle consisting of 5% dimethyl sulfoxide (DMSO), 300 mg/mL hydroxypropyl-β-cyclodextrin (HPβCD), and 0.9% sodium chloride. Vehicle control solutions contained identical components, without Vorinostat. Mice were weighed weekly and received daily intraperitoneal injections for 28 consecutive days, administered on alternating sides. Animals were randomly assigned to either the Vorinostat treatment group (50 mg/kg) or the vehicle control group. Twenty-four hours after the final injection, grip strength testing was performed. Mice were then euthanized by intraperitoneal injection of Euthanyl or pentobarbital sodium (100–120 mg/kg), followed by

cervical dislocation after 15-20 minutes of reduced activity. The TA muscle from one hindlimb was collected for analysis of post-synaptic apparatus structure, while TA, EDL, and SOL muscles from the contralateral side were used for western blot analysis, as previously completed in non-injected and AAV-shRNA-injected endplates. Morphometric features of the endplates, including area, perimeter, and compactness, were quantified again and compared with those of previously analyzed endplates. HuR immunofluorescence analyses were also conducted to assess for any changes in HuR localization or distribution following drug treatment.

2.3.1 Animal Grip Strength Testing

Mice were habituated in the testing room for 30 minutes under standard lighting conditions. During forepaw grip strength assessment, each mouse was allowed to grasp the bar with both forepaws and was gently pulled away from the force meter until release occurred. Between trials, the animal was positioned on the apparatus's metal floor plate, and grip strength was recorded as grams of force (GF). A minimum of five trials was conducted per mouse. 30 minutes after the forepaw assessment, combined forelimb and hindlimb grip strength was evaluated by placing all four limbs on the grate and gently pulling the mouse away from the meter until the mouse released its grip. At least five trials were performed, with GF recorded for each. Body weight was measured before the animals were returned to their housing room. Data analysis included normalizing grip-strength values (grams) to body weight for both the forepaw and four-limb grip-strength measurements obtained from *mdx* vehicle-injected and *mdx* Vorinostat-treated mice, with higher grip-strength values indicating greater grip strength.

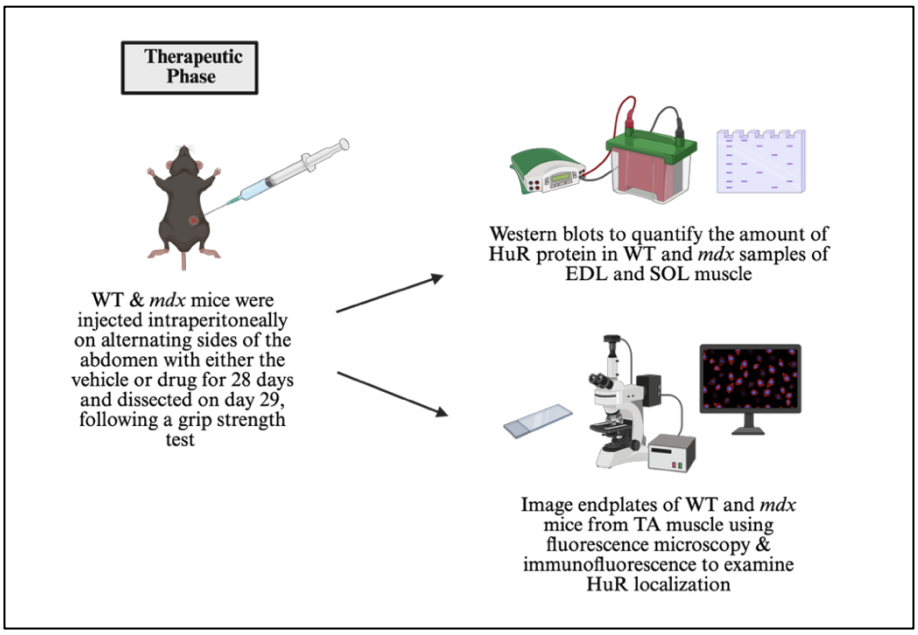


Figure 10. **Experimental Design Used to Evaluate the Therapeutic Effects of HuR Modulation in Dystrophic Skeletal Muscle.** *mdx* mice were treated daily with either the histone deacetylase inhibitor (HDACi) Vorinostat (50 mg/kg, intraperitoneal injection) or vehicle control for 28 days. Following treatment, skeletal muscle samples were collected to assess HuR and acetylated tubulin expression by western blot analysis. The effects of Vorinostat on endplate morphology, HuR abundance, and localization were also further evaluated by immunofluorescence staining and fluorescence microscopy of TA muscle cross-sections. This figure was created using BioRender.

2.4 Statistical Analyses of All Collected Data

All data were analyzed using GraphPad Prism 10 (GraphPad Software - Boston, Massachusetts), and data are presented as mean ± SEM. Immunofluorescence datasets were analyzed using the Mann-Whitney U test, with measurements from individual fibres averaged to generate a single value per mouse prior to statistical analysis. Western blot datasets were analyzed using unpaired Student's t-tests. Endplate compactness measurements from three experimental groups were analyzed using one-way ANOVA followed by Sidak's multiple-comparisons test. Differences in the distribution of blinded endplate morphology classifications were evaluated using Fisher's exact test. For all analyses, each mouse was treated as a biological replicate, and a p-value< 0.05 was considered statistically significant.

Chapter 3 – Results

3.1 Analyses of the Structure of the Post-synaptic Membrane in *mdx* and WT Muscles and Expression Pattern of the RNA-Binding Protein HuR

3.1.1 *mdx Mice Exhibit Disorganized Morphology of the Post-synaptic Apparatus*

In a first series of experiments, we sought to confirm the previously reported NMJ endplate disruption in *mdx* mice by fluorescent labelling of the AChR α-subunit at the post-synaptic membrane (Banks et al., 2009; Iyer et al., 2021; Jerusalem et al., 1974; Lovering et al., 2020; Lyons et al., 1991; Shiao, 2004). Blinded classification was performed using the Single Image Analysis Library (SIAL) plug-in on ImageJ/Fiji, which randomized and anonymized image file names to eliminate scoring bias (Tyrpak et al., 2020). Approximately 100 images of NMJ post-synaptic membranes from WT and *mdx* mice (n =3) were acquired and subsequently subjected to blinded analysis (Figure 11). Endplates were ranked by morphology from most organized (phenotype score 1) to most disorganized (phenotype score 3) (Osseni et al., 2020, 2022). As expected, *mdx* mice exhibited greater fragmentation and discontinuity, while endplates from WT controls were most often continuous and organized. This was reflected by a significant increase in the proportion of disorganized post-synaptic membrane in *mdx* muscles compared to WT ($p<0.0001$) (Banks et al., 2009; Iyer et al., 2021; Jerusalem et al., 1974; Lovering et al., 2020; Lyons et al., 1991; Shiao, 2004).

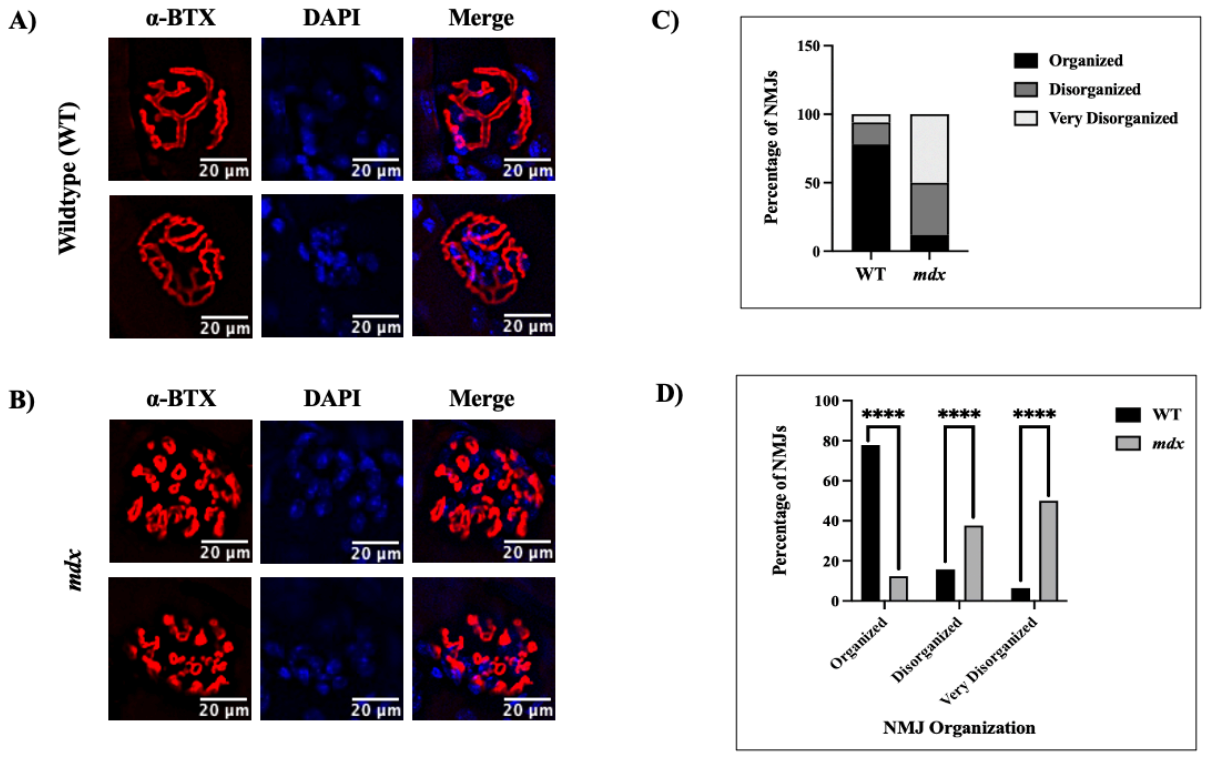


Figure 11. *mdx* Mice Exhibit Fragmented and Disorganized Post-synaptic Endplate Morphology Compared to WT Controls. Representative images of post-synaptic endplates from the tibialis anterior (TA) muscle of 12-20-week-old wild-type (WT; panel A) and *mdx* (panel B) mice are shown. Additionally, the distribution of endplate morphology categories after blinded scoring is shown (panel C), along with the corresponding statistical analysis (panel D). *mdx* mice exhibited increased fragmentation, reduced structural integrity, a lower proportion of organized endplates, and a greater proportion of disorganized and very disorganized endplates compared to WT controls. Acetylcholine receptors (AChRs) were labelled using Alexa Fluor 594-conjugated α-bungarotoxin (α-BTX; red), and nuclei were counterstained with DAPI (blue). Images were acquired using a Leica Thunder microscope at 10× magnification (numerical aperture 0.32) using the same exposure and intensity for all images. Computational clearing (60% strength) and uniform brightness and contrast adjustments were applied consistently across all samples. Endplates were randomized and classified using the SIAL plugin in ImageJ/Fiji according to a phenotype scale ranging from 1 (organized) to 3 (very disorganized). Data represent n=3 mice per group, with 50–60 endplates analyzed per mouse. Statistical significance was determined using Fisher's exact test (*p < 0.05, **p < 0.01, ***p < 0.001, ****p < 0.0001, ns = not significant). Scale bar: 20 µm.

3.1.2 *HuR Protein Levels are Upregulated in mdx Mice Across Different Ages and Muscles*

Next, we investigated HuR protein expression in WT and *mdx* mice across multiple muscles with varying fibre-type compositions, including the Tibialis Anterior (TA), Diaphragm (DIA), Extensor Digitorum Longus (EDL), and Soleus (SOL) and at ages 4-24+ weeks (Figures 12-15). This analysis was performed to establish HuR expression in dystrophic muscle and determine if this expression changed across muscles and throughout disease progression.

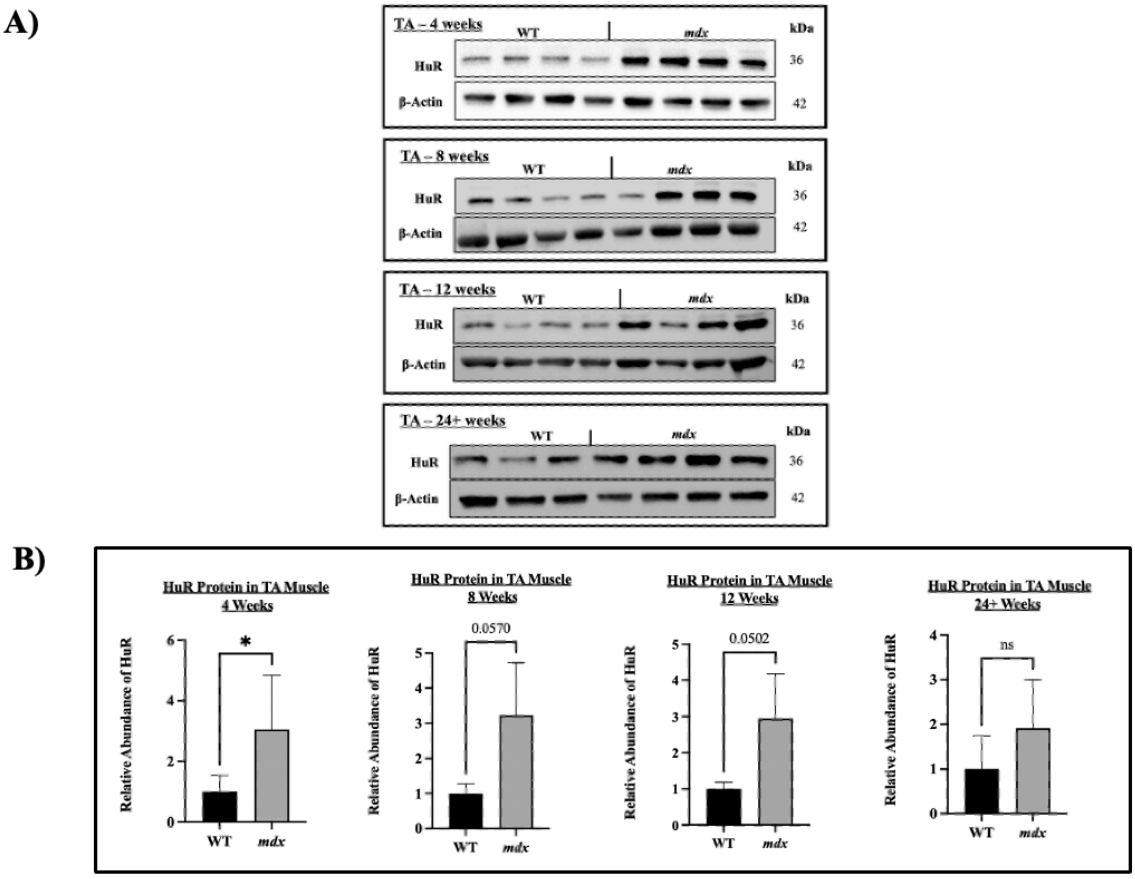


Figure 12. HuR Protein Levels Are Elevated in *mdx* TA Muscle From 4-12 Weeks. Panel A displays representative western blots of HuR protein expression in the tibialis anterior (TA) muscle of wild-type (WT) and *mdx* mice at 4, 8, 12, and 24+ weeks. Panel B provides the corresponding quantification, confirming a significant increase in HuR protein abundance in *mdx* mice at 4 weeks, with similarly strong upward trends at 8-12 weeks, and a non-significant trend towards an increase at 24+ weeks. HuR protein levels were normalized to β-actin. Data represent n = 3-4 mice per group, with 2-3 technical replicates completed per Western blot. Statistical analysis was performed using unpaired t-tests (*p< 0.05, **p< 0.01, ***p< 0.001, ****p< 0.0001, ns = not significant).

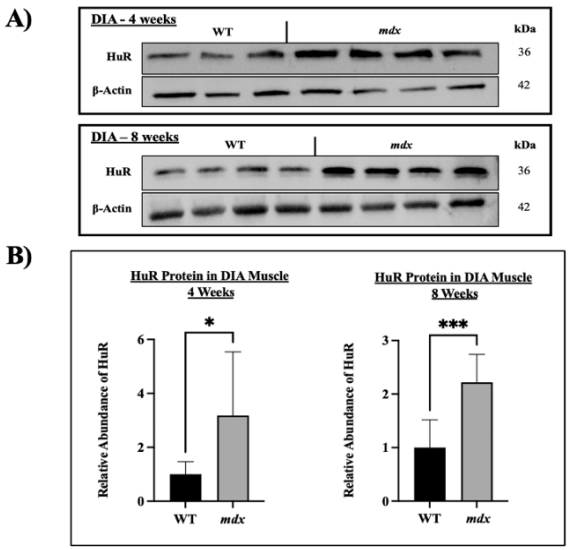


Figure 13. HuR Protein Levels Are Increased in *mdx* DIA Muscle at 4-8 Weeks. Panel A depicts representative western blots of HuR protein expression in the diaphragm (DIA) muscle of wild-type (WT) and *mdx* mice at 4 and 8 weeks. Panel B provides the corresponding quantification, confirming a significant increase in HuR protein abundance in *mdx* mice at both time points. HuR protein levels were normalized to β-actin. Data represent n = 3-4 mice per group, with 2-3 technical replicates conducted per Western blot. Statistical analysis was performed using unpaired t-tests (*p< 0.05, **p< 0.01, ***p< 0.001, ****p< 0.0001, ns = not significant).

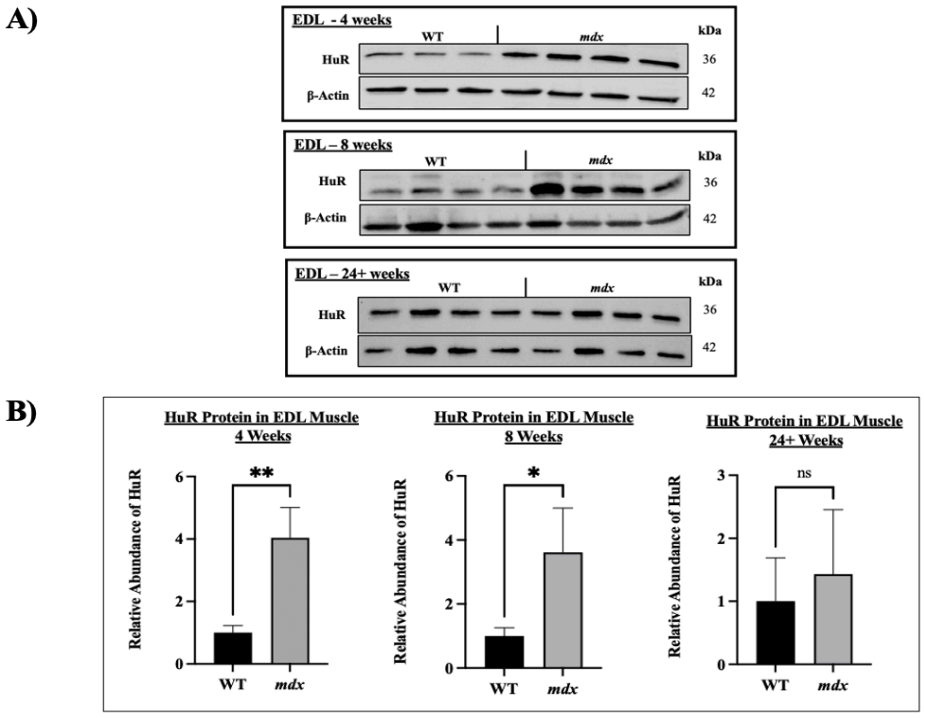


Figure 14. HuR Protein Levels Are Elevated in *mdx* EDL Muscle with Significance at 4-8 Weeks. Panel A displays representative western blots of HuR protein expression in the extensor digitorum longus (EDL) muscle of wild-type (WT) and *mdx* mice at 4, 8, and 24+ weeks. Panel B summarizes the quantification, indicating significantly increased HuR protein abundance in *mdx* mice at 4 and 8 weeks, while levels at 24+ weeks remain elevated but are not statistically different from WT. HuR protein levels were normalized to β-actin. Data represent n = 3-4 mice per group, with 1-3 technical replicates completed per Western blot. Statistical analysis was performed using unpaired t-tests (*p< 0.05, **p< 0.01, ***p< 0.001, ****p< 0.0001, ns = not significant).

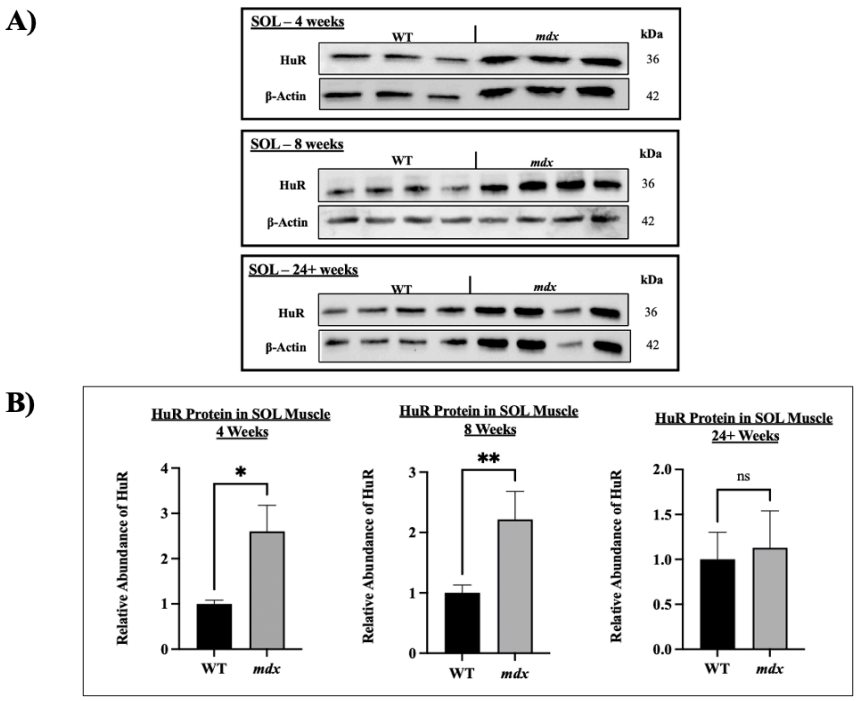


Figure 15. HuR Protein Levels are Increased in *mdx* SOL Muscle at 4-8 Weeks. Panel A illustrates representative western blots of HuR protein expression in the soleus (SOL) muscle of wild-type (WT) and *mdx* mice at 4, 8, and 24+ weeks. Panel B presents the corresponding quantification, showing significantly higher HuR protein abundance in *mdx* mice at 4 and 8 weeks, while levels at 24+ weeks remain elevated but do not reach statistical significance. HuR protein levels were normalized to β-actin. Data represent n = 3-4 mice per group, with 1-3 technical replicates conducted per Western blot. Statistical analysis was performed using unpaired t-tests (*p< 0.05, **p< 0.01, ***p< 0.001, ****p< 0.0001, ns = not significant).

Across most muscle types (fast- or slow-twitch) and ages, HuR protein expression was consistently elevated in *mdx* mice compared with WT controls. The greatest increases were generally observed at earlier time points, at which HuR expression reached statistical significance across all muscles (Table 1). Although the magnitude of these differences appeared to diminish with age, HuR protein levels remained elevated in *mdx* muscle at later time points, including 24+ weeks, though they did not always reach statistical significance. This pattern was observed across both fast- and slow-twitch muscles, indicating that increased HuR expression is a common feature of dystrophic skeletal muscle rather than being restricted to a specific muscle type or stage of disease progression.

Muscle	4 Weeks	8 Weeks	12 Weeks	24+ Weeks
Tibialis Anterior (TA)	↑	p = 0.0570	p = 0.0502	ns
Diaphragm (DIA)	↑	↑↑↑	-	-
Extensor Digitorum Longus (EDL)	↑↑	↑	-	ns
Soleus (SOL)	↑	↑↑	-	ns

Table 1. Summary of Statistical Analyses of Elevated HuR Protein Levels in *mdx* Mice Across Muscles and Ages. Overview of statistical comparisons for HuR protein expression in *mdx* mice relative to wild-type (WT) controls across TA, DIA, EDL, and SOL muscles at 4-24+ weeks. Significant increases are observed at most early time points across multiple muscles, while later time points show a consistent trend toward higher HuR levels that do not reach statistical significance. ↑ $p < 0.05$, ↑↑ $p < 0.01$, ↑↑↑ $p < 0.001$, ns = not significant. "–" indicates that the muscle was not collected.

3.1.3 *Elevated Nuclear HuR Protein with Limited Cytoplasmic Redistribution in mdx Muscle*

The observation that HuR protein expression was elevated across most muscle types at earlier ages in *mdx* mice prompted further investigation into its distribution in dystrophic muscle. This was especially important given that HuR's function is closely associated with its intracellular localization and is regulated by its post-translational modifications that govern its nucleocytoplasmic shuttling and RNA-binding activity (Grammatikakis et al., 2017; Srikantan et al., 2012a). Thus, we performed subcellular fractionation to isolate and quantify HuR protein in the nuclear and cytoplasmic fractions of the muscle fibres.

Nuclear and cytoplasmic protein fractions were isolated from 11-week-old WT and *mdx* TA muscles. The TA muscle was selected because it is highly susceptible to contraction-induced injury and displays pronounced dystrophic pathology in *mdx* mice (Dellorusso et al., 2001). The 11-week time point was chosen as an established stage of disease progression at which elevated

HuR protein expression had already been observed, enabling assessment of its subcellular localization within dystrophic muscle fibres. Histone H3 and α-tubulin were used as nuclear and cytoplasmic markers, respectively, to verify successful separation of the two fractions (Dimauro et al., 2012). Histone H3 was detected, predominantly in the nuclear fraction, whereas α-tubulin was detected with greater abundance in the cytoplasmic fraction, indicating effective isolation of nuclear and cytoplasmic proteins. HuR abundance was subsequently quantified in each compartment by Western blotting (Figure 16). Nuclear HuR was significantly increased in *mdx* muscle relative to WT controls ($p<0.001$). In contrast, cytoplasmic HuR exhibited a similar upward trend but did not reach statistical significance. Although HuR levels appeared elevated in both compartments, the increase was predominantly associated with the nuclear fraction, indicating preferential localization of HuR within the nuclear compartment of dystrophic muscle.

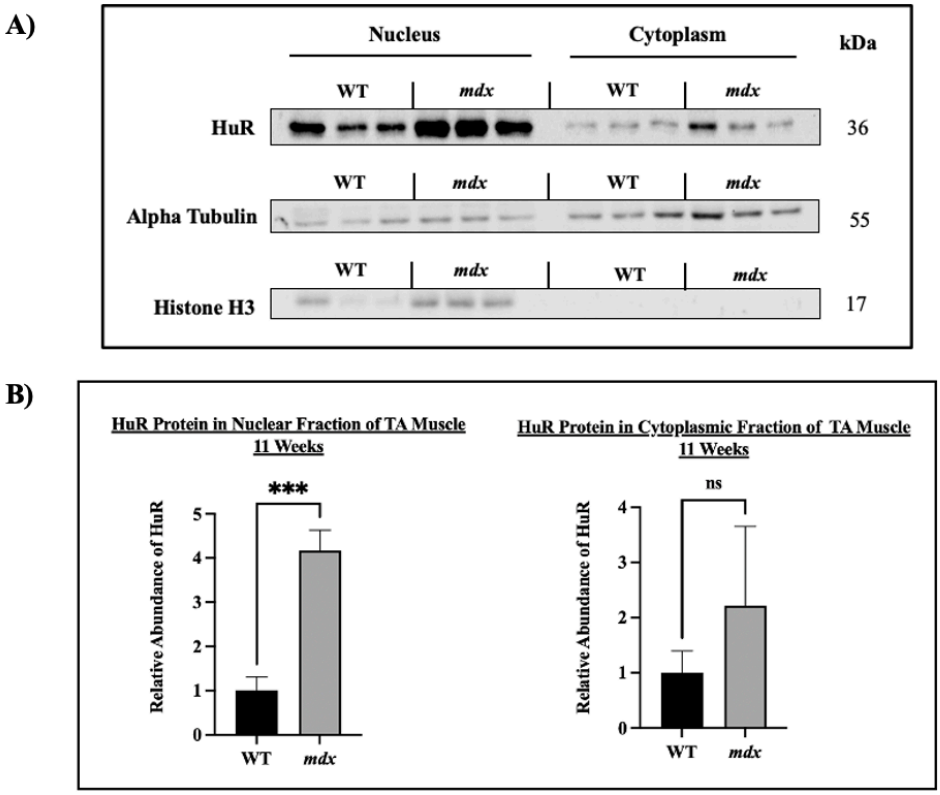


Figure 16. Subcellular Fractionation Reveals Increased Nuclear HuR Protein in *mdx* TA Muscle at 11 Weeks. Panel A shows representative immunoblots of HuR protein levels in nuclear and cytoplasmic fractions from Wild-type (WT) and *mdx* TA muscle, with α-tubulin and histone H3 used as cytoplasmic and nuclear markers, respectively. Panel B displays quantification of HuR protein levels in each fraction. HuR protein was significantly increased in the nuclear fraction of *mdx* muscle compared to WT, while a trend toward increased levels was observed in the cytoplasmic fraction that was not significant. Data are presented as relative abundance normalized to appropriate loading controls. n=3, with 2–3 trials conducted per Western blot. Statistical analysis was performed using unpaired t-tests (*p< 0.05, **p< 0.01, ***p< 0.001, ****p<0.0001, ns = not significant).

3.1.4 *HuR Localization in WT and mdx TA Muscle Across Disease Progression as Revealed by Immunofluorescence*

In addition to the subcellular fractionation findings, HuR immunofluorescence was performed on TA muscle cross-sections from WT and *mdx* mice aged 4 to 24+ weeks (Figures 17-19). Sections were stained for HuR, laminin, and DAPI to visualize HuR distribution within muscle fibres across the disease course. This analysis provided spatial context for the fractionation data and enabled assessment of potential changes in HuR localization with disease progression. Immunofluorescence staining confirmed the presence of HuR within the TA muscle fibres of both WT and *mdx* mice at all ages examined (Figures 17-19). HuR signal was detected in both nuclear

and cytoplasmic compartments, while laminin staining outlined muscle fibre borders. Consistent with dystrophic pathology, *mdx* muscle sections exhibited greater fibre-size heterogeneity and an increased proportion of nuclei relative to WT controls (Duddy et al., 2015; Watkins et al., 1982).

4 weeks

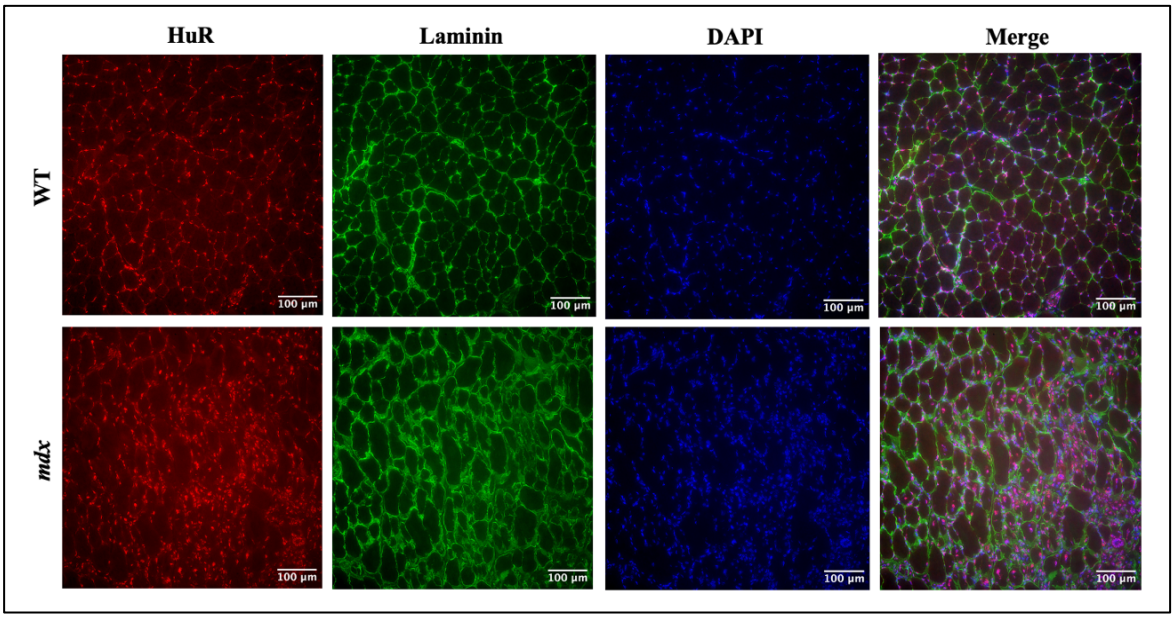


Figure 17. HuR Immunofluorescence in WT and *mdx* TA Muscle at 4 Weeks. HuR staining (red) appears increased in *mdx* muscle relative to WT. Laminin (green) outlines muscle fibre boundaries, and nuclei are counterstained with DAPI (blue). Images were acquired using a Leica Thunder microscope at 40× magnification (numerical aperture 1.25) using the same exposure and intensity for all images. Computational clearing (60% strength) and uniform brightness and contrast adjustments were also applied consistently across all samples. Scale bar: 100 µm.

8 weeks

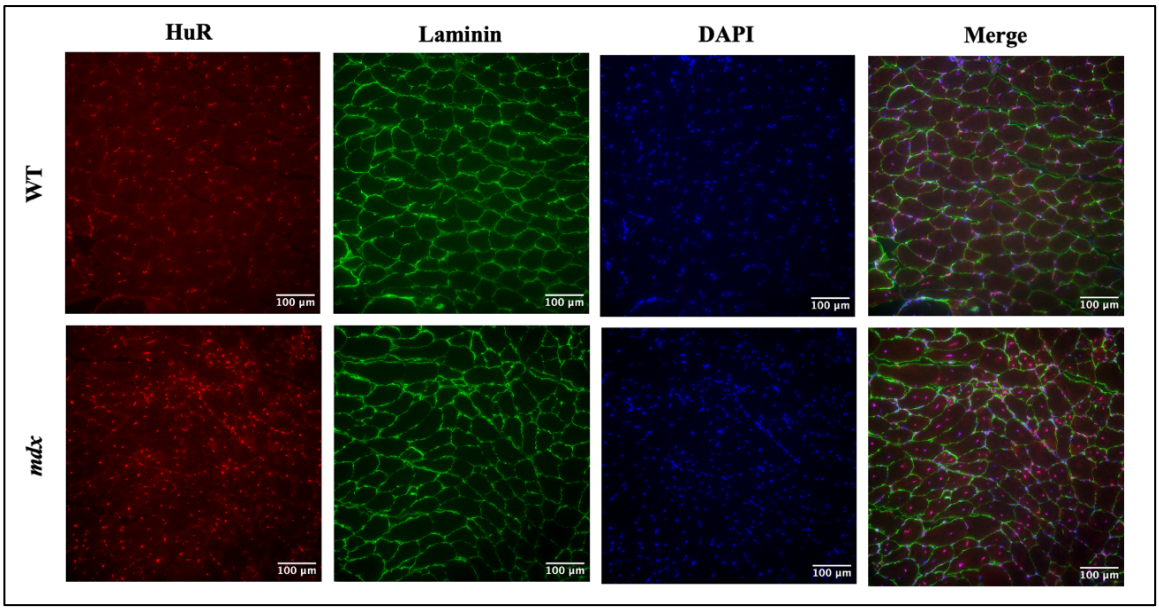


Figure 18. HuR Immunofluorescence in WT and *mdx* TA Muscle at 8 Weeks. HuR staining (red) appears increased in *mdx* muscle relative to WT. Laminin (green) outlines muscle fibre boundaries, and nuclei are counterstained with DAPI (blue). Images were acquired using a Leica Thunder microscope at 40× magnification (numerical aperture 1.25) using the same exposure and intensity for all images. Computational clearing (60% strength) and uniform brightness and contrast adjustments were also applied consistently across all samples. Scale bar: 100 µm.

24+ weeks

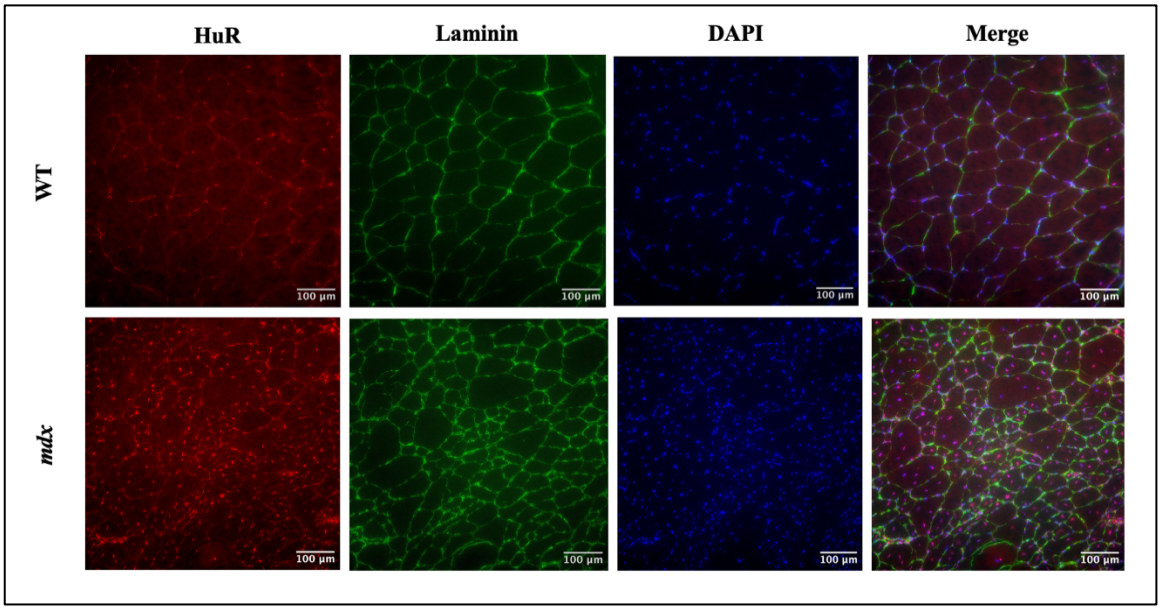


Figure 19. HuR Immunofluorescence in WT and *mdx* TA Muscle at 24+ Weeks. HuR staining (red) appears increased in *mdx* muscle relative to WT. Laminin (green) outlines muscle fibre boundaries, and nuclei are counterstained with DAPI (blue). Images were acquired using a Leica Thunder microscope at 40× magnification (numerical aperture 1.25) with glycerol immersion using the same exposure and intensity for all images. Computational clearing (60% strength) and uniform brightness and contrast adjustments were also applied consistently across all samples. Scale bar: 100 µm.

To quantify these observations, immunofluorescence images were segmented into nuclear and cytoplasmic compartments using the machine learning-based Labkit plugin in ImageJ/Fiji (Figure 20) (Kelley et al., 2019). When all ages were combined (4–24+ weeks), nuclear HuR abundance was higher in *mdx* TA muscle fibres than in WT controls and approached statistical significance (p=0.0541). In contrast, cytoplasmic HuR abundance did not differ significantly between genotypes.

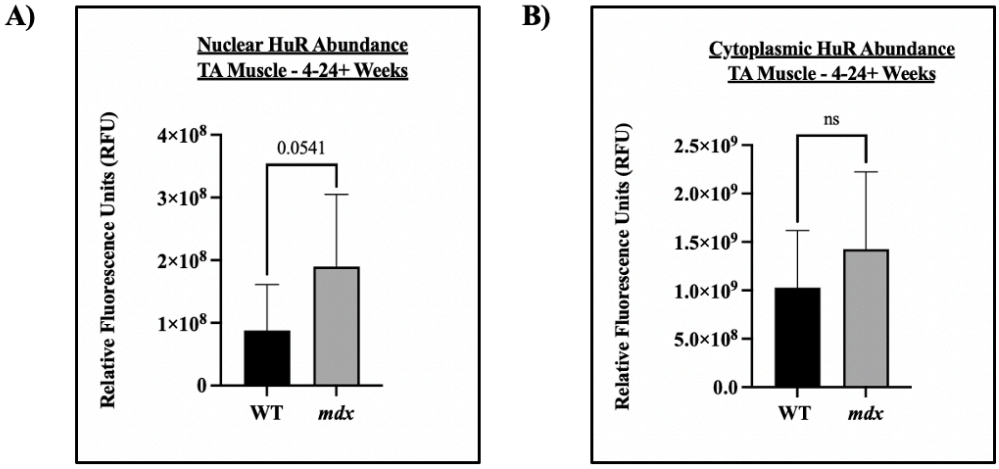


Figure 20. HuR Localization Exhibits a Strong Trend Toward Increased Nuclear Abundance in *mdx* TA Muscle. Panel A shows the quantification of nuclear HuR abundance, and panel B depicts the cytoplasmic HuR abundance (both representing integrated density in RFU) from the tibialis anterior (TA) muscle cross-sections from Wild-type (WT) and *mdx* mice aged 4-24+ weeks. Measurements from 2-3 cross-sectional images per mouse were averaged prior to statistical analysis, with a total of n=7-8 mice across all ages. Statistical analyses were performed using Mann-Whitney tests (*p < 0.05, **p < 0.01, ***p < 0.001, ****p < 0.0001, ns = not significant).

3.1.5 *Minimal HuR-Macrophage Co-localization by Immunofluorescence*

HuR immunofluorescence staining was performed in combination with the F4/80 pan-macrophage surface marker to determine whether the elevated HuR levels observed in *mdx* TA muscle from 4-24+ weeks are associated with intrinsic HuR expression within muscle fibres or influenced by macrophage infiltration (Figures 21-23) (Villalta et al., 2009). Given the well-established increase in macrophage presence in dystrophic muscle, this approach enabled simultaneous evaluation of HuR localization and macrophage distribution within the same tissue sections (Rosenberg et al., 2015; Tripodi et al., 2021).

4 weeks

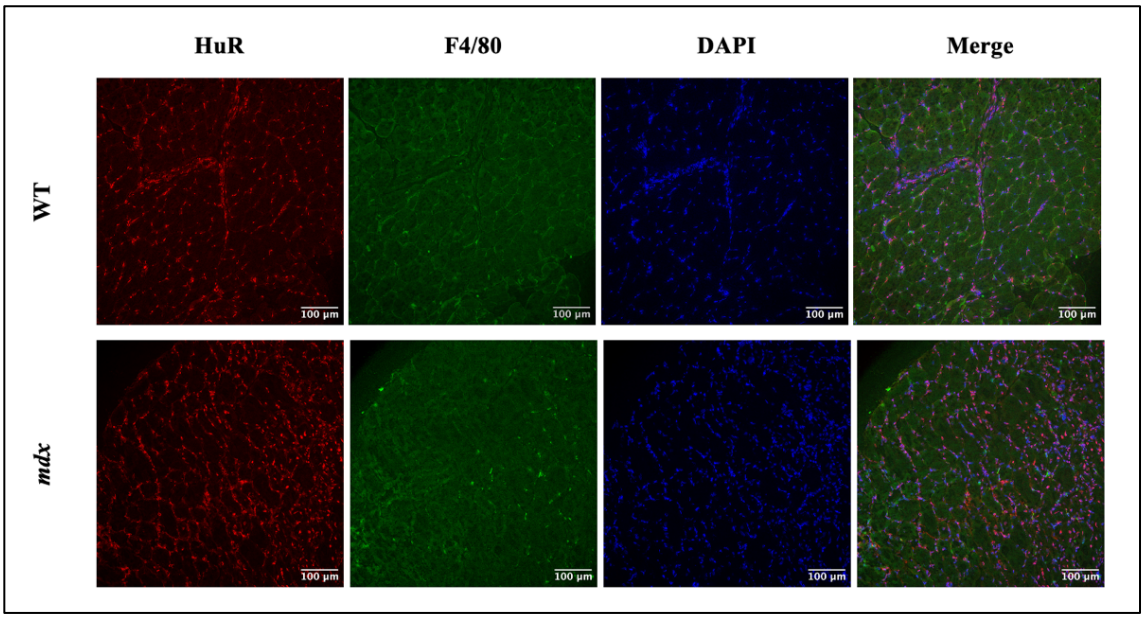


Figure 21. HuR Signal Shows Limited Co-Localization with Macrophages at 4 Weeks in *mdx* TA Muscle. Representative HuR and macrophage surface marker F4/80 immunofluorescence images in tibialis anterior (TA) muscle cross-sections from 4-week-old Wild-type (WT; top) and *mdx* (bottom) mice. HuR is shown in red, F4/80-positive macrophages in green, and nuclei are counterstained with DAPI (blue). Images were acquired using a Leica Thunder microscope at 40× magnification (numerical aperture 1.25) with glycerol immersion using the same exposure and intensity for all images. Computational clearing (60% strength) and uniform brightness and contrast adjustments were also applied consistently across all samples. Scale bar: 100 µm.

8 weeks

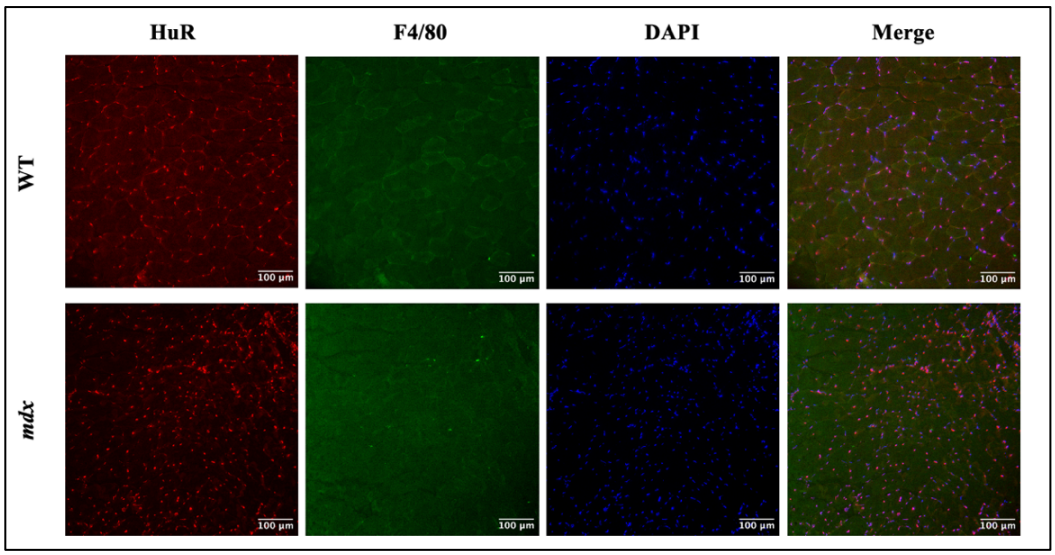


Figure 22. HuR Signal Shows Limited Co-Localization with Macrophages at 8 Weeks in *mdx* TA Muscle. Representative HuR and macrophage surface marker F4/80 immunofluorescence images in tibialis anterior (TA) muscle cross-sections from 8-week-old Wild-type (WT; top) and *mdx* (bottom) mice. HuR is shown in red, F4/80-positive macrophages in green, and nuclei are counterstained with DAPI (blue). Images were acquired using a Leica Thunder microscope at 40× magnification (numerical aperture 1.25) with glycerol immersion using the same exposure and intensity for all images. Computational clearing (60% strength) and uniform brightness and contrast adjustments were applied consistently across all samples. Scale bar: 100 µm.

24 weeks

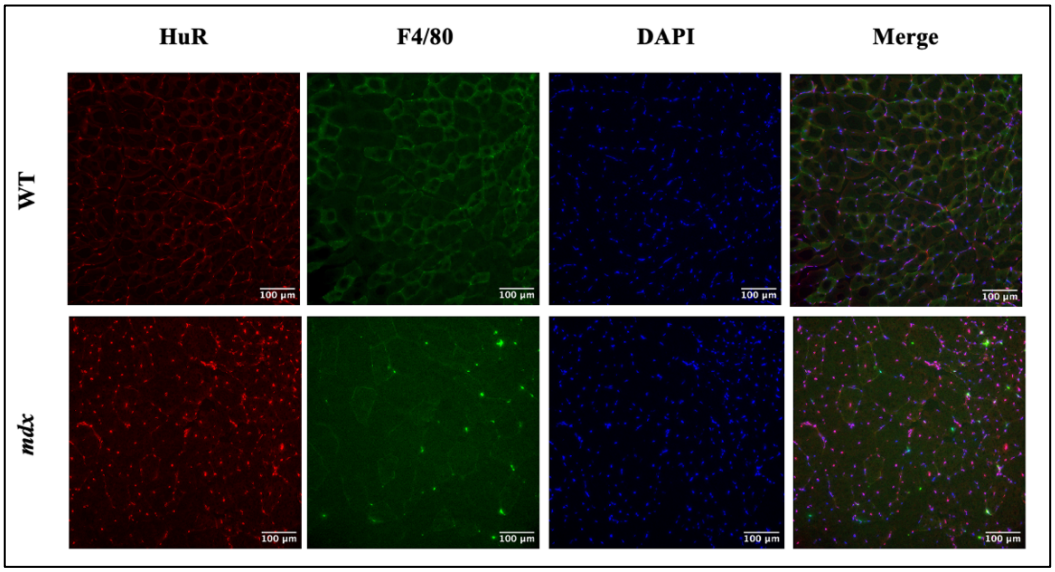


Figure 23. HuR Signal Shows Limited Co-Localization with Macrophages at 24+ Weeks in *mdx* TA Muscle. Representative HuR and macrophage surface marker F4/80 immunofluorescence images in tibialis anterior (TA) muscle cross-sections from 24+ week-old Wild-type (WT; top) and *mdx* (bottom) mice. HuR is shown in red, F4/80-positive macrophages in green, and nuclei are counterstained with DAPI (blue). Images were acquired using a Leica Thunder microscope at 40× magnification (numerical aperture 1.25) with glycerol immersion using the same exposure and intensity for all images. Computational clearing (60% strength) and uniform brightness and contrast adjustments were also applied consistently across all samples. Scale bar: 100 µm.

To assess the contribution of macrophages to total HuR expression, the percentage of F4/80-expressing macrophages to total nuclei was calculated. Additionally, macrophage-associated HuR expression was also computed as the percentage of HuR-expressing macrophages (Mac^{HuR}) to HuR-expressing nuclei (Nuc^{HuR}). Macrophage infiltration was increased in *mdx* TA muscle relative to WT controls ($p<0.001$) (Figure 24). Despite this, HuR-positive macrophages accounted for a small fraction of the total HuR-positive nuclei. This indicates that infiltrating macrophages contribute minimally to overall nuclear HuR expression, accounting for only 2.85% of total HuR-positive nuclei and are therefore unlikely to represent the primary source of the elevated HuR localization observed in *mdx* muscle ($p<0.01$).

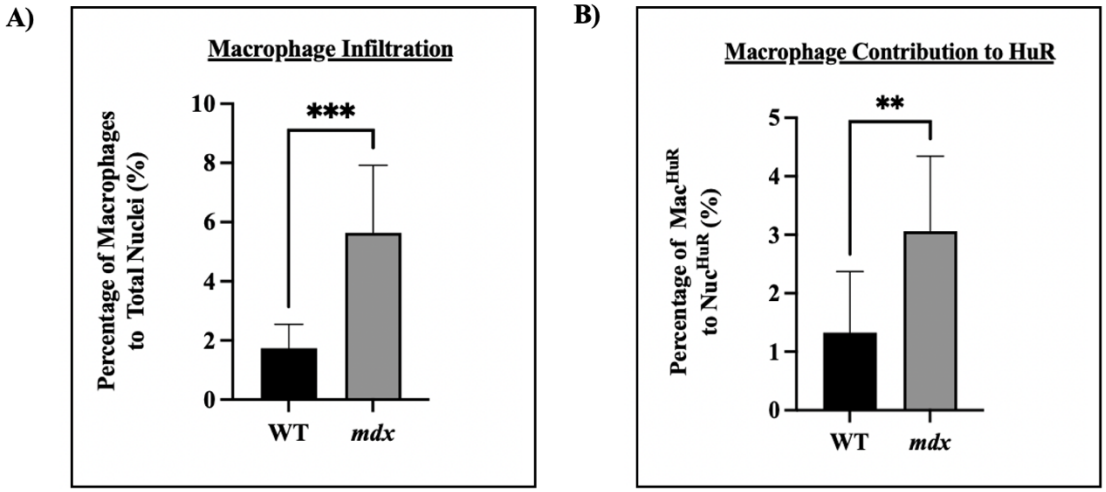


Figure 24. Macrophages Contribute Minimally to Total Nuc^{HuR} Despite Increased Infiltration in *mdx* TA Muscle. Panel A depicts macrophage infiltration expressed as a percentage of total nuclei in Wild-type (WT) and *mdx* TA muscle across all ages. Panel B shows the percentage of macrophages expressing HuR (Mac^{HuR}) relative to the total nuclei expressing HuR (Nuc^{HuR}). Statistical analyses were completed using Mann-Whitney tests for n = 2- 3 mice per age group from 4- 24+ weeks (*p< 0.05, **p< 0.01, ***p< 0.001, ****p<0.0001, ns = not significant).

3.2 The Impact of HuR Knockdown on the Organization of the Post-synaptic Membrane in *mdx* Muscle

3.2.1 *HuR Knockdown Normalizes Elevated HuR Protein Levels in mdx Muscle*

Building on the observed upregulation of HuR in *mdx* muscle, we next investigated whether targeted reduction of HuR would improve the structure of the post-synaptic apparatus. A recombinant AAV expressing a short-hairpin RNA targeting HuR (shHuR) was used to reduce HuR expression, while an AAV expressing a short-hairpin RNA directed against luciferase (shLuc) served as a non-targeting control to account for potential effects of viral transduction (Ji et al., 2020; Manini et al., 2022; Moore et al., 2010; Zincarelli et al., 2008). Following AAV-shHuR administration, confirmation of this knockdown was necessary to ensure that any observed changes in post-synaptic membrane morphology and downstream molecular outcomes could be directly attributed to reduced HuR expression. To this end, western blot analysis was performed, and results demonstrated an approximate 2.5-fold reduction (or 60%) in HuR protein expression in the shHuR-injected TA muscle relative to the contralateral shLuc-injected TA muscle (Figure 25, $p<0.01$). HuR levels following shHuR treatment were comparable in magnitude to those previously measured in WT TA muscle during the initial characterization phase of this project (Figure 12); however, these measurements were obtained from separate Western blot experiments, as WT mice were not included in the HuR knockdown experiments.

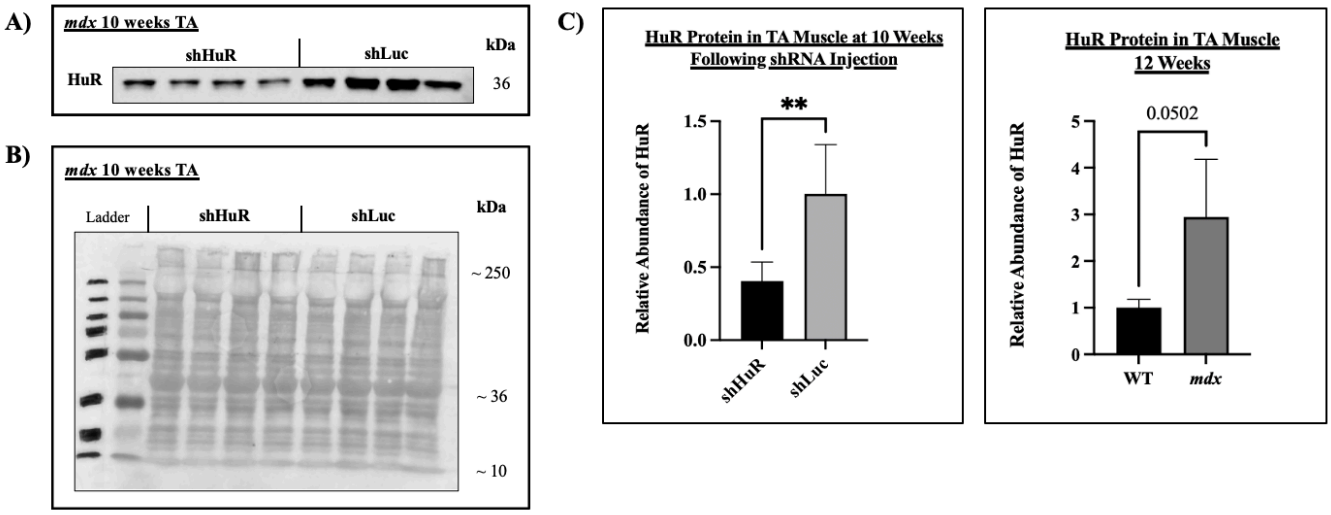


Figure 25. AAV-Mediated HuR Knockdown Significantly Reduces HuR Protein Expression in *mdx* TA Muscle. Panel A displays representative chemiluminescent western blots of HuR expression in tibialis anterior (TA) muscle from 10-week-old *mdx* mice following injection with short-hairpin HuR (shHuR) or short-hairpin luciferase (shLuc). Panel B shows the corresponding total protein staining using Ponceau. Panel C presents the quantitative analysis of HuR protein abundance. The left graph in panel C shows a significant reduction in HuR protein levels after shHuR treatment compared with shLuc controls, while the right graph in this panel is included as a reference and shows the elevated HuR protein abundance in *mdx* TA muscle compared with WT controls at 12 weeks of age, first presented in Figure 12. Data are presented as relative protein abundance normalized to total protein (n=4, 2-3 independent trials). Statistical analyses were conducted using unpaired t-tests (where *$p < 0.05$, **$p < 0.01$, ***$p < 0.001$, ****$p < 0.0001$, ns = not significant).

3.2.2 *HuR Knockdown Partially Improved Endplate Morphology in mdx Muscle*

Having confirmed successful HuR knockdown by western blotting, the effects of reduced HuR expression on post-synaptic endplate morphology were examined next. Representative endplates from shLuc-injected and shHuR-treated muscles exhibited varying degrees of structural organization and fragmentation and were subsequently classified under blinded assessment (Figure 26). Qualitatively, endplates from shHuR-treated muscle appeared more compact and structurally intact, while shLuc-injected post-synaptic membranes more frequently exhibited extensive fragmentation and dispersed AChR clusters. Additionally, WT non-injected endplates and WT shLuc-injected endplates were also included in these analyses to serve as references for normal endplate morphology and to assess potential effects associated with AAV delivery independent of HuR knockdown, respectively.

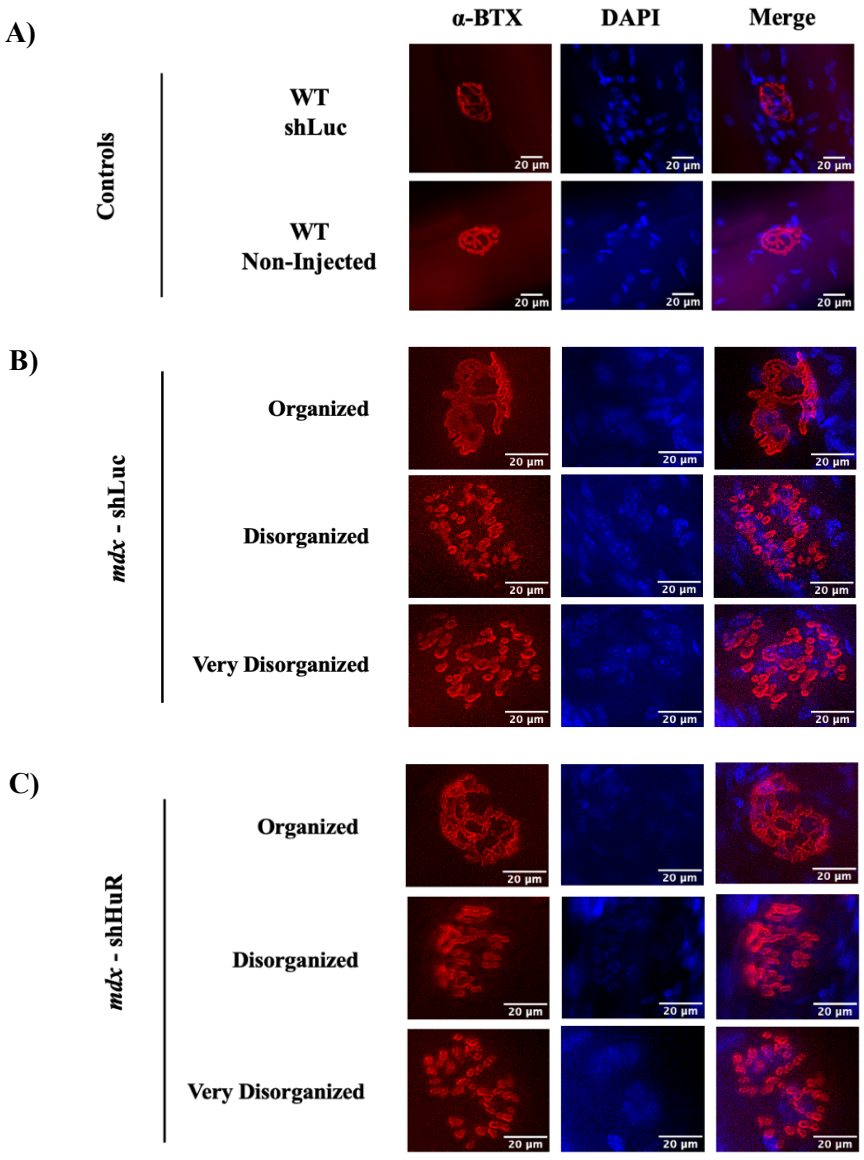


Figure 26. Representative Images of Post-synaptic Endplates in Non-Injected or shLuc-injected WT Mice and *mdx* Mice Injected with either shLuc or shHuR. All endplates were obtained from the tibialis anterior (TA) muscle and stained with α-bungarotoxin (α-BTX; red) to label the α-subunit of the acetylcholine receptor (AChR) and DAPI (blue) to label nuclei. Panel A shows endplates from WT mice injected with Adeno-Associated Virus (AAV)-shLuc (top) or age-matched non-injected Wild-type (WT) controls (bottom). Images in Panel A were acquired using a Zeiss microscope at 20× magnification (numerical aperture 0.8). Panels B and C show endplates from 10-week-old *mdx* mice collected 4 weeks following intramuscular injection with short-hairpin luciferase (shLuc; Panel B) or short-hairpin HuR (shHuR; Panel C). Images in Panels B and C were acquired using a Leica Thunder microscope at 40× magnification under glycerol immersion (numerical aperture 1.25) using the same exposure and intensity for all images. Computational clearing (60% strength) and uniform brightness and contrast adjustments were also applied consistently across all samples. Scale bar: 20 µm.

3.2.3 *Blinded NMJ Scoring Reveals Fewer Severely Disorganized Endplates Following HuR Knockdown*

Earlier analyses of WT and *mdx* TA muscle identified substantial abnormalities in post-synaptic endplate morphology, with dystrophic endplates exhibiting increased fragmentation and disruption of the characteristic pretzel-like endplate morphology. After confirming successful HuR knockdown, the post-synaptic apparatus was re-examined to assess whether reduced HuR expression influenced these structural abnormalities (Figure 27). Endplates were first analyzed using blinded morphological classification, followed by quantitative measurements (Osseni et al., 2020, 2022). Relative to untreated *mdx* muscle, shLuc-injected endplates exhibited a modest increase in the proportion of disorganized endplates and a corresponding reduction in very disorganized endplates. shHuR knockdown further shifted endplate morphology toward the disorganized category, with a greater proportion of endplates classified as disorganized and fewer classified as very disorganized compared with both *mdx* and shLuc controls. The proportion of organized endplates remained low and did not differ significantly between groups. In contrast, the proportion of disorganized endplates was significantly greater in shHuR-treated muscle than in both shLuc-injected ($p< 0.01$) and untreated *mdx* muscle ($p<0.001$), whereas the proportion of very disorganized endplates was significantly reduced relative to both shLuc-injected ($p<0.01$) and untreated *mdx* muscle ($p<0.0001$). These findings indicate that HuR knockdown altered endplate morphology distribution, primarily by reducing the frequency of very disorganized endplates and shifting them toward disorganized endplates.

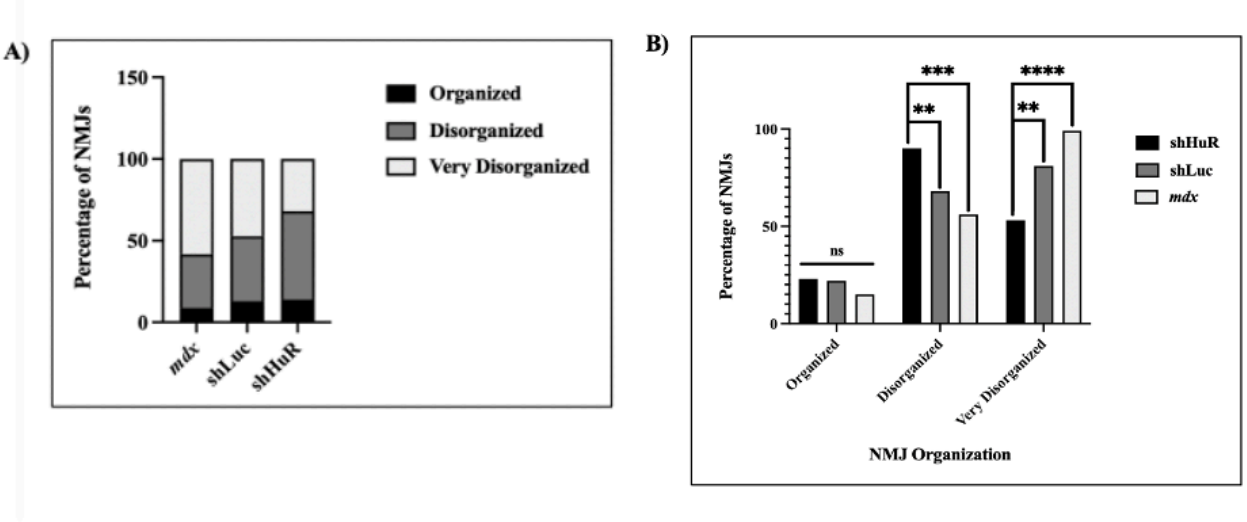


Figure 27. HuR Knockdown Partially Improves Endplate Organization in *mdx* TA Muscle. Panel A illustrates the distribution of neuromuscular junction (NMJ) phenotype scores (organized, disorganized, very disorganized) in non-injected *mdx*, short-hairpin Luciferase (shLuc), and short-hairpin HuR (shHuR) injected muscles. Panel B represents the quantification of NMJ endplate morphology, demonstrating a significant reduction in highly disorganized NMJs and a corresponding shift toward disorganized NMJs in shHuR-treated muscle compared to controls. NMJ endplates were randomized and classified using a blinded scoring system (1-3), where 1 indicates organized morphology, and 3 indicates very disorganized morphology. Statistical significance was determined through post hoc comparisons using Fisher's exact test for n=3 mice per condition and 40-50 NMJ endplates examined per mouse per condition (*p< 0.05, **p< 0.01, ***p< 0.001, ****p< 0.0001, ns = not significant).

To complement the blinded morphological classification, AChR compactness was quantified as an objective measure of post-synaptic endplate organization (Figure 28). Compactness was calculated as the proportion of the total endplate area occupied by AChRs, with higher values reflecting greater AChR clustering and a more structurally intact post-synaptic apparatus (Jones et al., 2016; Minty et al., 2020). Compactness was significantly increased in shLuc-injected muscle relative to untreated *mdx* controls ($p<0.01$). HuR knockdown further increased compactness, with shHuR-treated endplates exhibiting greater compactness than shLuc-injected controls ($p<0.05$). Overall, compactness was significantly higher in shHuR-treated muscle compared with untreated *mdx* muscle ($p<0.0001$), suggesting that HuR knockdown reduced the AChR dispersion typically observed in *mdx* endplates and promoted a more organized post-synaptic apparatus.

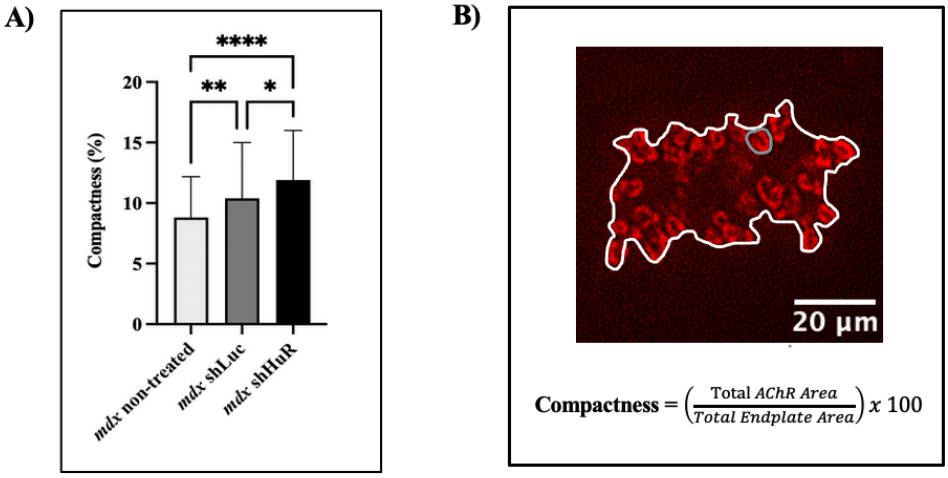


Figure 28. Quantification of AChR Compactness Following HuR Knockdown in *mdx* TA Muscle at 10 Weeks. Panel A presents quantification of endplate compactness (%), demonstrating a significant increase in short-hairpin (shHuR) injected muscle compared to short-hairpin-Luciferase (shLuc) and *mdx* controls. Panel B shows a representative endplate used to quantify acetylcholine receptor (AChR) compactness. Compactness was calculated as the ratio of the total AChR area (inner grey outline) to the total endplate area (outer white outline) × 100, where higher values indicate a more compact post-synaptic endplate. Statistical analyses were completed using an ordinary one-way ANOVA with multiple comparisons for n = 3 mice per group (*p< 0.05, **p< 0.01, ***p< 0.001, ****p<0.0001, ns = not significant). Scale bar: 20 µm.

3.3 The Pharmacological Treatment of *mdx* Mice to Modulate the Expression and Localization of HuR in Muscle

After observing that HuR expression is elevated in *mdx* muscle and that AAV-mediated HuR knockdown partially improves post-synaptic membrane organization, we next examined whether HuR expression could be decreased pharmacologically to produce similar effects. The experimental rationale was based, in part, on our initial interpretation that elevated HuR expression in *mdx* muscle was associated with increased cytoplasmic HuR localization in dystrophic muscle fibres relative to WT controls. Vorinostat (SAHA) was selected based on evidence from cancer models showing that HDAC inhibition can alter HuR localization and reduce its cytoplasmic abundance (Pryzbylkowski et al., 2008). Furthermore, Vorinostat has previously shown beneficial effects in skeletal muscle in a mouse model of Myotonic Dystrophy type 1 (DM1), including improvements in disease-associated splicing abnormalities and muscle histopathology (Neault et

al., 2023). In addition, HDAC inhibition increases protein acetylation, a post-translational modification that can influence protein interactions, stability, and localization; as HuR undergoes dynamic nucleocytoplasmic shuttling, changes in its acetylation status may therefore influence its intracellular distribution and function (Grammatikakis et al., 2017; Schultz et al., 2020). For these reasons, Vorinostat or the corresponding vehicle control (DMSO, HPβCD, and saline) was administered to *mdx* mice by intraperitoneal injection using a treatment regimen adapted from Neault et al. (2023). Vorinostat treatment was hypothesized to reduce overall HuR protein abundance and its presumed cytoplasmic localization in dystrophic muscle, with potential effects on post-synaptic endplate organization (Allegri et al., 2018; Kim et al., 2011; Natarajan et al., 2021; Osseni et al., 2022; Pryzbylkowski et al., 2008).

3.3.1 *Grip Strength Following Vorinostat-Treated mdx Mice*

First, we evaluated functional outcomes following Vorinostat treatment by examining whole-body weight and muscle function in *mdx* mice. Body weight was monitored weekly, and grip strength was measured in both forelimbs and all limbs following treatment. This was not done prior to the vehicle and Vorinostat injections due to administrative constraints. Analysis revealed no significant difference in grip strength between *mdx* mice receiving Vorinostat and those receiving vehicle control. Additionally, body weight increased slightly over the treatment period in all groups, with no significant differences observed between them (Figure 29).

A)

	Initial Weight (g)	Final Weight (g)
***mdx* vehicle**	27.63	28.35
***mdx* Vorinostat**	32.90	33.18

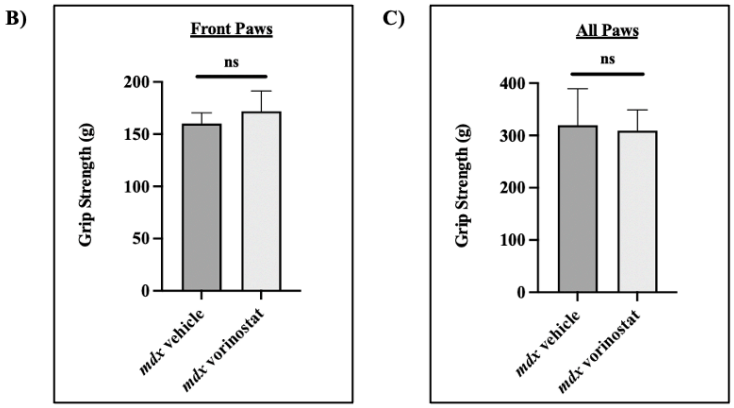


Figure 29. Body Weight and Grip Strength in Vehicle- and Vorinostat-injected *mdx* Mice. Whole-body weight and functional assessments are shown for the vehicle-injected and Vorinostat-treated groups. Mice were weighed weekly, and grip strength in the forelimbs and all limbs was measured 24 hours after the final dose. Statistical analyses were completed using unpaired t-tests for n = 3 (*p< 0.05, **p< 0.01, ***p< 0.001, ****p<0.0001, ns = not significant).

3.3.2 *Post-Synaptic Organization Following Vorinostat Treatment in mdx Mice*

Next, we examined the effects of Vorinostat on post-synaptic membrane organization in TA muscles from vehicle-injected and Vorinostat-treated *mdx* mice, with representative endplates shown in Figure 30. Similar examples of organized, disorganized, and very disorganized endplates were observed in both groups of mice, with no noticeable qualitative differences in endplate structure/organization.

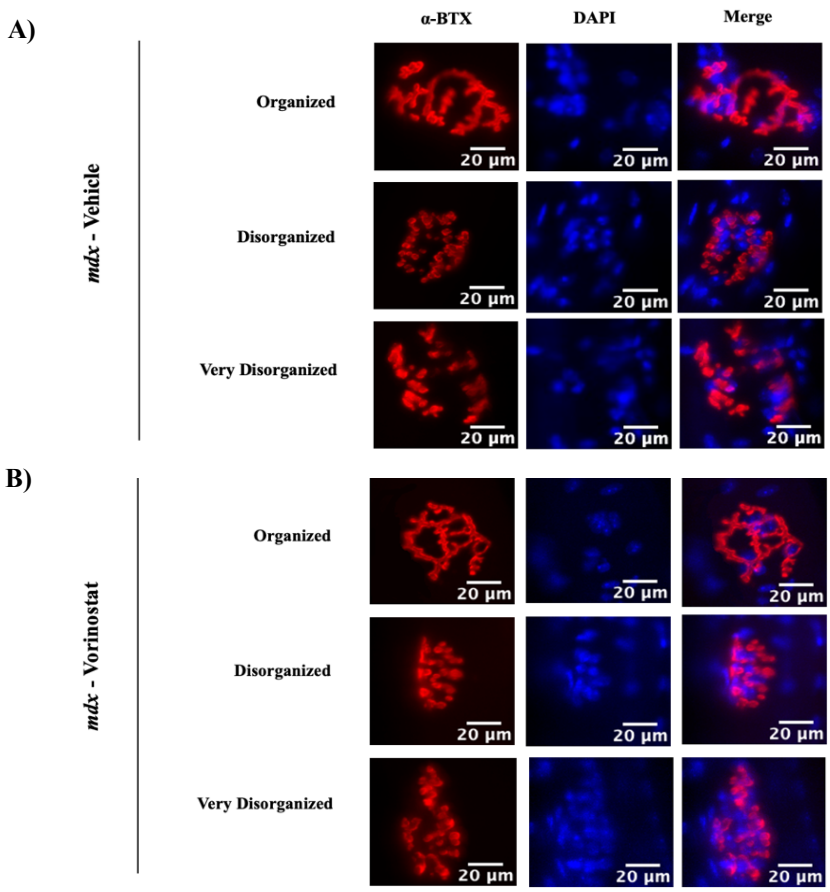


Figure 30. Organization of the Post-Synaptic Apparatus in *mdx* TA Muscle Following Vorinostat Treatment. Representative images of neuromuscular junction (NMJ) endplates from the tibialis anterior (TA) muscle of 17–20-week-old *mdx* mice, 4 weeks following daily intraperitoneal injection with either vehicle (Panel A) or Vorinostat (Panel B). The α-subunit of the acetylcholine receptor (AChR) was labelled using α-bungarotoxin conjugated to Alexa Fluor 594 (red), and nuclei were counterstained with DAPI (blue). Images were acquired using a Zeiss microscope at 20× magnification (numerical aperture 0.8). Brightness and contrast were adjusted uniformly across all samples. Scale bar: 20 µm.

Similarly, blinded assessment of post-synaptic membrane morphology demonstrated no significant difference in endplate organization between Vorinostat- and vehicle- injected *mdx* muscle (Figure 31). Although Vorinostat-treated muscles exhibited a strong trend toward fewer disorganized post-synaptic endplates ($p=0.059$), this change was not associated with a corresponding increase in organized endplates, and the overall distribution of endplate phenotypes remained comparable between treatment groups. Overall, no significant differences in post-synaptic endplate organization were detected between the groups under the conditions examined.

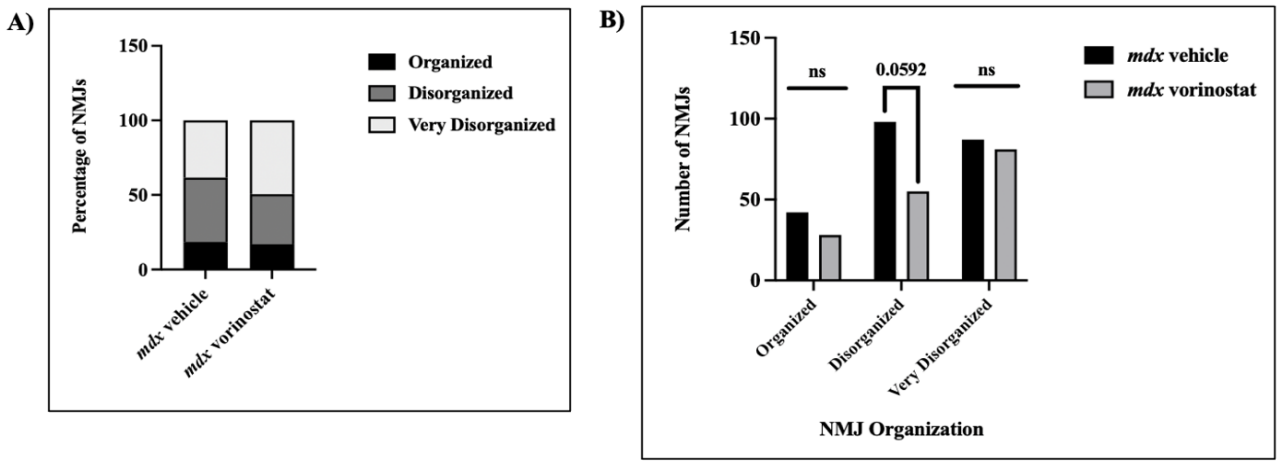


Figure 31. Endplate Organization in *mdx* Muscle Following Vorinostat Treatment. Panel A exhibits the distribution of neuromuscular (NMJ) endplate phenotype scores (organized, disorganized, very disorganized) in vehicle-injected and Vorinostat-treated *mdx* mice. Panel B shows the quantification of post-synaptic membrane organization, with no significant differences observed between groups; however, a trend toward a reduced proportion of disorganized NMJs was noted in Vorinostat-treated muscle. Endplates were classified using a blinded scoring system (1-3), where 1 represents organized morphology, and 3 represents very disorganized morphology. Statistical analyses were conducted using post hoc comparisons with Fisher's exact test for n=3 (*p< 0.05, **p< 0.01, ***p< 0.001, ****p< 0.0001, ns = not significant). The data in both panels were produced by Dr. Lola Lessard.

3.3.3 *HuR Protein Expression and Localization Following Vorinostat Treatment*

As HuR protein expression was elevated in *mdx* muscle and Vorinostat was hypothesized to influence its regulation through acetylation-dependent mechanisms, HuR protein abundance was evaluated in the EDL and SOL muscles following treatment. Western blot analysis revealed a non-significant trend toward reduced HuR protein expression in EDL muscle relative to vehicle-injected controls, while insufficient sample availability in the SOL precluded statistical analysis (Figures 32-33).

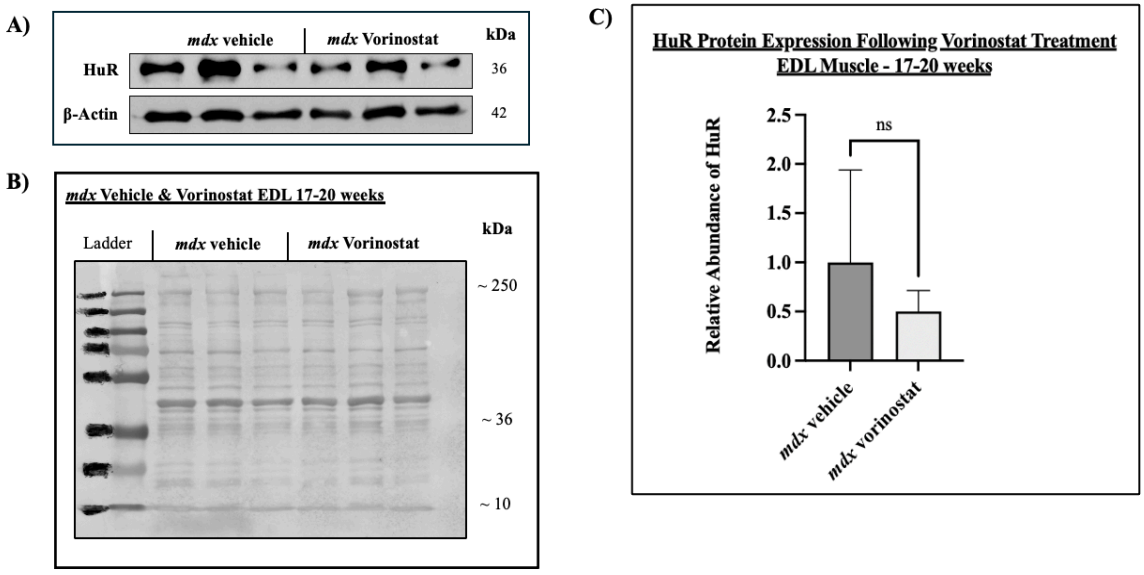


Figure 32. HuR Protein Levels in Vehicle-Injected and Vorinostat-Treated *mdx* EDL Muscle. Panel A exhibits representative chemiluminescent Western blot images of HuR expression in vehicle-injected and Vorinostat-treated *mdx* extensor digitorum longus (EDL) muscle. Panel B displays the corresponding total protein staining (Ponceau), and Panel C shows quantification of HuR protein levels after normalization to total protein. Statistical analyses were completed using unpaired t-tests for n = 3 mice over 2-3 independent trials (*p< 0.05, **p< 0.01, ***p< 0.001, ****p<0.0001, ns = not significant).

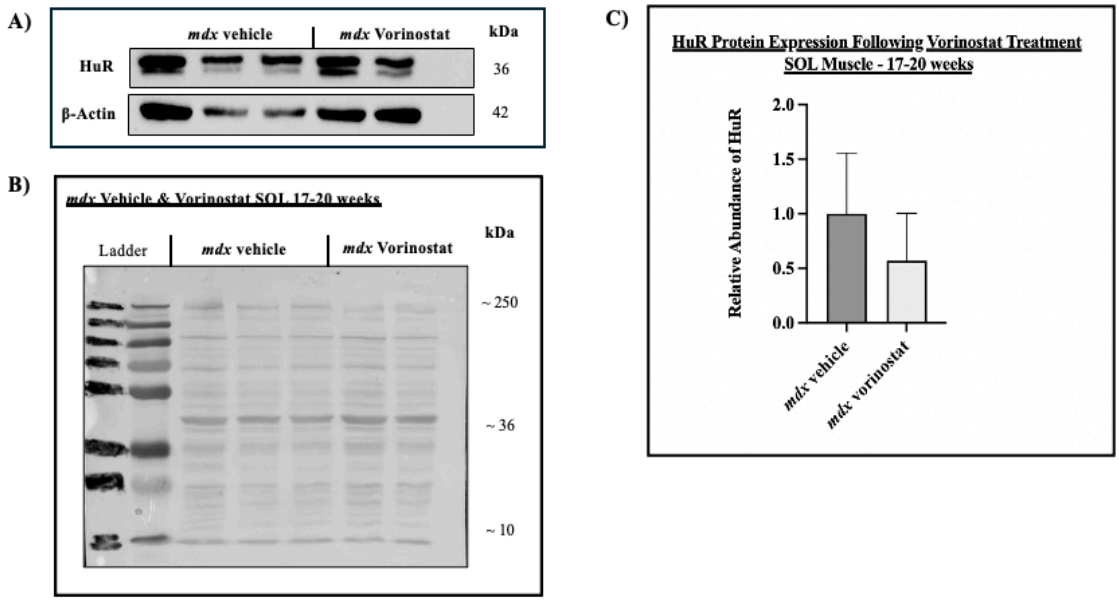


Figure 33. HuR Protein Expression in Vehicle-Injected and Vorinostat-Treated *mdx* SOL Muscle. Panel A shows representative chemiluminescent Western blot images of HuR expression in vehicle-injected and Vorinostat-treated *mdx* soleus (SOL) muscle. Panel B presents the corresponding total protein staining (Ponceau), and Panel C shows quantification of HuR protein levels, normalized to total protein, for n = 2-3 mice across 2-3 independent trials.

Next, immunofluorescence analyses were conducted to assess HuR localization in *mdx* TA muscle fibre cross-sections (Figure 34). In both vehicle-injected and Vorinostat-treated mice, HuR exhibited a similar pattern of nuclear and cytoplasmic localization, with no obvious differences observed following treatment. Similarly, laminin staining enabled the visualization of muscle fibre morphology and the characteristic variation in fibre size associated with dystrophic pathology (Watkins et al., 1982).

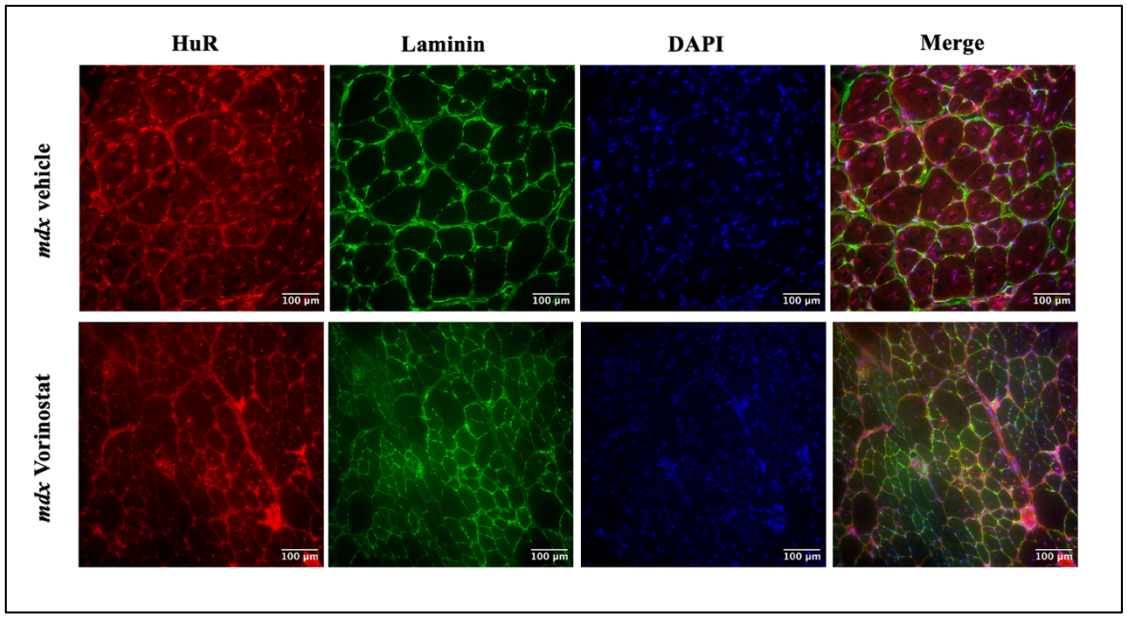


Figure 34. HuR Localization Following Vorinostat Treatment in *mdx* TA Muscle Fibre Cross-Sections. Representative immunofluorescence images of tibialis anterior (TA) muscle from *mdx* vehicle-injected (top) and *mdx* Vorinostat-treated (bottom) mice. HuR was detected using a 3A2 primary antibody (red), laminin delineated muscle fibre boundaries (green), and nuclei were counterstained with DAPI (blue). Images were acquired using a Leica Thunder microscope at 40× magnification (numerical aperture 1.25) with glycerol immersion using the same exposure and intensity for all images. Computational clearing (60% strength) and uniform brightness and contrast adjustments were also applied consistently across all samples. Scale bar: 100 µm.

Quantification of cytoplasmic HuR abundance and concentration showed that they were relatively lower in Vorinostat-treated *mdx* muscle relative to vehicle-injected controls, but neither measurement reached statistical significance. Nevertheless, both parameters exhibited a similar downward trend ($p=0.20$) following treatment (Figure 35). The nuclear-to-cytoplasmic (N/C) ratio was subsequently examined as a measure of HuR's intracellular distribution between nuclear and cytoplasmic compartments, with values >1 indicating predominantly nuclear localization. No

significant difference in N/C ratio was detected between vehicle-injected and Vorinostat-treated mice, as N/C ratios remained >1 in both groups, indicating that HuR retained predominantly nuclear localization regardless of treatment. In general, no significant differences in HuR abundance or subcellular localization were detected between Vorinostat- and vehicle-injected groups in *mdx* TA muscle.

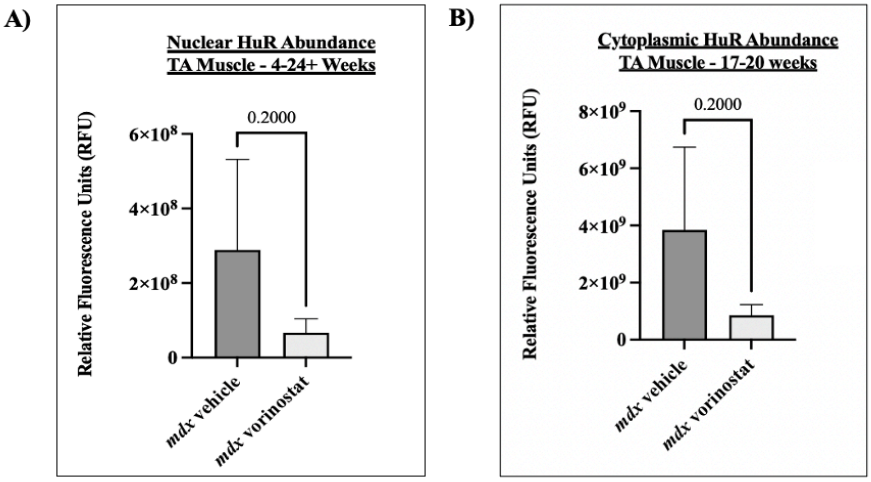


Figure 35. Quantification of Nuclear and Cytoplasmic HuR Abundance following Vorinostat Treatment in *mdx* TA Muscle. Panel A shows the total nuclear HuR abundance, while Panel B depicts the total cytoplasmic HuR abundance after quantification in vehicle-injected and Vorinostat-treated *mdx* mice following 28 days of treatment. Measurements obtained from 2-3 cross-sectional images were averaged for each mouse (for an n of 3 per group) prior to statistical analysis. Statistical analyses were performed using Mann-Whitney tests for n = 3 (*p< 0.05, **p< 0.01, ***p< 0.001, ****p<0.0001, ns = not significant).

3.3.4 *No Significant Effects on Tubulin Acetylation After Vorinostat Treatment in mdx Muscle*

Lastly, to assess HDAC inhibition following Vorinostat treatment, acetylated tubulin levels were measured in EDL and SOL muscles following treatment and normalized to α-tubulin levels. HDACs mediate the deacetylation of α-tubulin, and inhibition of HDAC activity is expected to increase the abundance of acetylated tubulin (de Ruijter et al., 2003; Hubbert et al., 2002). Acetylated tubulin was therefore assessed as a marker of HDAC inhibition and microtubule stabilization within the treated muscles (Osseni et al., 2020). However, no significant differences in acetylated tubulin abundance were detected between Vorinostat-and vehicle-injected groups in either muscle (Figures 36-37).

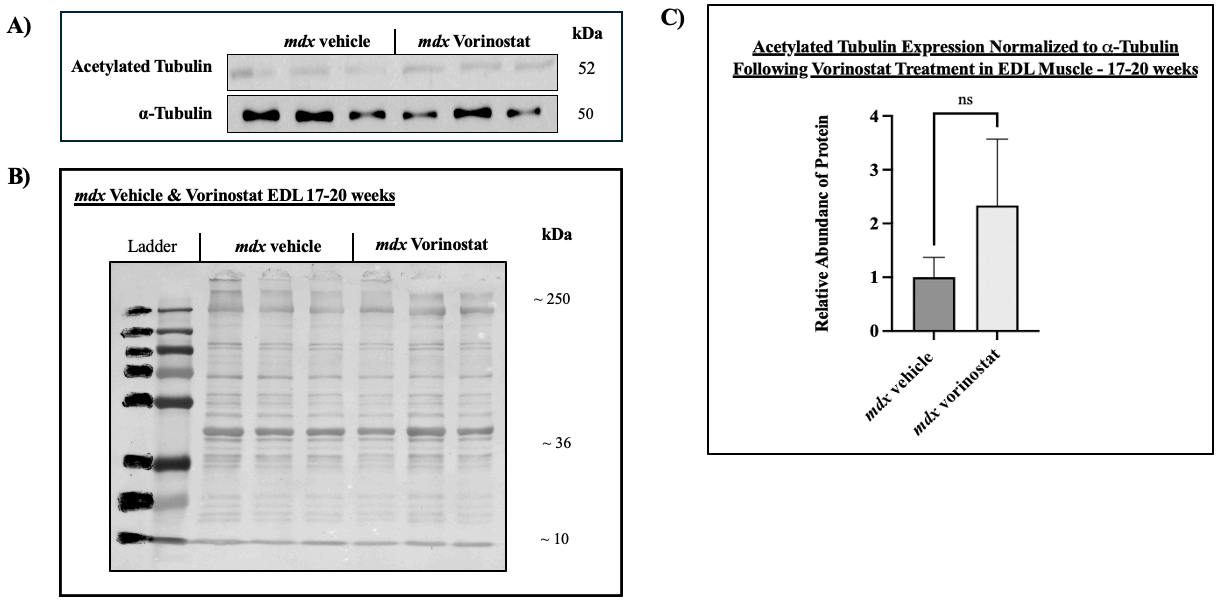


Figure 36. Acetylated Tubulin Levels in the EDL Muscles of Vehicle- and Vorinostat-injected *mdx* mice. Panel A presents representative Western blot images of acetylated tubulin normalized to α-tubulin in vehicle-injected and Vorinostat-treated *mdx* extensor digitorum longus (EDL) muscle. Panel B shows the corresponding total protein staining (Ponceau), and Panel C depicts the quantification of acetylated tubulin normalized to α-tubulin. Statistical analyses were completed using unpaired t-tests for n = 3 mice over 2-3 independent trials (*p< 0.05, **p< 0.01, ***p< 0.001, ****p<0.0001, ns = not significant).

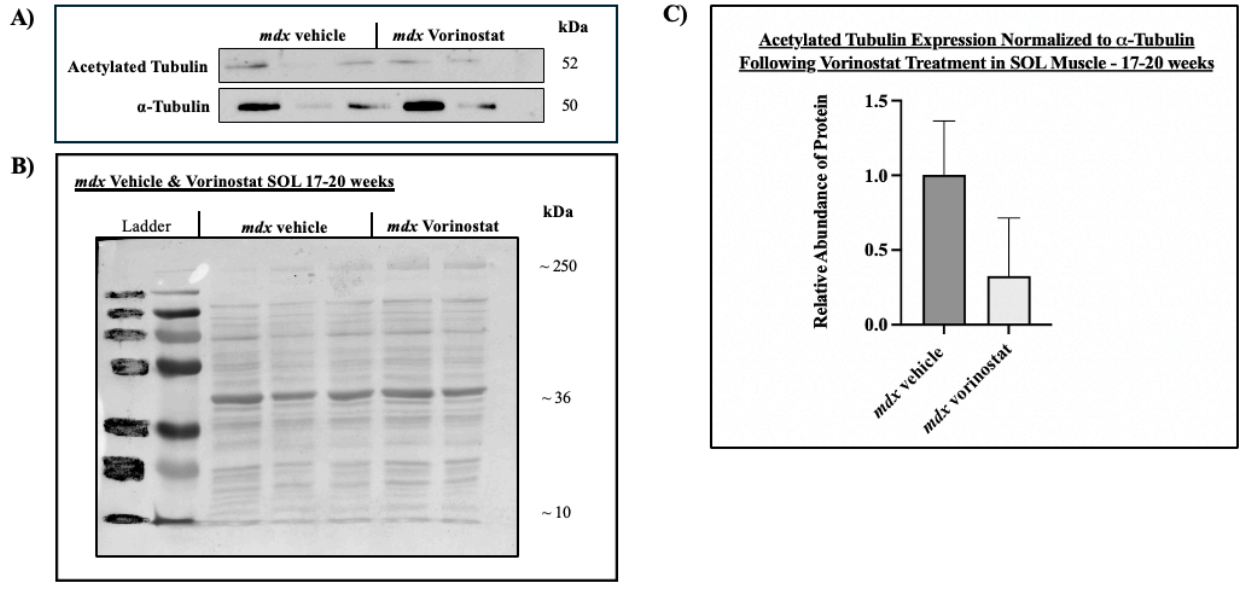


Figure 37. Acetylated Tubulin Levels in the SOL Muscles of Vehicle- and Vorinostat-injected *mdx* mice. Panel A shows representative Western blot images of acetylated tubulin normalized to α-tubulin in vehicle-injected and Vorinostat-treated *mdx* soleus (SOL) muscle. Panel B shows the corresponding total protein staining (Ponceau), and Panel C presents quantification of acetylated tubulin, normalized to α-tubulin, for n=2-3 mice across 2 independent trials.

Chapter 4 - Discussion

This project's primary aim was to characterize the role of the RBP HuR in the post-synaptic membrane of the NMJ in *mdx* mice. First, we confirmed that *mdx* mice exhibit an extensively more disorganized post-synaptic apparatus than WT controls, accompanied by significantly elevated HuR protein levels across multiple muscles and ages. HuR was also found to be predominantly localized to the nucleus in *mdx* muscle, while macrophages represented only a small fraction of HuR expression. These findings suggest that the increased HuR abundance observed in dystrophic muscle primarily reflects changes occurring within the muscle fibres rather than infiltrating inflammatory cells. Notably, AAV-mediated HuR knockdown restored HuR protein levels to those observed in WT control levels and partially improved post-synaptic endplate morphology, as evidenced by increased AChR compactness relative to shLuc-injected and non-injected *mdx* mice. Lastly, pharmacological treatment of *mdx* mice with the HDAC inhibitor Vorinostat resulted in non-significant reductions in HuR expression with no improvement in the morphology of the post-synaptic apparatus in dystrophic fibres. However, non-significant changes in acetylated tubulin levels across the EDL and SOL muscles were also seen, indicating insufficient HDAC inhibition following Vorinostat treatment, which may have contributed to the limited effects observed. Collectively, these findings show that HuR expression is dysregulated in dystrophic muscle and suggest its possible involvement in the disorganization of the post-synaptic apparatus observed in *mdx* mice.

4.1 NMJ Disorganization as a Central Pathological Feature in DMD

We first confirmed that the post-synaptic membrane of NMJs in *mdx* mice exhibits significant disorganization relative to WT controls, consistent with previous reports (Harriman, 1976; Pratt et al., 2015b). These endplate abnormalities reflect the absence of dystrophin, which

binds to the DGC at the sarcolemma, anchors the internal cytoskeleton to the external ECM of the muscle fibre, and stabilizes the post-synaptic membrane (Figueroa et al., 2003; van der Giessen et al., 2007). As such, NMJs are strikingly fragmented, with abnormal post-synaptic folding and nerve terminal sprouting seen in all DMD mouse models and patients with DMD (Banks et al., 2009; Jerusalem et al., 1974; Lyons et al., 1991; Shiao, 2004). These structural defects impair neuromuscular transmission efficiency, exacerbating muscle weakness and contributing to a progressive decline in contractile performance (Banks et al., 2009; Shiao, 2004). These findings validated substantial post-synaptic membrane abnormalities in dystrophic muscle and provided the rationale for investigating HuR as a potential regulator of endplate organization.

4.2 Elevated HuR Protein Expression in Dystrophic Muscle

Consistent increases in HuR protein expression across multiple *mdx* muscles and disease stages suggest that HuR dysregulation is a prominent feature of dystrophic skeletal muscle. Such sustained elevation may reflect the chronic degenerative and regenerative environment characteristic of DMD, in which sources of cellular stress (such as metabolic or mechanical stress) also persist throughout disease progression (Duan et al., 2021). As a regulator of mRNA stability, HuR has been well established in promoting the expression of several transcripts involved in these processes (Figueroa et al., 2003; van der Giessen et al., 2007; von Roretz et al., 2011). Thus, upregulated HuR expression in *mdx* muscle may represent an adaptive response to support the continuous regenerative demands imposed by chronic muscle damage (Chang et al., 2023). Other mechanisms that could contribute to the increased HuR protein observed in dystrophic muscle include altered post-translational regulation of HuR, wherein modifications such as phosphorylation enhance its stability, localization, and function (Grammatikakis et al., 2017). Additionally, microRNAs (miRNAs), including miR-519, miR-125a, and miR-16, can suppress

HuR protein production (Srikantan et al., 2012b), raising the possibility that changes in miRNA-mediated regulation could also contribute to HuR elevation in dystrophic muscle.

Moreover, the extent of HuR upregulation seemed to vary among muscle types, with fast-twitch muscles (TA and EDL) generally showing greater increases in HuR expression than slow-twitch muscles (SOL and DIA) (Table 1). However, these observations should be interpreted as descriptive trends rather than as evidence of muscle-type-specific differences in HuR expression, as statistical comparisons between muscle types and fibre-type analyses within specific muscles were not performed. Differences among muscle types likely reflected the distinct metabolic and contractile properties of individual muscle groups and their differential susceptibility to dystrophic pathology (Talbot et al., 2016). Fast-twitch glycolytic fibres are known to be more susceptible to degeneration in DMD due to their greater force-generating capacity and increased susceptibility to contraction-induced mechanical damage (Talbot et al., 2016; Webster et al., 1988). HuR has also previously been implicated in promoting glycolytic type II fibre formation, raising the possibility that elevated HuR expression may preferentially associate with fast-twitch fibre types that are particularly susceptible to dystrophic degeneration in DMD (Janice Sánchez et al., 2019). Moreover, age-dependent differences in HuR expression were more apparent with greater HuR upregulation in *mdx* mice relative to WT controls at earlier time points (4 weeks) than at later ones (24+ weeks). This finding may reflect the pronounced regenerative activity that characterizes the early stages of disease progression in *mdx* muscle, when myofibre degeneration is particularly active (Pastoret et al., 1995; Turk et al., 2005).

4.3 HuR Localization Remains Largely Nuclear in Dystrophic Skeletal Muscle

Subcellular localization is a key determinant of HuR function, with many post-transcriptional regulatory activities occurring after translocation from the nucleus to the cytoplasm

(von Roretz et al., 2011). Accordingly, the chronic regenerative environment characteristic of dystrophic muscle was expected to favour increased cytoplasmic localization of HuR, particularly within newly regenerated fibres (Duan et al., 2021, Figueroa et al., 2003). Increased cytoplasmic HuR would be consistent with its established role in promoting the stability and translation of transcripts involved in myogenesis and adaptive stress responses (Figueroa et al., 2003; van der Giessen et al., 2007; von Roretz et al., 2011). Contrary to this expectation, subcellular fractionation analyses revealed that elevated HuR expression in *mdx* TA muscle at 11 weeks was predominantly nuclear, suggesting that increased HuR expression alone is insufficient to drive cytoplasmic accumulation in dystrophic muscle. This finding also indicates that the mechanisms regulating HuR abundance and subcellular distribution may be independently dysregulated, potentially through alterations in HuR nucleocytoplasmic trafficking, impaired or absent signalling pathways that promote nuclear export, post-translational modifications favouring nuclear retention, and/or dysregulated stress-response signalling mechanisms (Beauchamp et al., 2010; Kim et al., 2008; von Roretz et al., 2011). Further, increased nuclear HuR may reflect enhanced regulation of transcripts associated with myogenesis or cellular stress responses characteristic of dystrophic muscle. Given that HuR's function is highly dependent on its subcellular localization (Grammatikakis et al., 2017), the preferential nuclear accumulation observed in *mdx* muscle may also alter the repertoire of transcripts subject to HuR-mediated regulation (Srikantan et al., 2012a). In summary, these results imply that changes in HuR intracellular distribution may contribute to its dysregulation in dystrophic muscle and influence its regulatory activity independently of overall protein abundance.

To determine whether this localization pattern extended beyond the single time point examined by subcellular fractionation, HuR distribution was further assessed by

immunofluorescence in the TA muscle across the disease course (4-24+ weeks). Consistent with the fractionation findings, HuR remained predominantly nuclear in both WT and *mdx* muscle fibres. Although HuR abundance was higher in *mdx* muscle in both the nuclear and cytoplasmic compartments, only modest, non-significant increases in cytoplasmic HuR abundance were observed relative to WT controls. Taken together, these data show that elevated HuR expression in dystrophic muscle remains predominantly nuclear throughout disease progression, despite the chronic cellular stress characteristic of DMD, which is often associated with cytoplasmic HuR localization (Figueroa et al., 2003; von Roretz et al., 2011). Thus, this nuclear localization pattern warrants further investigation.

4.4 Contribution of Immune Cells to Elevated HuR Expression

Chronic inflammation is a defining feature of DMD and contributes substantially to disease progression (Bez Batti Angulski et al., 2023). Since the loss of dystrophin compromises myofibre stability, it results in repeated contraction-induced injury and the release of damage-associated molecular patterns (DAMPs), which activate innate immune signalling pathways within skeletal muscle (Rosenberg et al., 2015; Tripodi et al., 2021). This promotes persistent recruitment of inflammatory cells, including neutrophils and macrophages, along with sustained elevations in pro-inflammatory cytokines such as IL-6 (Tulangekar, 2021). Rather than resolving following injury, inflammatory signalling becomes chronically activated in dystrophic muscle, impairing effective tissue repair and contributing to progressive fibrosis and muscle degeneration (Rosenberg et al., 2015; Tripodi et al., 2021).

Given that HuR is a stress-responsive RBP, it is known to regulate the stability of numerous inflammatory and stress response-associated transcripts (e.g., cytokines, interleukins, p21, p53, etc.). As such, it was important to determine whether the elevated HuR expression observed in

mdx muscle originated primarily from infiltrating immune cells or from the muscle fibres themselves (Govindaraju et al., 2013; Srikantan et al., 2012a). To address this, co-localization analyses were performed using HuR and the macrophage surface marker F4/80. Minimal overlap between HuR and macrophage staining was observed, indicating that F4/80-positive macrophages accounted for only a small proportion of HuR-positive nuclei. This finding suggests that the elevated HuR expression in dystrophic muscle is unlikely to be due to inflammatory cell infiltration. Instead, chronic dystrophic stress within muscle fibres themselves may contribute to sustained HuR accumulation, potentially through activation of stress-responsive pathways, such as the p38 MAPK pathway (Lafarga et al., 2009).

4.5 Genetic and Pharmacological Modulation of HuR Expression and Localization and Their Effects on Post-Synaptic Morphology

Despite the consistent elevation of HuR expression in dystrophic muscle, its contribution to disease pathology remained unclear. Previous studies have demonstrated that HuR is involved in the post-transcriptional regulation of transcripts involved in post-synaptic maintenance (Deschênes-Furry et al., 2005; Joassard et al., 2015; Karmouch et al., 2020). This led us to hypothesize that HuR dysregulation may contribute to the endplate abnormalities characteristic of DMD. Accordingly, HuR expression was reduced in *mdx* TA muscle using rAAV2/9-mediated shRNA delivery to evaluate its effects on dystrophic endplate pathology. The partial improvement in endplate morphology observed following HuR knockdown suggests that elevated HuR expression may contribute to processes underlying post-synaptic disorganization rather than functioning solely as a marker of dystrophic pathology. In particular, the subsequent increase in AChR compactness following HuR reduction indicated that HuR dysregulation may contribute to the fragmentation and dispersion of post-synaptic receptor clusters characteristic of dystrophic

muscle. As AChR compactness reflects the structural integrity and organization of the post-synaptic apparatus, improvements in compactness may also indicate enhanced stabilization of receptor clusters and reduced pathological remodelling of the endplate (Osseni et al., 2020). The limited nature of this improvement, however, suggests that HuR likely represents one component of a broader network of molecular alterations contributing to defects in post-synaptic membrane organization. Nevertheless, HuR knockdown partially improves post-synaptic organization, supporting a role for HuR in regulating endplate morphology and identifying HuR as a potential contributor to dystrophic endplate pathology.

As a pharmacological approach, Vorinostat was evaluated as an indirect strategy to reduce HuR expression and modulate its localization through HDAC inhibition. HDAC inhibitors have demonstrated beneficial effects in dystrophic muscle, while acetylation has been shown to influence HuR activity and subcellular localization in other disease contexts, including DM1 and cancer (Consalvi et al., 2013; Grammatikakis et al., 2017; Neault et al., 2023; Pryzbylkowski et al., 2008). These observations raised the possibility that Vorinostat could influence HuR function in dystrophic muscle and potentially alter the post-transcriptional regulation of transcripts involved in endplate organization (Glozak et al., 2005; Joassard et al., 2015; Wang et al., 2004). In addition to its potential effects on HuR, Vorinostat was expected to improve post-synaptic morphology through mechanisms involving microtubule acetylation, as HDAC6 inhibition promotes AChR cluster stability and improves endplate morphology in dystrophic muscle (Osseni et al., 2020, 2022). No significant differences were noted in HuR expression, localization, or post-synaptic morphology between the Vorinostat- and vehicle-injected groups; however, acetylated tubulin levels were also unchanged, suggesting that adequate HDAC inhibition may not have been achieved (Hubbert et al., 2002; Osseni et al., 2020, 2022). Therefore, the absence of effects on

HuR and post-synaptic morphology may reflect insufficient HDAC inhibition rather than a lack of biological efficacy. Overall, direct genetic reduction of HuR improved post-synaptic organization, while the effects of indirect HuR modulation with Vorinostat remain unclear.

4.6 Limitations

A few limitations should be considered when interpreting the findings of this project. First, subcellular fractionation was only performed in the TA muscle at 11 weeks. While immunofluorescence analyses revealed a strong trend toward increased nuclear HuR abundance in dystrophic muscle when data were compiled across ages, it remains unknown whether similar alterations in HuR localization are present across muscles other than the TA. Future studies incorporating additional muscle types and ages, using subcellular fractionation, would help determine the extent to which preferential nuclear HuR localization is conserved throughout disease progression.

In addition, although AAV-mediated HuR knockdown partly improved post-synaptic endplate morphology, AChR compactness was also increased in shLuc-injected muscles compared to untreated *mdx* controls. This finding suggests that factors independent of HuR knockdown may have contributed to the observed changes in endplate organization. Intramuscular AAV administration can potentially induce local muscle injury, regeneration, inflammatory responses, and tissue remodelling, all of which may affect endplate morphology independently of the shRNA sequence (Muraine et al., 2020; Tasfaout et al., 2018). Moreover, it is also possible that some of the changes observed in shLuc-treated muscle were related to shRNA expression itself. Exogenous shRNAs are processed by the endogenous RNA interference machinery and, at adequate expression levels, may compete with endogenous factors involved in miRNA production or function, potentially altering the expression of non-target genes (Grimm et al., 2006; Isenmann et

al., 2023). Thus, both vector-associated effects and nonspecific consequences of shRNA expression may have influenced the differences observed between shLuc-treated and untreated *mdx* muscles. Nevertheless, the greater improvement observed following shHuR treatment relative to shLuc supports a contribution of HuR reduction to partial improvement in post-synaptic organization. Future studies incorporating saline-injected, empty-vector, and wild-type controls would help distinguish the effects of intramuscular injection, vector delivery, and shRNA expression from those attributable to HuR reduction. These controls were not included in the present study because of time constraints and difficulty breeding sufficient numbers of *mdx* mice.

Moreover, interpretation of the Vorinostat experiments should consider the lack of a measurable increase in acetylated tubulin following treatment as a notable limitation. Although no differences were detected in HuR expression, localization, or post-synaptic organization, the absence of increased tubulin acetylation makes it unclear whether these negative findings reflect a true lack of involvement of HDAC-dependent pathways in dystrophic endplate pathology or insufficient HDAC inhibition under the treatment conditions employed in this project (Hubbert et al., 2002; Osseni et al., 2020, 2022; Neault et al., 2023). Despite this, the absence of significant improvements following Vorinostat treatment does not rule out the possibility that alternative HDAC inhibitor approaches to HuR modulation may influence endplate organization in dystrophic muscle and remains to be studied.

Lastly, the *mdx* mouse model represents an important limitation of this project. Though the *mdx* mouse is among the most widely used models of DMD, it exhibits a considerably milder disease phenotype and a longer lifespan than DMD patients, largely due to its robust regenerative capacity, which partially compensates for ongoing muscle degeneration (McGreevy et al., 2015). Consequently, pathological features such as severe fibrosis, scoliosis, and cardiomyopathy

develop later and are generally less pronounced than those observed in human disease (McGreevy et al., 2015). These differences may limit the extent to which the alterations in HuR expression, localization, and NMJ morphology identified in *mdx* muscle reflect the pathological mechanisms underlying DMD in human patients. While alternative models such as the D2.mdx mouse display more severe early disease manifestations, including extensive muscle necrosis and fibrosis, they also fail to fully recapitulate the progressive nature of DMD, with certain pathological features seemingly resolving with age (Aartsma-Rus et al., 2023; McGreevy et al., 2015).

4.7 Future Directions

The present findings suggest that HuR upregulation contributes to post-synaptic endplate disorganization in dystrophic muscle; however, the molecular mechanisms underlying this effect remain unclear. Future studies should therefore investigate the downstream mRNA targets and signalling pathways regulated by HuR in skeletal muscle to determine how HuR dysregulation contributes to endplate abnormalities. This could be achieved using approaches such as ribonucleoprotein immunoprecipitation (RIP) and cross-linking immunoprecipitation (CLIP), coupled with transcriptomic analyses, thereby enabling the identification of transcripts associated with or directly bound by HuR (Li et al., 2014; Tenenbaum et al., 2000; Ule et al., 2003). Such studies may further clarify HuR's role in regulating post-synaptic organization and provide mechanistic insight into the endplate abnormalities observed in DMD.

Another important future direction would be to cross *mdx* mice with muscle-specific HuR knockout mice and assess the long-term effects of this HuR knockout on post-synaptic endplate organization. While rAAV-mediated HuR knockdown demonstrated that reducing HuR expression partially improves endplate morphology, this approach was localized to a single muscle and achieved only partial reduction of HuR expression. In contrast, a muscle-specific HuR knockout

model would permit sustained reduction of HuR throughout skeletal muscle, allowing its contribution to disease progression to be evaluated across multiple muscles and disease stages. Evaluating endplate morphology in dystrophic mice lacking HuR specifically in skeletal muscle would also help determine whether the improvements observed following AAV-mediated knockdown are sustained over time, further elucidating the role of HuR at dystrophic endplates.

Moreover, despite AAV-mediated HuR knockdown partially improving post-synaptic endplate morphology, it remains unclear whether these structural improvements translate into enhanced neuromuscular function. Future studies should therefore aim to incorporate functional assessments of neuromuscular performance, including measurements of nerve-evoked muscle responses, synaptic transmission efficiency, muscle fatigability, and ex vivo muscle contractile assays (Rozand et al., 2015; Zanetti et al., 2018). Given that alterations in post-synaptic endplate abnormalities have been implicated in impaired neuromuscular transmission, reduced force production, and safety factor in dystrophic muscle, such functional testing would provide important insight into whether HuR contributes to disease progression beyond its partial effects on endplate organization (Personius et al., 2006; Wood et al., 1997).

The lack of evidence for effective HDAC inhibition in this study highlights the need to further optimize pharmacological approaches targeting HDAC-regulated pathways to modulate HuR. Accordingly, Vorinostat's effects on HuR expression, localization, endplate morphology, and grip strength remain inconclusive. Future studies should optimize dosing, treatment duration, and routes of administration to achieve more effective HDAC inhibition. In addition, evaluation of isoform-specific HDAC inhibitors may help clarify whether the lack of response observed with Vorinostat reflects the broad nature of pan-HDAC inhibition. As individual HDAC isoforms regulate distinct aspects of skeletal muscle homeostasis, microtubule dynamics, and NMJ maintenance, selective

inhibition may provide greater therapeutic specificity than broad-spectrum HDAC inhibition (Bertoldi et al., 2025; de Ruijter et al., 2003; Tian et al., 2020). For example, the HDAC6-selective inhibitor Tubastatin A has been shown to increase α-tubulin acetylation and improve post-synaptic endplate organization in dystrophic muscle, highlighting the value of investigating individual HDAC isoforms in greater detail (Osseni et al., 2022). Moreover, small-molecule inhibitors of HuR, including MS-444 and Pyrvinium Pamoate, may provide an alternative approach for directly targeting HuR activity, as these compounds disrupt HuR function by inhibiting HuR nucleocytoplasmic shuttling or interfering with HuR-mRNA interactions (Blanco et al., 2016; Chae et al., 2009; Guo et al., 2016; Schultz et al., 2020). Direct pharmacological inhibition of HuR would be a valuable approach to further define the molecular pathways linking HuR upregulation to post-synaptic endplate disorganization in *mdx* mice.

Finally, examining post-synaptic endplate morphology, as well as HuR expression and localization, in skeletal muscle biopsies from DMD patients and D2.mdx mice across disease progression would be an important next step in validating the translational relevance of these findings (Aartsma-Rus et al., 2023). These studies would help determine whether the alterations in HuR expression observed in *mdx* muscle are conserved across multiple DMD models and in human disease. Further, assessing the relationship between HuR dysregulation, age, and endplate abnormalities could improve understanding of HuR's contribution to post-synaptic defects and its potential as a therapeutic target in DMD.

4.8 Conclusion

The primary objective of this thesis was to characterize the role of HuR in the post-synaptic membrane of *mdx* mice and determine whether HuR influences endplate organization in DMD. The results support the central hypothesis that HuR contributes to the molecular mechanisms underlying

post-synaptic membrane defects, showing that HuR is dysregulated in dystrophic muscle and that its reduction can partially improve endplate morphology. More broadly, these results highlight the importance of considering post-transcriptional regulatory mechanisms when investigating endplate abnormalities in DMD and support a partial role for HuR in regulating post-synaptic apparatus organization.

Works Cited

Aartsma-Rus, A., van Putten, M., Mantuano, P., & De Luca, A. (2023). On the use of D2.B10-Dmdmdx/J (D2.mdx) Versus C57BL/10ScSn-Dmdmdx/J (mdx) Mouse Models for Preclinical Studies on Duchenne Muscular Dystrophy: A Cautionary Note from Members of the TREAT-NMD Advisory Committee on Therapeutics. *Journal of Neuromuscular Diseases*, *10*(1), 155–158. https://doi.org/10.3233/JND-221547

Abdelmohsen, K. (2010). Posttranscriptional regulation of cancer traits by HuR. *Wiley Interdisciplinary Reviews. RNA*, *1*(2), 214–229. https://doi.org/10.1002/wrna.4

Abdelmohsen, K., Kuwano, Y., Kim, H. H., & Gorospe, M. (2008). *Posttranscriptional gene regulation by RNA-binding proteins during oxidative stress: Implications for cellular senescence*. *389*(3), 243–255. https://doi.org/10.1515/BC.2008.022

Abdel-Salam, E., Abdel-Meguid, I., & Korraa, S. S. (2009). Markers of degeneration and regeneration in Duchenne muscular dystrophy. *Acta Myologica: Myopathies and Cardiomyopathies: Official Journal of the Mediterranean Society of Myology*, *28*(3), 94–100.

Akaaboune, M., Culican, S. M., Turney, S. G., & Lichtman, J. W. (1999). Rapid and reversible effects of activity on acetylcholine receptor density at the neuromuscular junction in vivo. *Science*, *286*(5439), 503–507. https://doi.org/10.1126/science.286.5439.503

Allegri, L., Mio, C., Russo, D., Filetti, S., & Baldan, F. (2018). Effects of HuR downregulation on anaplastic thyroid cancer cells. *Oncology Letters*, *15*(1), 575–579. https://doi.org/10.3892/ol.2017.7289

Alvarez-Suarez, P., Gawor, M., & Prószyński, T. J. (2020). Perisynaptic schwann cells—The multitasking cells at the developing neuromuscular junctions. *Seminars in Cell &*

Developmental Biology, Differentiation of Skeletal Muscles, *104*, 31–38. https://doi.org/10.1016/j.semcdb.2020.02.011

Amirouche, A., Tadesse, H., Lunde, J. A., Bélanger, G., Côté, J., & Jasmin, B. J. (2013). Activation of p38 signaling increases utrophin A expression in skeletal muscle via the RNA-binding protein KSRP and inhibition of AU-rich element-mediated mRNA decay: Implications for novel DMD therapeutics. *Human Molecular Genetics*, *22*(15), 3093–3111. https://doi.org/10.1093/hmg/ddt165

An, M. C., Lin, W., Yang, J., Dominguez, B., Padgett, D., Sugiura, Y., Aryal, P., Gould, T. W., Oppenheim, R. W., Hester, M. E., Kaspar, B. K., Ko, C.-P., & Lee, K.-F. (2010). Acetylcholine negatively regulates development of the neuromuscular junction through distinct cellular mechanisms. *Proceedings of the National Academy of Sciences of the United States of America*, *107*(23), 10702–10707. https://doi.org/10.1073/pnas.1004956107

Angus, L. M., Chakkalakal, J. V., Méjat, A., Eibl, J. K., Bélanger, G., Megeney, L. A., Chin, E. R., Schaeffer, L., Michel, R. N., & Jasmin, B. J. (2005). Calcineurin-NFAT signaling, together with GABP and peroxisome PGC-1{alpha}, drives utrophin gene expression at the neuromuscular junction. *American Journal of Physiology. Cell Physiology*, *289*(4), C908-917. https://doi.org/10.1152/ajpcell.00196.2005

Apponi, L. H., Corbett, A. H., & Pavlath, G. K. (2011). RNA-binding proteins and gene regulation in myogenesis. *Trends in Pharmacological Sciences*, *32*(11), 652–658. https://doi.org/10.1016/j.tips.2011.06.004

Baker, R. W. (2016). Chaperoning SNARE assembly and disassembly. *Nature Reviews. Molecular Cell Biology*, *17*(8), 465–479. https://doi.org/10.1038/nrm.2016.65

Banks, G. B., Chamberlain, J. S., & Froehner, S. C. (2009). Truncated dystrophins can influence neuromuscular synapse structure. *Molecular and Cellular Neuroscience*, *40*(4), 433–441. https://doi.org/10.1016/j.mcn.2008.12.011

Barbosa-Morais, N. L., Irimia, M., Pan, Q., Xiong, H. Y., Gueroussov, S., Lee, L. J., Slobodeniuc, V., Kutter, C., Watt, S., Colak, R., Kim, T., Misquitta-Ali, C. M., Wilson, M. D., Kim, P. M., Odom, D. T., Frey, B. J., & Blencowe, B. J. (2012). The evolutionary landscape of alternative splicing in vertebrate species. *Science*, *338*(6114), 1587–1593. https://doi.org/10.1126/science.1230612

Barik, A., Lu, Y., Sathyamurthy, A., Bowman, A., Shen, C., Li, L., Xiong, W., & Mei, L. (2014). LRP4 is critical for neuromuscular junction maintenance. *The Journal of Neuroscience: The Official Journal of the Society for Neuroscience*, *34*(42), 13892–13905. https://doi.org/10.1523/JNEUROSCI.1733-14.2014

Beauchamp, P., Nassif, C., Hillock, S., van der Giessen, K., von Roretz, C., Jasmin, B. J., & Gallouzi, I.-E. (2010). The cleavage of HuR interferes with its transportin-2-mediated nuclear import and promotes muscle fiber formation. *Cell Death & Differentiation*, *17*(10), 1588–1599. https://doi.org/10.1038/cdd.2010.34

Belaya, K., Finlayson, S., Slater, C. R., Cossins, J., Liu, W. W., Maxwell, S., McGowan, S. J., Maslau, S., Twigg, S. R. F., Walls, T. J., Pascual Pascual, S. I., Palace, J., & Beeson, D. (2012). Mutations in DPAGT1 cause a limb-girdle congenital myasthenic syndrome with tubular aggregates. *American Journal of Human Genetics*, *91*(1), 193–201. https://doi.org/10.1016/j.ajhg.2012.05.022

Belhasan, D. C., Akaaboune, M. (2020). The role of the dystrophin glycoprotein complex on the neuromuscular system. *Neuroscience Letters*, *722*, 134833. https://doi.org/10.1016/j.neulet.2020.134833

Belotti, E. (2020). Regulation of Gene expression at the neuromuscular Junction. *Neuroscience Letters*, *735*, 135163. https://doi.org/10.1016/j.neulet.2020.135163

Bergamin, E., Hallock, P. T., Burden, S. J., & Hubbard, S. R. (2010). The cytoplasmic adaptor protein Dok7 activates the receptor tyrosine kinase MuSK via dimerization. *Molecular Cell*, *39*(1), 100–109. https://doi.org/10.1016/j.molcel.2010.06.007

Bertoldi, M., Albamonte, E., Bello, L., D'amico, A., Masson, R., Nigro, V., Pane, M., Panicucci, C., Sframeli, M., & Ricci, F. (2025). Histone deacetylases in Duchenne muscular dystrophy: A role in the mechanism of disease and a target for inhibition. *Clinical Epigenetics*, *18*, 9. https://doi.org/10.1186/s13148-025-02031-7

Bez Batti Angulski, A., Hosny, N., Cohen, H., Martin, A. A., Hahn, D., Bauer, J., & Metzger, J. M. (2023a). Duchenne muscular dystrophy: Disease mechanism and therapeutic strategies. *Frontiers in Physiology*, *14*, 1183101. https://doi.org/10.3389/fphys.2023.1183101

Bez Batti Angulski, Hosny, N., Cohen, H., Martin, A. A., Hahn, D., Bauer, J., & Metzger, J. M. (2023b). Duchenne muscular dystrophy: Disease mechanism and therapeutic strategies. *Frontiers in Physiology*, *14*, 1183101. https://doi.org/10.3389/fphys.2023.1183101

Bhatnagar, S. (2010). Therapeutic Targeting of Signaling Pathways in Muscular Dystrophy. *Journal of Molecular Medicine (Berlin, Germany)*, *88*(2), 155–166. https://doi.org/10.1007/s00109-009-0550-4

Birnkrant, D. J., Bushby, K., Bann, C. M., Apkon, S. D., Blackwell, A., Brumbaugh, D., Case, L. E., Clemens, P. R., Hadjiyannakis, S., Pandya, S., Street, N., Tomezsko, J., Wagner, K. R., Ward, L. M., Weber, D. R., & DMD Care Considerations Working Group. (2018). Diagnosis and management of Duchenne muscular dystrophy, part 1: Diagnosis, and neuromuscular, rehabilitation, endocrine, and gastrointestinal and nutritional management. *The Lancet. Neurology*, *17*(3), 251–267. https://doi.org/10.1016/S1474-4422(18)30024-3

Bladen, C. L., Salgado, D., Monges, S., Foncuberta, M. E., Kekou, K., Kosma, K., Dawkins, H., Lamont, L., Roy, A. J., Chamova, T., Guergueltcheva, V., Chan, S., Korngut, L., Campbell, C., Dai, Y., Wang, J., Barišić, N., Brabec, P., Lahdetie, J., … Lochmüller, H. (2015). The TREAT-NMD DMD Global Database: Analysis of More than 7,000 Duchenne Muscular Dystrophy Mutations. *Human Mutation*, *36*(4), 395–402. https://doi.org/10.1002/humu.22758

Blanco, F. F., Preet, R., Aguado, A., Vishwakarma, V., Stevens, L. E., Vyas, A., Padhye, S., Xu, L., Weir, S. J., Anant, S., Meisner-Kober, N., Brody, J. R., & Dixon, D. A. (2016). Impact of HuR inhibition by the small molecule MS-444 on colorectal cancer cell tumorigenesis. *Oncotarget*, *7*(45), 74043–74058. https://doi.org/10.18632/oncotarget.12189

Boëx, M., Messéant, J., Bauché, S., Fontaine, B., Legay, C., & Strochlic, L. (2018). Regulation of mammalian neuromuscular junction formation and maintenance by Wnt signaling. *Current Opinion in Physiology, Neuromuscular Junctions*, *4*, 88–95. https://doi.org/10.1016/j.cophys.2018.07.002

Borges, L. S., & Ferns, M. (2001). Agrin-induced phosphorylation of the acetylcholine receptor regulates cytoskeletal anchoring and clustering. *The Journal of Cell Biology*, *153*(1), 1–12. https://doi.org/10.1083/jcb.153.1.1

Borges, L. S., Yechikhov, S., Lee, Y. I., Rudell, J. B., Friese, M. B., Burden, S. J., & Ferns, M. J. (2008). Identification of a Motif in the Acetylcholine Receptor β Subunit Whose Phosphorylation Regulates Rapsyn Association and Postsynaptic Receptor Localization. *The Journal of Neuroscience*, *28*(45), 11468–11476. https://doi.org/10.1523/JNEUROSCI.2508-08.2008

Brennan, C. M., Steitz, J.A. (2001). HuR and mRNA stability. *Cellular and Molecular Life Sciences CMLS*, *58*(2), 266–277. https://doi.org/10.1007/PL00000854

Briguet, A., Ruegg, Markus (2000). The Ets Transcription Factor GABP Is Required for Postsynaptic Differentiation In Vivo. *The Journal of Neuroscience*, *20*(16), 5989–5996. https://doi.org/10.1523/JNEUROSCI.20-16-05989.2000

Cardone, N., Taglietti, V., Baratto, S., Kefi, K., Periou, B., Gitiaux, C., Barnerias, C., Lafuste, P., Pharm, F. L., Pharm, J. N., Panicucci, C., Desguerre, I., Bruno, C., Authier, F.-J., Fiorillo, C., Relaix, F., & Malfatti, E. (2023). Myopathologic trajectory in Duchenne muscular dystrophy (DMD) reveals lack of regeneration due to senescence in satellite cells. *Acta Neuropathologica Communications*, *11*(1), 167. https://doi.org/10.1186/s40478-023-01657-z

Cartaud, A., Strochlic, L., Guerra, M., Blanchard, B., Lambergeon, M., Krejci, E., Cartaud, J., & Legay, C. (2004). MuSK is required for anchoring acetylcholinesterase at the neuromuscular junction. *Journal of Cell Biology*, *165*(4), 505–515. https://doi.org/10.1083/jcb.200307164

Chae, M.-J., Sung, H. Y., Kim, E.-H., Lee, M., Kwak, H., Chae, C. H., Kim, S., & Park, W.-Y. (2009). Chemical inhibitors destabilize HuR binding to the AU-rich element of TNF-alpha mRNA. *Experimental & Molecular Medicine*, *41*(11), 824–831. https://doi.org/10.3858/emm.2009.41.11.088

Chakkalakal, J. V., & Jasmin, B. J. (2003). Localizing synaptic mRNAs at the neuromuscular junction: It takes more than transcription. *BioEssays: News and Reviews in Molecular, Cellular and Developmental Biology*, *25*(1), 25–31. https://doi.org/10.1002/bies.10205

Chakkalakal, J. V., Stocksley, M. A., Harrison, M.-A., Angus, L. M., Deschenes-Furry, J., St-Pierre, S., Megeney, L. A., Chin, E. R., Michel, R. N., & Jasmin, B. J. (2003). Expression of utrophin A mRNA correlates with the oxidative capacity of skeletal muscle fiber types and is regulated by calcineurin/NFAT signaling. *Proceedings of the National Academy of Sciences of the United States of America*, *100*(13), 7791–7796. https://doi.org/10.1073/pnas.0932671100

Chamberlain, J. R., & Chamberlain, J. S. (2017). Progress toward Gene Therapy for Duchenne Muscular Dystrophy. *Molecular Therapy: The Journal of the American Society of Gene Therapy*, *25*(5), 1125–1131. https://doi.org/10.1016/j.ymthe.2017.02.019

Chan, M. C., Rowe, G. C., Raghuram, S., Patten, I. S., Farrell, C., & Arany, Z. (2014). Post-natal induction of PGC-1α protects against severe muscle dystrophy independently of utrophin. *Skeletal Muscle*, *4*(1), 2. https://doi.org/10.1186/2044-5040-4-2

Chang, M., Cai, Y., Gao, Z., Chen, X., Liu, B., Zhang, C., Yu, W., Cao, Q., Shen, Y., Yao, X., Chen, X., & Sun, H. (2023). Duchenne muscular dystrophy: Pathogenesis and promising therapies. *Journal of Neurology*, *270*(8), 3733–3749. https://doi.org/10.1007/s00415-023-11796-x

Chen, F., Qian, L., Yang, Z.-H., Huang, Y., Ngo, S. T., Ruan, N.-J., Wang, J., Schneider, C., Noakes, P. G., Ding, Y.-Q., Mei, L., & Luo, Z.-G. (2007). Rapsyn interaction with calpain stabilizes AChR clusters at the neuromuscular junction. *Neuron*, *55*(2), 247–260. https://doi.org/10.1016/j.neuron.2007.06.031

Chia, R., Chiò, A., & Traynor, B. J. (2018). Novel genes associated with amyotrophic lateral sclerosis: Diagnostic and clinical implications. *The Lancet. Neurology*, *17*(1), 94–102. https://doi.org/10.1016/S1474-4422(17)30401-5

Clark, M. E., Farinha, A., Morrison, A. R., & Lisi, G. P. (2025). Structural, biological, and biomedical implications of mRNA interactions with the master regulator HuR. *NAR Molecular Medicine*, *2*(1), ugaf002. https://doi.org/10.1093/narmme/ugaf002

Cohn, R. D. (2000). Molecular basis of muscular dystrophies. *Muscle & Nerve*, *23*(10), 1456–1471. https://doi.org/10.1002/1097-4598(200010)23:10<1456::aid-mus2>3.0.co;2-t

Colombrita. (2013). *ELAV proteins along evolution: Back to the nucleus? - PubMed*. https://pubmed.ncbi.nlm.nih.gov/23439364/

Consalvi, S., Mozzetta, C., Bettica, P., Germani, M., Fiorentini, F., Del Bene, F., Rocchetti, M., Leoni, F., Monzani, V., Mascagni, P., Puri, P. L., & Saccone, V. (2013). Preclinical Studies in the mdx Mouse Model of Duchenne Muscular Dystrophy with the Histone Deacetylase Inhibitor Givinostat. *Molecular Medicine*, *19*(1), 79–87. https://doi.org/10.2119/molmed.2013.00011

Covault, J., & Sanes, J. R. (1986). Distribution of N-CAM in synaptic and extrasynaptic portions of developing and adult skeletal muscle. *The Journal of Cell Biology*, *102*(3), 716–730. https://doi.org/10.1083/jcb.102.3.716

Daniels, M. P. (2012). The Role of Agrin in Synaptic Development, Plasticity and Signaling in the Central Nervous System. *Neurochemistry International*, *61*(6), 848–853. https://doi.org/10.1016/j.neuint.2012.02.028

Darras, B. T., Urion, D. K., & Ghosh, P. S. (1993). Dystrophinopathies. In M. P. Adam, J. Feldman, G. M. Mirzaa, R. A. Pagon, S. E. Wallace, L. J. Bean, K. W. Gripp, & A. Amemiya (Eds.), *GeneReviews®*. University of Washington, Seattle. http://www.ncbi.nlm.nih.gov/books/NBK1119/

Dassi, E. (2017). Handshakes and Fights: The Regulatory Interplay of RNA-Binding Proteins. *Frontiers in Molecular Biosciences*, *4*, 67. https://doi.org/10.3389/fmolb.2017.00067

Davis, L. A., Fogarty, M. J., Brown, A., & Sieck, G. C. (2022). Structure and Function of the Mammalian Neuromuscular Junction. *Comprehensive Physiology*, *12*(4), 3731–3766. https://doi.org/10.1002/cphy.c210022

de Ruijter, A. J. M., van Gennip, A. H., Caron, H. N., Kemp, S., & van Kuilenburg, A. B. P. (2003). Histone deacetylases (HDACs): Characterization of the classical HDAC family. *Biochemical Journal*, *370*(Pt 3), 737–749. https://doi.org/10.1042/BJ20021321

Deasy, B. M., Feduska, J. M., Payne, T. R., Li, Y., Ambrosio, F., & Huard, J. (2009). Effect of VEGF on the Regenerative Capacity of Muscle Stem Cells in Dystrophic Skeletal Muscle. *Molecular Therapy*, *17*(10), 1788–1798. https://doi.org/10.1038/mt.2009.136

Dellorusso, C., Crawford, R. W., Chamberlain, J. S., & Brooks, S. V. (2001). Tibialis anterior muscles in mdx mice are highly susceptible to contraction-induced injury. *Journal of Muscle Research and Cell Motility*, *22*(5), 467–475. https://doi.org/10.1023/a:1014587918367

Deschênes-Furry, J., Bélanger, G., Mwanjewe, J., Lunde, J. A., Parks, R. J., Perrone-Bizzozero, N., & Jasmin, B. J. (2005). The RNA-binding Protein HuR Binds to Acetylcholinesterase Transcripts andRegulates Their Expression in Differentiating Skeletal MuscleCells*. *Journal of Biological Chemistry*, *280*(27), 25361–25368. https://doi.org/10.1074/jbc.M410929200

Di Marco, S., Mazroui, R., Dallaire, P., Chittur, S., Tenenbaum, S. A., Radzioch, D., Marette, A., & Gallouzi, I.-E. (2005). NF-kappa B-mediated MyoD decay during muscle wasting requires nitric oxide synthase mRNA stabilization, HuR protein, and nitric oxide release. *Molecular and Cellular Biology*, *25*(15), 6533–6545. https://doi.org/10.1128/MCB.25.15.6533-6545.2005

Dimauro, I., Pearson, T., Caporossi, D., & Jackson, M. J. (2012). A simple protocol for the subcellular fractionation of skeletal muscle cells and tissue. *BMC Research Notes*, *5*, 513. https://doi.org/10.1186/1756-0500-5-513

Duan, D., Goemans, N., Takeda, S., Mercuri, E., & Aartsma-Rus, A. (2021). Duchenne muscular dystrophy. *Nature Reviews Disease Primers*, *7*(1), 1–19. https://doi.org/10.1038/s41572-021-00248-3

Duddy, W., Duguez, S., Johnston, H., Cohen, T. V., Phadke, A., Gordish-Dressman, H., Nagaraju, K., Gnocchi, V., Low, S., & Partridge, T. (2015). Muscular dystrophy in the mdx mouse is a severe myopathy compounded by hypotrophy, hypertrophy and hyperplasia. *Skeletal Muscle*, *5*, 16. https://doi.org/10.1186/s13395-015-0041-y

Dumont, N. A. (2016). Targeting muscle stem cell intrinsic defects to treat Duchenne muscular dystrophy. *NPJ Regenerative Medicine*, *1*, 16006. https://doi.org/10.1038/npjregenmed.2016.6

Dumont, N. A., Wang, Y. X., von Maltzahn, J., Pasut, A., Bentzinger, C. F., Brun, C. E., & Rudnicki, M. A. (2015). Dystrophin expression in muscle stem cells regulates their polarity and asymmetric division. *Nature Medicine*, *21*(12), 1455–1463. https://doi.org/10.1038/nm.3990

Dzierlega, K., & Yokota, T. (2020). Optimization of antisense-mediated exon skipping for Duchenne muscular dystrophy. *Gene Therapy*, *27*(9), 407–416. https://doi.org/10.1038/s41434-020-0156-6

Efimova, A. D., Ovchinnikov, R. K., Roman, A. Y., Maltsev, A. V., Grigoriev, V. V., Kovrazhkina, E. A., & Skvortsova, V. I. (2017). [The FUS protein: Physiological functions and a role in amyotrophic lateral sclerosis]. *Molekuliarnaia Biologiia*, *51*(3), 387–399. https://doi.org/10.7868/S0026898417020094

Eftimie, R., Brenner, H. R., & Buonanno, A. (1991). Myogenin and MyoD join a family of skeletal muscle genes regulated by electrical activity. *Proceedings of the National Academy of Sciences of the United States of America*, *88*(4), 1349–1353. https://doi.org/10.1073/pnas.88.4.1349

Eguchi, T., Tezuka, T., Miyoshi, S., & Yamanashi, Y. (2016). Postnatal knockdown of dok-7 gene expression in mice causes structural defects in neuromuscular synapses and myasthenic pathology. *Genes to Cells: Devoted to Molecular & Cellular Mechanisms*, *21*(6), 670–676. https://doi.org/10.1111/gtc.12370

Englund, D. A., Jolliffe, A., Aversa, Z., Zhang, X., Sturmlechner, I., Sakamoto, A. E., Zeidler, J. D., Warner, G. M., McNinch, C., White, T. A., Chini, E. N., Baker, D. J., van Deursen, J. M., & LeBrasseur, N. K. (2022). P21 induces a senescence program and skeletal muscle

dysfunction. *Molecular Metabolism*, *67*, 101652. https://doi.org/10.1016/j.molmet.2022.101652

Fallini, C., Rouanet, J. P., Donlin-Asp, P. G., Guo, P., Zhang, H., Singer, R. H., Rossoll, W., & Bassell, G. J. (2014). Dynamics of survival of motor neuron (SMN) protein interaction with the mRNA-binding protein IMP1 facilitates its trafficking into motor neuron axons. *Developmental Neurobiology*, *74*(3), 319–332. https://doi.org/10.1002/dneu.22111

Fan, X. C., & Steitz, J. A. (1998). HNS, a nuclear-cytoplasmic shuttling sequence in HuR. *Proceedings of the National Academy of Sciences of the United States of America*, *95*(26), 15293–15298. https://doi.org/10.1073/pnas.95.26.15293

Farooq, F., Balabanian, S., Liu, X., Holcik, M., & MacKenzie, A. (2009). P38 Mitogen-activated protein kinase stabilizes SMN mRNA through RNA binding protein HuR. *Human Molecular Genetics*, *18*(21), 4035–4045. https://doi.org/10.1093/hmg/ddp352

Feige, P., Brun, C. E., Ritso, M., & Rudnicki, M. A. (2018). Orienting Muscle Stem Cells for Regeneration in Homeostasis, Aging, and Disease. *Cell Stem Cell*, *23*(5), 653–664. https://doi.org/10.1016/j.stem.2018.10.006

Ferraro, E., Molinari, F., & Berghella, L. (2012). Molecular control of neuromuscular junction development. *Journal of Cachexia, Sarcopenia and Muscle*, *3*(1), 13–23. https://doi.org/10.1007/s13539-011-0041-7

Figueroa, A., Cuadrado, A., Fan, J., Atasoy, U., Muscat, G. E., Muñoz-Canoves, P., Gorospe, M., & Muñoz, A. (2003). Role of HuR in Skeletal Myogenesis through Coordinate Regulation of Muscle Differentiation Genes. *Molecular and Cellular Biology*, *23*(14), 4991–5004. https://doi.org/10.1128/MCB.23.14.4991-5004.2003

Florczyk-Soluch, U., Polak, K., & Dulak, J. (2021). The multifaceted view of heart problem in Duchenne muscular dystrophy. *Cellular and Molecular Life Sciences: CMLS*, *78*(14), 5447–5468. https://doi.org/10.1007/s00018-021-03862-2

Friese, M. B., Blagden, C. S., & Burden, S. J. (2007). Synaptic differentiation is defective in mice lacking acetylcholine receptor beta-subunit tyrosine phosphorylation. *Development*, *134*(23), 4167–4176. https://doi.org/10.1242/dev.010702

Fromm, L., Burden, Steven. (2001). Neuregulin-1-stimulated phosphorylation of GABP in skeletal muscle cells. *Biochemistry*, *40*(17), 5306–5312. https://doi.org/10.1021/bi002649m

Fu, A. K. Y., Ip, F. C. F., Fu, W.-Y., Cheung, J., Wang, J. H., Yung, W.-H., & Ip, N. Y. (2005). Aberrant motor axon projection, acetylcholine receptor clustering, and neurotransmission in cyclin-dependent kinase 5 null mice. *Proceedings of the National Academy of Sciences of the United States of America*, *102*(42), 15224–15229. https://doi.org/10.1073/pnas.0507678102

García-Cruz, C., Aragón, J., Lourdel, S., Annan, A., Roger, J. E., Montanez, C., & Vaillend, C. (2020). *Tissue- and cell-specific whole-transcriptome meta-analysis from brain and retina reveals differential expression of dystrophin complexes and new dystrophin spliced isoforms*. https://dx.doi.org/10.1093/hmg/ddac236

Gautam, M., Noakes, P. G., Mudd, J., Nichol, M., Chu, G. C., Sanes, J. R., & Merlie, J. P. (1995). Failure of postsynaptic specialization to develop at neuromuscular junctions of rapsyn-deficient mice. *Nature*, *377*(6546), 232–236. https://doi.org/10.1038/377232a0

Gehle, V. M., Walcott, E. C., Nishizaki, T., & Sumikawa, K. (1997). N-glycosylation at the conserved sites ensures the expression of properly folded functional ACh receptors. *Brain*

Research. Molecular Brain Research, *45*(2), 219–229. https://doi.org/10.1016/s0169-328x(96)00256-2

Ghasemizadeh, A., Christin, E., Guiraud, A., Couturier, N., Abitbol, M., Risson, V., Girard, E., Jagla, C., Soler, C., Laddada, L., Sanchez, C., Jaque-Fernandez, F.-I., Jacquemond, V., Thomas, J.-L., Lanfranchi, M., Courchet, J., Gondin, J., Schaeffer, L., & Gache, V. (2021). MACF1 controls skeletal muscle function through the microtubule-dependent localization of extra-synaptic myonuclei and mitochondria biogenesis. *eLife*, *10*, e70490. https://doi.org/10.7554/eLife.70490

Giessen, K. van der, Di-Marco, S., Clair, E., & Gallouzi, I. E. (2003). RNAi-mediated HuR Depletion Leads to the Inhibition of Muscle Cell Differentiation *. *Journal of Biological Chemistry*, *278*(47), 47119–47128. https://doi.org/10.1074/jbc.M308889200

Glisovic, T., Bachorik, J. L., Yong, J., & Dreyfuss, G. (2008). RNA-binding proteins and post-transcriptional gene regulation. *FEBS Letters*, *582*(14), 1977–1986. https://doi.org/10.1016/j.febslet.2008.03.004

Glozak, M. A., Sengupta, N., Zhang, X., & Seto, E. (2005). Acetylation and deacetylation of non-histone proteins. *Gene*, *363*, 15–23. https://doi.org/10.1016/j.gene.2005.09.010

Goddeeris, M. M., Wu, B., Venzke, D., Yoshida-Moriguchi, T., Saito, F., Matsumura, K., Moore, S. A., & Campbell, K. P. (2013). LARGE glycans on dystroglycan function as a tunable matrix scaffold to prevent dystrophy. *Nature*, *503*(7474), 136–140. https://doi.org/10.1038/nature12605

Goulet, B. B., Kothary, R., & Parks, R. J. (2013). At the “junction” of spinal muscular atrophy pathogenesis: The role of neuromuscular junction dysfunction in SMA disease

progression. *Current Molecular Medicine*, *13*(7), 1160–1174. https://doi.org/10.2174/15665240113139990044

Grady, R. M., Akaaboune, M., Cohen, A. L., Maimone, M. M., Lichtman, J. W., & Sanes, J. R. (2003). Tyrosine-phosphorylated and nonphosphorylated isoforms of alpha-dystrobrevin: Roles in skeletal muscle and its neuromuscular and myotendinous junctions. *The Journal of Cell Biology*, *160*(5), 741–752. https://doi.org/10.1083/jcb.200209045

Grady, R. M., Zhou, H., Cunningham, J. M., Henry, M. D., Campbell, K. P., & Sanes, J. R. (2000). Maturation and maintenance of the neuromuscular synapse: Genetic evidence for roles of the dystrophin--glycoprotein complex. *Neuron*, *25*(2), 279–293. https://doi.org/10.1016/s0896-6273(00)80894-6

Grammatikakis, I., Abdelmohsen, K., & Gorospe, M. (2017a). Posttranslational control of HuR function. *Wiley Interdisciplinary Reviews. RNA*, *8*(1). https://doi.org/10.1002/wrna.1372

Grammatikakis, I., Abdelmohsen, K., & Gorospe, M. (2017b). Posttranslational control of HuR function. *WIREs RNA*, *8*(1), e1372. https://doi.org/10.1002/wrna.1372

Gramolini, A. O., Bélanger, G., & Jasmin, B. J. (2001). Distinct regions in the 3′ untranslated region are responsible for targeting and stabilizing utrophin transcripts in skeletal muscle cells. *The Journal of Cell Biology*, *154*(6), 1173–1184. https://doi.org/10.1083/jcb.200101108

Gramolini, A. O., Bélanger, G., Thompson, J. M., Chakkalakal, J. V., & Jasmin, B. J. (2001). Increased expression of utrophin in a slow vs. A fast muscle involves posttranscriptional events. *American Journal of Physiology. Cell Physiology*, *281*(4), C1300-1309. https://doi.org/10.1152/ajpcell.2001.281.4.C1300

Grimm, D., Streetz, K. L., Jopling, C. L., Storm, T. A., Pandey, K., Davis, C. R., Marion, P., Salazar, F., & Kay, M. A. (2006). Fatality in mice due to oversaturation of cellular microRNA/short hairpin RNA pathways. *Nature*, *441*(7092), 537–541. https://doi.org/10.1038/nature04791

Guiraud, S., Edwards, B., Babbs, A., Squire, S. E., Berg, A., Moir, L., Wood, M. J., & Davies, K. E. (2019). The potential of utrophin and dystrophin combination therapies for Duchenne muscular dystrophy. *Human Molecular Genetics*, *28*(13), 2189–2200. https://doi.org/10.1093/hmg/ddz049

Guo, J., Lv, J., Chang, S., Chen, Z., Lu, W., Xu, C., Liu, M., & Pang, X. (2016). Inhibiting cytoplasmic accumulation of HuR synergizes genotoxic agents in urothelial carcinoma of the bladder. *Oncotarget*, *7*(29), 45249–45262. https://doi.org/10.18632/oncotarget.9932

Haeussler, J., Haeusler, J., Striebel, A. M., Assum, G., Vogel, W., Furneaux, H., & Krone, W. (2000). Tumor antigen HuR binds specifically to one of five protein-binding segments in the 3'-untranslated region of the neurofibromin messenger RNA. *Biochemical and Biophysical Research Communications*, *267*(3), 726–732. https://doi.org/10.1006/bbrc.1999.2019

Handschin, C., Kobayashi, Y. M., Chin, S., Seale, P., Campbell, K. P., & Spiegelman, B. M. (2007). PGC-1α regulates the neuromuscular junction program and ameliorates Duchenne muscular dystrophy. *Genes & Development*, *21*(7), 770–783. https://doi.org/10.1101/gad.1525107

Hanson, B., Wood, M. J. A., & Roberts, T. C. (2021). Molecular correction of Duchenne muscular dystrophy by splice modulation and gene editing. *RNA Biology*, *18*(7), 1048–1062. https://doi.org/10.1080/15476286.2021.1874161

Hara, Y., Balci-Hayta, B., Yoshida-Moriguchi, T., Kanagawa, M., Beltrán-Valero de Bernabé, D., Gündeşli, H., Willer, T., Satz, J. S., Crawford, R. W., Burden, S. J., Kunz, S., Oldstone, M. B. A., Accardi, A., Talim, B., Muntoni, F., Topaloğlu, H., Dinçer, P., & Campbell, K. P. (2011). A dystroglycan mutation associated with limb-girdle muscular dystrophy. *The New England Journal of Medicine*, *364*(10), 939–946. https://doi.org/10.1056/NEJMoa1006939

Harriman, D. G. (1976). A comparison of the fine structure of motor end-plates in Duchenne dystrophy and in human neurogenic diseases. *Journal of the Neurological Sciences*, *28*(2), 233–247. https://doi.org/10.1016/0022-510x(76)90106-4

Hata, K., Maeno-Hikichi, Y., Yumoto, N., Burden, S. J., & Landmesser, L. T. (2018). Distinct Roles of Different Presynaptic and Postsynaptic NCAM Isoforms in Early Motoneuron–Myotube Interactions Required for Functional Synapse Formation. *The Journal of Neuroscience*, *38*(2), 498–510. https://doi.org/10.1523/JNEUROSCI.1014-17.2017

Herndon, C. A. (2008). Neuregulin-1 induces acetylcholine receptor transcription in the absence of GABPα phosphorylation. *Journal of Neuroscience Research*, *86*(5), 982–991. https://doi.org/10.1002/jnr.21563

Hinman, M. N. (2008). Diverse molecular functions of Hu proteins. *Cellular and Molecular Life Sciences*, *65*(20), 3168–3181. https://doi.org/10.1007/s00018-008-8252-6

Hoffman, E. P., Brown, R. H., & Kunkel, L. M. (1987). Dystrophin: The protein product of the duchenne muscular dystrophy locus. *Cell*, *51*(6), 919–928. https://doi.org/10.1016/0092-8674(87)90579-4

Hollinger, K., Gardan-Salmon, D., Santana, C., Rice, D., Snella, E., & Selsby, J. T. (2013). Rescue of dystrophic skeletal muscle by PGC-1α involves restored expression of

dystrophin-associated protein complex components and satellite cell signaling. *American Journal of Physiology-Regulatory, Integrative and Comparative Physiology*, *305*(1), R13–R23. https://doi.org/10.1152/ajpregu.00221.2012

Hörnberg, H. (2013). RNA-binding proteins and translational regulation in axons and growth cones. *Frontiers in Neuroscience*, *7*, 81. https://doi.org/10.3389/fnins.2013.00081

Houang, E. M., Sham, Y. Y., Bates, F. S., & Metzger, J. M. (2018). Muscle membrane integrity in Duchenne muscular dystrophy: Recent advances in copolymer-based muscle membrane stabilizers. *Skeletal Muscle*, *8*(1), 31. https://doi.org/10.1186/s13395-018-0177-7

Hui, T., Jing, H., Zhou, T., Chen, P., Liu, Z., Dong, X., Yan, M., Ren, D., Zou, S., Wang, S., Fei, E., Hong, D., & Lai, X. (2021). Increasing LRP4 diminishes neuromuscular deficits in a mouse model of Duchenne muscular dystrophy. *Human Molecular Genetics*, *30*(17), 1579–1590. https://doi.org/10.1093/hmg/ddab135

Isenmann, M., Stoddart, M. J., Schmelzeisen, R., Gross, C., Della Bella, E., & Rothweiler, R. M. (2023). Basic Principles of RNA Interference: Nucleic Acid Types and In Vitro Intracellular Delivery Methods. *Micromachines*, *14*(7), 1321. https://doi.org/10.3390/mi14071321

Ismaeel, A., Kim, J.-S., Kirk, J. S., Smith, R. S., Bohannon, W. T., & Koutakis, P. (2019). Role of Transforming Growth Factor-β in Skeletal Muscle Fibrosis: A Review. *International Journal of Molecular Sciences*, *20*(10), 2446. https://doi.org/10.3390/ijms20102446

Iyer, S. R., Shah, S. B., & Lovering, R. M. (2021). The Neuromuscular Junction: Roles in Aging and Neuromuscular Disease. *International Journal of Molecular Sciences*, *22*(15), 8058. https://doi.org/10.3390/ijms22158058

Janice Sánchez, B., Tremblay, A.-M. K., Leduc-Gaudet, J.-P., Hall, D. T., Kovacs, E., Ma, J. F., Mubaid, S., Hallauer, P. L., Phillips, B. L., Vest, K. E., Corbett, A. H., Kontoyiannis, D. L., Hussain, S. N. A., Hastings, K. E. M., Di Marco, S., & Gallouzi, I.-E. (2019a). Depletion of HuR in murine skeletal muscle enhances exercise endurance and prevents cancer-induced muscle atrophy. *Nature Communications*, *10*(1), Article 1. https://doi.org/10.1038/s41467-019-12186-6

Jerusalem, F., Engel, A. G., & Gomez, M. R. (1974). DUCHENNE DYSTROPHY: II. MORPHOMETRIC STUDY OF MOTOR END-PLATE FINE STRUCTURE. *Brain*, *97*(1), 123–130. https://doi.org/10.1093/brain/97.1.123

Ji, X., Adams, S. T., & Miller, S. C. (2020). Bioluminescence imaging in mice with synthetic luciferin analogues. *Methods in Enzymology*, *640*, 165–183. https://doi.org/10.1016/bs.mie.2020.04.033

Joassard, O. R., Bélanger, G., Karmouch, J., Lunde, J. A., Shukla, A. H., Chopard, A., Legay, C., & Jasmin, B. J. (2015). HuR Mediates Changes in the Stability of AChR β-Subunit mRNAs after Skeletal Muscle Denervation. *The Journal of Neuroscience: The Official Journal of the Society for Neuroscience*, *35*(31), 10949–10962. https://doi.org/10.1523/JNEUROSCI.1043-15.2015

Jones, R. A., Harrison, C., Eaton, S. L., Llavero Hurtado, M., Graham, L. C., Alkhammash, L., Oladiran, O. A., Gale, A., Lamont, D. J., Simpson, H., Simmen, M. W., Soeller, C., Wishart, T. M., & Gillingwater, T. H. (2017). Cellular and Molecular Anatomy of the Human Neuromuscular Junction. *Cell Reports*, *21*(9), 2348–2356. https://doi.org/10.1016/j.celrep.2017.11.008

Jones, R. A., Reich, C. D., Dissanayake, K. N., Kristmundsdottir, F., Findlater, G. S., Ribchester, R. R., Simmen, M. W., & Gillingwater, T. H. (2016). NMJ-morph reveals principal components of synaptic morphology influencing structure–function relationships at the neuromuscular junction. *Open Biology*, *6*(12), 160240. https://doi.org/10.1098/rsob.160240

Karmouch, J., Delers, P., Semprez, F., Soyed, N., Areias, J., Bélanger, G., Ravel-Chapuis, A., Dobbertin, A., Jasmin, B. J., & Legay, C. (2020). AChR β-Subunit mRNAs Are Stabilized by HuR in a Mouse Model of Congenital Myasthenic Syndrome With Acetylcholinesterase Deficiency. *Frontiers in Molecular Neuroscience*, *13*, 568171. https://doi.org/10.3389/fnmol.2020.568171

Katsanou, V., Milatos, S., Yiakouvaki, A., Sgantzis, N., Kotsoni, A., Alexiou, M., Harokopos, V., Aidinis, V., Hemberger, M., & Kontoyiannis, D. L. (2009). The RNA-Binding Protein Elavl1/HuR Is Essential for Placental Branching Morphogenesis and Embryonic Development. *Molecular and Cellular Biology*, *29*(10), 2762–2776. https://doi.org/10.1128/MCB.01393-08

Kelley, J. B. (2019). Fluorescence-based quantification of nucleocytoplasmic transport. *Methods, Nuclear Architecture and Transport*, *157*, 106–114. https://doi.org/10.1016/j.ymeth.2018.11.002

Khalil, B., Marwaha, K., & Bollu, P. C. (2026). Physiology, Neuromuscular Junction. In *StatPearls*. StatPearls Publishing. http://www.ncbi.nlm.nih.gov/books/NBK470413/

Kim, H. H., Abdelmohsen, K., Lal, A., Pullmann, R., Yang, X., Galban, S., Srikantan, S., Martindale, J. L., Blethrow, J., Shokat, K. M., & Gorospe, M. (2008). Nuclear HuR

accumulation through phosphorylation by Cdk1. *Genes & Development*, *22*(13), 1804–1815. https://doi.org/10.1101/gad.1645808

Kim, H.-J. (2011). Histone deacetylase inhibitors: Molecular mechanisms of action and clinical trials as anti-cancer drugs. *American Journal of Translational Research*, *3*(2), 166–179.

Klöss, S., Rodenbach, D., Bordel, R., & Mülsch, A. (2005). Human-antigen R (HuR) expression in hypertension: Downregulation of the mRNA stabilizing protein HuR in genetic hypertension. *Hypertension*, *45*(6), 1200–1206. https://doi.org/10.1161/01.HYP.0000165674.58470.8f

Kong, J. (1999). Dystrophin is required for organizing large acetylcholine receptor aggregates. *Brain Research*, *839*(2), 298–304. https://doi.org/10.1016/s0006-8993(99)01737-0

Kuwano, Y., Kim, H. H., Abdelmohsen, K., Pullmann, R., Martindale, J. L., Yang, X., & Gorospe, M. (2008). MKP-1 mRNA stabilization and translational control by RNA-binding proteins HuR and NF90. *Molecular and Cellular Biology*, *28*(14), 4562–4575. https://doi.org/10.1128/MCB.00165-08

Lafarga, V., Cuadrado, A., Lopez de Silanes, I., Bengoechea, R., Fernandez-Capetillo, O., & Nebreda, A. R. (2009). P38 Mitogen-Activated Protein Kinase- and HuR-Dependent Stabilization of p21Cip1 mRNA Mediates the G1/S Checkpoint. *Molecular and Cellular Biology*, *29*(16), 4341–4351. https://doi.org/10.1128/MCB.00210-09

Lai, Y., Choi, U. B., Leitz, J., Rhee, H. J., Lee, C., Altas, B., Zhao, M., Pfuetzner, R. A., Wang, A. L., Brose, N., Rhee, J., & Brunger, A. T. (2017). Molecular Mechanisms of Synaptic Vesicle Priming by Munc13 and Munc18. *Neuron*, *95*(3), 591-607.e10. https://doi.org/10.1016/j.neuron.2017.07.004

Landini, G. (2008). *Advanced shape analysis with ImageJ* [Computer software]. https://blog.bham.ac.uk/intellimic/g-landini-software/

Latvanlehto, A., Fox, M. A., Sormunen, R., Tu, H., Oikarainen, T., Koski, A., Naumenko, N., Shakirzyanova, A., Kallio, M., Ilves, M., Giniatullin, R., Sanes, J. R., & Pihlajaniemi, T. (2010). Muscle-derived collagen XIII regulates maturation of the skeletal neuromuscular junction. *Journal of Neuroscience*, *30*(37), 12230–12241. https://doi.org/10.1523/JNEUROSCI.5518-09.2010

Lee, E. B., Lee, V. M.-Y., & Trojanowski, J. Q. (2012). Gains or losses: Molecular mechanisms of TDP43-mediated neurodegeneration. *Nature Reviews Neuroscience*, *13*(1), 38–50. https://doi.org/10.1038/nrn3121

Lefebvre, S., Bürglen, L., Reboullet, S., Clermont, O., Burlet, P., Viollet, L., Benichou, B., Cruaud, C., Millasseau, P., & Zeviani, M. (1995). Identification and characterization of a spinal muscular atrophy-determining gene. *Cell*, *80*(1), 155–165. https://doi.org/10.1016/0092-8674(95)90460-3

Li, D. K., Tisdale, S., Lotti, F., & Pellizzoni, L. (2014). SMN control of RNP assembly: From post-transcriptional gene regulation to motor neuron disease. *Seminars in Cell & Developmental Biology*, *0*, 22–29. https://doi.org/10.1016/j.semcdb.2014.04.026

Li, L., Xiong, W.-C., & Mei, L. (2018). Neuromuscular Junction Formation, Aging, and Disorders. *Annual Review of Physiology*, *80*(1), 159–188. https://doi.org/10.1146/annurev-physiol-022516-034255

Li, L., Zhou, J., James, G., Heller-Harrison, R., Czech, M. P., & Olson, E. N. (1992). FGF inactivates myogenic helix-loop-helix proteins through phosphorylation of a conserved

protein kinase C site in their DNA-binding domains. *Cell*, *71*(7), 1181–1194. https://doi.org/10.1016/s0092-8674(05)80066-2

Li, X., Kazan, H., Lipshitz, H. D., & Morris, Q. D. (2014). Finding the target sites of RNA-binding proteins. *Wiley Interdisciplinary Reviews. RNA*, *5*(1), 111–130. https://doi.org/10.1002/wrna.1201

Liang, Z., Chen, X., & Nourbakhsh, M. (2026). New Insights into Neuromuscular Junction Biology: Evidence from Human and Animal Research. *International Journal of Molecular Sciences*, *27*(3), 1253. https://doi.org/10.3390/ijms27031253

Lin, J., Wu, P.-H., Tarr, P. T., Lindenberg, K. S., St-Pierre, J., Zhang, C.-Y., Mootha, V. K., Jäger, S., Vianna, C. R., Reznick, R. M., Cui, L., Manieri, M., Donovan, M. X., Wu, Z., Cooper, M. P., Fan, M. C., Rohas, L. M., Zavacki, A. M., Cinti, S., … Spiegelman, B. M. (2004). Defects in adaptive energy metabolism with CNS-linked hyperactivity in PGC-1alpha null mice. *Cell*, *119*(1), 121–135. https://doi.org/10.1016/j.cell.2004.09.013

Lin, W., Dominguez, B., Yang, J., Aryal, P., Brandon, E. P., Gage, F. H., & Lee, K.-F. (2005). Neurotransmitter acetylcholine negatively regulates neuromuscular synapse formation by a Cdk5-dependent mechanism. *Neuron*, *46*(4), 569–579. https://doi.org/10.1016/j.neuron.2005.04.002

Lovering, R. M., Iyer, S. R., Edwards, B., & Davies, K. E. (2020). Alterations of neuromuscular junctions in Duchenne muscular dystrophy. *Neuroscience Letters*, *737*, 135304. https://doi.org/10.1016/j.neulet.2020.135304

Lyons, P. R., & Slater, C. R. (1991). Structure and function of the neuromuscular junction in young adultmdx mice. *Journal of Neurocytology*, *20*(12), 969–981. https://doi.org/10.1007/BF01187915

Macpherson, P., Kostrominova, T., Tang, H., & Goldman, D. (2002). Protein kinase C and calcium/calmodulin-activated protein kinase II (CaMK II) suppress nicotinic acetylcholine receptor gene expression in mammalian muscle. A specific role for CaMK II in activity-dependent gene expression. *The Journal of Biological Chemistry*, *277*(18), 15638–15646. https://doi.org/10.1074/jbc.M109864200

Manini, A., Abati, E., Nuredini, A., Corti, S., & Comi, G. P. (2022). Adeno-Associated Virus (AAV)-Mediated Gene Therapy for Duchenne Muscular Dystrophy: The Issue of Transgene Persistence. *Frontiers in Neurology*, *12*, 814174. https://doi.org/10.3389/fneur.2021.814174

Martin, P. T. (2007). Congenital Muscular Dystrophies Involving the O-Mannose Pathway. *Current Molecular Medicine*, *7*(4), 417–425. https://doi.org/10.2174/156652407780831601

Martin, P. T., Scott, L. J., Porter, B. E., & Sanes, J. R. (1999). Distinct structures and functions of related pre- and postsynaptic carbohydrates at the mammalian neuromuscular junction. *Molecular and Cellular Neurosciences*, *13*(2), 105–118. https://doi.org/10.1006/mcne.1999.0737

Massopust, R. T., Lee, Y. il, Pritchard, A. L., Nguyen, V.-K. M., McCreedy, D. A., & Thompson, W. J. (2020). Lifetime analysis of mdx skeletal muscle reveals a progressive pathology that leads to myofiber loss. *Scientific Reports*, *10*, 17248. https://doi.org/10.1038/s41598-020-74192-9

Mazroui, R., Di Marco, S., Clair, E., von Roretz, C., Tenenbaum, S. A., Keene, J. D., Saleh, M., & Gallouzi, I.-E. (2008). Caspase-mediated cleavage of HuR in the cytoplasm contributes

to pp32/PHAP-I regulation of apoptosis. *The Journal of Cell Biology*, *180*(1), 113–127. https://doi.org/10.1083/jcb.200709030

McGreevy, J. W., Hakim, C. H., McIntosh, M. A., & Duan, D. (2015). Animal models of Duchenne muscular dystrophy: From basic mechanisms to gene therapy. *Disease Models & Mechanisms*, *8*(3), 195–213. https://doi.org/10.1242/dmm.018424

Mei, L., & Nave, K.-A. (2014). Neuregulin-ERBB signaling in the nervous system and neuropsychiatric diseases. *Neuron*, *83*(1), 27–49. https://doi.org/10.1016/j.neuron.2014.06.007

Meier, T., Masciulli, F., Moore, C., Schoumacher, F., Eppenberger, U., Denzer, A. J., Jones, G., & Brenner, H. R. (1998). Agrin can mediate acetylcholine receptor gene expression in muscle by aggregation of muscle-derived neuregulins. *The Journal of Cell Biology*, *141*(3), 715–726. https://doi.org/10.1083/jcb.141.3.715

Memme, J. M., Oliveira, A. N., & Hood, D. A. (2021). P53 regulates skeletal muscle mitophagy and mitochondrial quality control following denervation-induced muscle disuse. *The Journal of Biological Chemistry*, *298*(2), 101540. https://doi.org/10.1016/j.jbc.2021.101540

Mercuri, E., Pane, M., Cicala, G., Brogna, C., & Ciafaloni, E. (2023). Detecting early signs in Duchenne muscular dystrophy: Comprehensive review and diagnostic implications. *Frontiers in Pediatrics*, *11*, 1276144. https://doi.org/10.3389/fped.2023.1276144

Messéant, J., Ezan, J., Delers, P., Glebov, K., Marchiol, C., Lager, F., Renault, G., Tissir, F., Montcouquiol, M., Sans, N., Legay, C., & Strochlic, L. (2017). Wnt proteins contribute to neuromuscular junction formation through distinct signaling pathways. *Development*, *144*(9), 1712–1724. https://doi.org/10.1242/dev.146167

Min, Y.-L., Li, H., Rodriguez-Caycedo, C., Mireault, A. A., Huang, J., Shelton, J. M., McAnally, J. R., Amoasii, L., Mammen, P. P. A., Bassel-Duby, R., & Olson, E. N. (2019). CRISPR-Cas9 corrects Duchenne muscular dystrophy exon 44 deletion mutations in mice and human cells. *Science Advances*, *5*(3), eaav4324. https://doi.org/10.1126/sciadv.aav4324

Minty, G., Hoppen, A., Boehm, I., Alhindi, A., Gibb, L., Potter, E., Wagner, B. C., Miller, J., Skipworth, R. J. E., Gillingwater, T. H., & Jones, R. A. (2020). aNMJ-morph: A simple macro for rapid analysis of neuromuscular junction morphology. *Royal Society Open Science*, *7*(4), 200128. https://doi.org/10.1098/rsos.200128

Miro, J., Bougé, A.-L., Murauer, E., Beyne, E., Da Cunha, D., Claustres, M., Koenig, M., & Tuffery-Giraud, S. (2020). First Identification of RNA-Binding Proteins That Regulate Alternative Exons in the Dystrophin Gene. *International Journal of Molecular Sciences*, *21*(20), 7803. https://doi.org/10.3390/ijms21207803

Misgeld, T., Burgess, R. W., Lewis, R. M., Cunningham, J. M., Lichtman, J. W., & Sanes, J. R. (2002). Roles of neurotransmitter in synapse formation: Development of neuromuscular junctions lacking choline acetyltransferase. *Neuron*, *36*(4), 635–648. https://doi.org/10.1016/s0896-6273(02)01020-6

Misquitta, C. M., Iyer, V. R., Werstiuk, E. S., & Grover, A. K. (2001). The role of 3'-untranslated region (3'-UTR) mediated mRNA stability in cardiovascular pathophysiology. *Molecular and Cellular Biochemistry*, *224*(1–2), 53–67. https://doi.org/10.1023/a:1011982932645

Molina, T., Fabre, P., & Dumont, N. A. (2021). Fibro-adipogenic progenitors in skeletal muscle homeostasis, regeneration and diseases. *Open Biology*, *11*(12), 210110. https://doi.org/10.1098/rsob.210110

Montagna, C., Maiani, E., Pieroni, L., & Consalvi, S. (2025). Duchenne Muscular Dystrophy: Integrating Current Clinical Practice with Future Therapeutic and Diagnostic Horizons. *International Journal of Molecular Sciences*, *26*(14), 6742. https://doi.org/10.3390/ijms26146742

Moore, C. B., Guthrie, E. H., Huang, M. T.-H., & Taxman, D. J. (2010). Short Hairpin RNA (shRNA): Design, Delivery, and Assessment of Gene Knockdown. *Methods in Molecular Biology (Clifton, N.J.)*, *629*, 141–158. https://doi.org/10.1007/978-1-60761-657-3_10

Morales, A. (2023). Dystrophinopathies. In *StatPearls*. StatPearls Publishing. http://www.ncbi.nlm.nih.gov/books/NBK534245/

Moransard, M., Borges, L. S., Willmann, R., Marangi, P. A., Brenner, H. R., Ferns, M. J., & Fuhrer, C. (2003). Agrin regulates rapsyn interaction with surface acetylcholine receptors, and this underlies cytoskeletal anchoring and clustering. *The Journal of Biological Chemistry*, *278*(9), 7350–7359. https://doi.org/10.1074/jbc.M210865200

Moscoso, L. M., Chu, G. C., Gautam, M., Noakes, P. G., Merlie, J. P., & Sanes, J. R. (1995). Synapse-associated expression of an acetylcholine receptor-inducing protein, ARIA/heregulin, and its putative receptors, ErbB2 and ErbB3, in developing mammalian muscle. *Developmental Biology*, *172*(1), 158–169. https://doi.org/10.1006/dbio.1995.0012

Mozzetta, C., Sartorelli, V., Steinkuhler, C., & Puri, P. L. (2024). HDAC inhibitors as pharmacological treatment for Duchenne muscular dystrophy: A discovery journey from bench to patients. *Trends in Molecular Medicine*, *30*(3), 278–294. https://doi.org/10.1016/j.molmed.2024.01.007

Muntoni, F., Torelli, S., & Ferlini, A. (2003). Dystrophin and mutations: One gene, several proteins, multiple phenotypes. *The Lancet Neurology*, *2*(12), 731–740. https://doi.org/10.1016/S1474-4422(03)00585-4

Muraine, L., Bensalah, M., Dhiab, J., Cordova, G., Arandel, L., Marhic, A., Chapart, M., Vasseur, S., Benkhelifa-Ziyyat, S., Bigot, A., Butler-Browne, G., Mouly, V., Negroni, E., & Trollet, C. (2020). Transduction Efficiency of Adeno-Associated Virus Serotypes After Local Injection in Mouse and Human Skeletal Muscle. *Human Gene Therapy*, *31*(3–4), 233–240. https://doi.org/10.1089/hum.2019.173

Nabors, L. B., Gillespie, G. Y., Harkins, L., & King, P. H. (2001). HuR, a RNA stability factor, is expressed in malignant brain tumors and binds to adenine- and uridine-rich elements within the 3' untranslated regions of cytokine and angiogenic factor mRNAs. *Cancer Research*, *61*(5), 2154–2161.

Nallamilli, B. R. R., Chaubey, A., Valencia, C. A., Stansberry, L., Behlmann, A. M., Ma, Z., Mathur, A., Shenoy, S., Ganapathy, V., Jagannathan, L., Ramachander, V., Ferlini, A., Bean, L., & Hegde, M. (2021). A single NGS-based assay covering the entire genomic sequence of the DMD gene facilitates diagnostic and newborn screening confirmatory testing. *Human Mutation*, *42*(5), 626–638. https://doi.org/10.1002/humu.24191

Namgoong, J. H., & Bertoni, C. (2016). Clinical potential of ataluren in the treatment of Duchenne muscular dystrophy. *Degenerative Neurological and Neuromuscular Disease*, *6*, 37–48. https://doi.org/10.2147/DNND.S71808

Natarajan, U., Venkatesan, T., & Rathinavelu, A. (2021). Effect of the HDAC Inhibitor on Histone Acetylation and Methyltransferases in A2780 Ovarian Cancer Cells. *Medicina*, *57*(5), 456. https://doi.org/10.3390/medicina57050456

Neault, N., Ravel-Chapuis, A., Baird, S. D., Lunde, J. A., Poirier, M., Staykov, E., Plaza-Diaz, J., Medina, G., Abadía-Molina, F., Jasmin, B. J., & MacKenzie, A. E. (2023). Vorinostat Improves Myotonic Dystrophy Type 1 Splicing Abnormalities in DM1 Muscle Cell Lines and Skeletal Muscle from a DM1 Mouse Model. *International Journal of Molecular Sciences*, *24*(4), 3794. https://doi.org/10.3390/ijms24043794

Newey, S. E., Gramolini, A. O., Wu, J., Holzfeind, P., Jasmin, B. J., Davies, K. E., & Blake, D. J. (2001). A novel mechanism for modulating synaptic gene expression: Differential localization of alpha-dystrobrevin transcripts in skeletal muscle. *Molecular and Cellular Neurosciences*, *17*(1), 127–140. https://doi.org/10.1006/mcne.2000.0918

Ng, S. Y. (2020). Recent insights into neuromuscular junction biology in Duchenne muscular dystrophy: Impacts, challenges, and opportunities. *EBioMedicine*, *61*, 103032. https://doi.org/10.1016/j.ebiom.2020.103032

Nguyen, H. H., Jayasinha, V., Xia, B., Hoyte, K., & Martin, P. T. (2002). Overexpression of the cytotoxic T cell GalNAc transferase in skeletal muscle inhibits muscular dystrophy in mdx mice. *Proceedings of the National Academy of Sciences of the United States of America*, *99*(8), 5616–5621. https://doi.org/10.1073/pnas.082613599

Noakes, P. G., Gautam, M., Mudd, J., Sanes, J. R., & Merlie, J. P. (1995). Aberrant differentiation of neuromuscular junctions in mice lacking s-laminin/laminin β2. *Nature*, *374*(6519), 258–262. https://doi.org/10.1038/374258a0

Nudelman, I., Glikin, D., Smolkin, B., Hainrichson, M., Belakhov, V., & Baasov, T. (2010). Repairing faulty genes by aminoglycosides: Development of new derivatives of geneticin (G418) with enhanced suppression of diseases-causing nonsense mutations. *Bioorganic & Medicinal Chemistry*, *18*(11), 3735–3746. https://doi.org/10.1016/j.bmc.2010.03.060

Ohno, K., Brengman, J., Tsujino, A., & Engel, A. G. (1998). Human endplate acetylcholinesterase deficiency caused by mutations in the collagen-like tail subunit (ColQ) of the asymmetric enzyme. *Proceedings of the National Academy of Sciences of the United States of America*, *95*(16), 9654–9659. https://doi.org/10.1073/pnas.95.16.9654

Osseni, A., Ravel-Chapuis, A., Belotti, E., Scionti, I., Gangloff, Y.-G., Moncollin, V., Mazelin, L., Mounier, R., Leblanc, P., Jasmin, B. J., & Schaeffer, L. (2022). Pharmacological inhibition of HDAC6 improves muscle phenotypes in dystrophin-deficient mice by downregulating TGF-β via Smad3 acetylation. *Nature Communications*, *13*(1), 7108. https://doi.org/10.1038/s41467-022-34831-3

Osseni, A., Ravel-Chapuis, A., Thomas, J.-L., Gache, V., Schaeffer, L., & Jasmin, B. J. (2020). HDAC6 regulates microtubule stability and clustering of AChRs at neuromuscular junctions. *Journal of Cell Biology*, *219*(8), e201901099. https://doi.org/10.1083/jcb.201901099

Oury, J., Liu, Y., Töpf, A., Todorovic, S., Hoedt, E., Preethish-Kumar, V., Neubert, T. A., Lin, W., Lochmüller, H., & Burden, S. J. (2019). MACF1 links Rapsyn to microtubule- and actin-binding proteins to maintain neuromuscular synapses. *The Journal of Cell Biology*, *218*(5), 1686–1705. https://doi.org/10.1083/jcb.201810023

Pascale, A., Amadio, M., & Quattrone, A. (2008). Defining a neuron: Neuronal ELAV proteins. *Cellular and Molecular Life Sciences: CMLS*, *65*(1), 128–140. https://doi.org/10.1007/s00018-007-7017-y

Pastoret, C. (1995). Mdx mice show progressive weakness and muscle deterioration with age. *Journal of the Neurological Sciences*, *129*(2), 97–105. https://doi.org/10.1016/0022-510x(94)00276-t

Patrick, G. N., Zukerberg, L., Nikolic, M., de la Monte, S., Dikkes, P., & Tsai, L. H. (1999). Conversion of p35 to p25 deregulates Cdk5 activity and promotes neurodegeneration. *Nature*, *402*(6762), 615–622. https://doi.org/10.1038/45159

Patterson, G., Conner, H., Groneman, M., Blavo, C., & Parmar, M. S. (2023). Duchenne muscular dystrophy: Current treatment and emerging exon skipping and gene therapy approach. *European Journal of Pharmacology*, *947*, 175675. https://doi.org/10.1016/j.ejphar.2023.175675

Patton, B. L., Miner, J. H., Chiu, A. Y., & Sanes, J. R. (1997). Distribution and function of laminins in the neuromuscular system of developing, adult, and mutant mice. *Journal of Cell Biology*, *139*(6), 1507–1521. https://doi.org/10.1083/jcb.139.6.1507

Péladeau, C., Adam, N., Bronicki, L. M., Coriati, A., Thabet, M., Al-Rewashdy, H., Vanstone, J., Mears, A., Renaud, J.-M., Holcik, M., & Jasmin, B. J. (2020). Identification of therapeutics that target eEF1A2 and upregulate utrophin A translation in dystrophic muscles. *Nature Communications*, *11*(1), Article 1. https://doi.org/10.1038/s41467-020-15971-w

Péladeau, C., Adam, N. J., & Jasmin, B. J. (2018). Celecoxib treatment improves muscle function in mdx mice and increases utrophin A expression. *The FASEB Journal*, *32*(9), 5090–5103. https://doi.org/10.1096/fj.201800081R

Perera, N. D., Sheean, R. K., Crouch, P. J., White, A. R., Horne, M. K., & Turner, B. J. (2016). Enhancing survival motor neuron expression extends lifespan and attenuates

neurodegeneration in mutant TDP-43 mice. *Human Molecular Genetics*, *25*(18), 4080–4093. https://doi.org/10.1093/hmg/ddw247

Personius, K. E., & Sawyer, R. P. (2006). Variability and failure of neurotransmission in the diaphragm of mdx mice. *Neuromuscular Disorders: NMD*, *16*(3), 168–177. https://doi.org/10.1016/j.nmd.2006.01.002

Pilgram, G. S. K., Potikanond, S., Baines, R. A., Fradkin, L. G., & Noordermeer, J. N. (2010). The Roles of the Dystrophin-Associated Glycoprotein Complex at the Synapse. *Molecular Neurobiology*, *41*(1), 1–21. https://doi.org/10.1007/s12035-009-8089-5

Pisani, C., Strimpakos, G., Gabanella, F., Di Certo, M. G., Onori, A., Severini, C., Luvisetto, S., Farioli-Vecchioli, S., Carrozzo, I., Esposito, A., Canu, T., Mattei, E., Corbi, N., & Passananti, C. (2018). Utrophin up-regulation by artificial transcription factors induces muscle rescue and impacts the neuromuscular junction in mdx mice. *Biochimica et Biophysica Acta*, *1864*(4Part A), 1172–1182. https://doi.org/10.1016/j.bbadis.2018.01.030

Podkalicka, P., Mucha, O., Dulak, J., & Loboda, A. (2019). Targeting angiogenesis in Duchenne muscular dystrophy. *Cellular and Molecular Life Sciences: CMLS*, *76*(8), 1507–1528. https://doi.org/10.1007/s00018-019-03006-7

Polymenidou, M., Lagier-Tourenne, C., Hutt, K. R., Huelga, S. C., Moran, J., Liang, T. Y., Ling, S.-C., Sun, E., Wancewicz, E., Mazur, C., Kordasiewicz, H., Sedaghat, Y., Donohue, J. P., Shiue, L., Bennett, C. F., Yeo, G. W., & Cleveland, D. W. (2011). Long pre-mRNA depletion and RNA missplicing contribute to neuronal vulnerability from loss of TDP-43. *Nature Neuroscience*, *14*(4), 459–468. https://doi.org/10.1038/nn.2779

Potter, R. A., Griffin, D. A., Heller, K. N., Peterson, E. L., Clark, E. K., Mendell, J. R., & Rodino-Klapac, L. R. (2021). Dose-Escalation Study of Systemically Delivered rAAVrh74.MHCK7.micro-dystrophin in the mdx Mouse Model of Duchenne Muscular Dystrophy. *Human Gene Therapy*, *32*(7–8), 375–389. https://doi.org/10.1089/hum.2019.255

Pratt, S. J. P., Shah, S. B., Ward, C. W., Kerr, J. P., Stains, J. P., & Lovering, R. M. (2015a). Recovery of altered neuromuscular junction morphology and muscle function in mdx mice after injury. *Cellular and Molecular Life Sciences: CMLS*, *72*(1), 153–164. https://doi.org/10.1007/s00018-014-1663-7

Pratt, S. J. P., Valencia, A. P., Le, G. K., Shah, S. B., & Lovering, R. M. (2015b). Pre- and postsynaptic changes in the neuromuscular junction in dystrophic mice. *Frontiers in Physiology*, *6*, 252. https://doi.org/10.3389/fphys.2015.00252

Pryzbylkowski, P., Obajimi, O., & Keen, J. C. (2008). Trichostatin A and 5 Aza-2' deoxycytidine decrease estrogen receptor mRNA stability in ER positive MCF7 cells through modulation of HuR. *Breast Cancer Research and Treatment*, *111*(1), 15–25. https://doi.org/10.1007/s10549-007-9751-0

Raj, B. (2015). Alternative Splicing in the Mammalian Nervous System: Recent Insights into Mechanisms and Functional Roles. *Neuron*, *87*(1), 14–27. https://doi.org/10.1016/j.neuron.2015.05.004

Ricotti, V., Mandy, W. P. L., Scoto, M., Pane, M., Deconinck, N., Messina, S., Mercuri, E., Skuse, D. H., & Muntoni, F. (2016). Neurodevelopmental, emotional, and behavioural problems in Duchenne muscular dystrophy in relation to underlying dystrophin gene

mutations. *Developmental Medicine and Child Neurology*, *58*(1), 77–84. https://doi.org/10.1111/dmcn.12922

Rimer, M., Prieto, A. L., Weber, J. L., Colasante, C., Ponomareva, O., Fromm, L., Schwab, M. H., Lai, C., & Burden, S. J. (2004). Neuregulin-2 is synthesized by motor neurons and terminal Schwann cells and activates acetylcholine receptor transcription in muscle cells expressing ErbB4. *Molecular and Cellular Neurosciences*, *26*(2), 271–281. https://doi.org/10.1016/j.mcn.2004.02.002

Rodríguez Cruz, P. M., Cossins, J., Beeson, D., & Vincent, A. (2020). The Neuromuscular Junction in Health and Disease: Molecular Mechanisms Governing Synaptic Formation and Homeostasis. *Frontiers in Molecular Neuroscience*, *13*. https://www.frontiersin.org/articles/10.3389/fnmol.2020.610964

Rosenberg, A. S., Puig, M., Nagaraju, K., Hoffman, E. P., Villalta, S. A., Rao, V. A., Wakefield, L. M., & Woodcock, J. (2015). Immune-mediated pathology in Duchenne muscular dystrophy. *Science Translational Medicine*, *7*(299), 299rv4. https://doi.org/10.1126/scitranslmed.aaa7322

Rozand, V., Grosprêtre, S., Stapley, P. J., & Lepers, R. (2015). Assessment of Neuromuscular Function Using Percutaneous Electrical Nerve Stimulation. *Journal of Visualized Experiments : JoVE*, (103), 52974. https://doi.org/10.3791/52974

Ryan, T. A. (2001). NCAM and Vesicle Cycling: The Importance of Good Glue in the Long Run. *Neuron*, *32*(5), 759–761. https://doi.org/10.1016/S0896-6273(01)00527-X

Sadasivam, G., Willmann, R., Lin, S., Erb-Vögtli, S., Kong, X. C., Rüegg, M. A., & Fuhrer, C. (2005). Src-Family Kinases Stabilize the Neuromuscular Synapse In Vivo via Protein Interactions, Phosphorylation, and Cytoskeletal Linkage of Acetylcholine Receptors. *The*

Journal of Neuroscience, *25*(45), 10479–10493. https://doi.org/10.1523/JNEUROSCI.2103-05.2005

Sam, C. (2026). Physiology, Acetylcholine. In *StatPearls*. StatPearls Publishing. http://www.ncbi.nlm.nih.gov/books/NBK557825/

Sanes, J. R. (2003). The basement membrane/basal lamina of skeletal muscle. *The Journal of Biological Chemistry*, *278*(15), 12601–12604. https://doi.org/10.1074/jbc.R200027200

Schmidt, N., Akaaboune, M., Gajendran, N., Martinez-Pena y Valenzuela, I., Wakefield, S., Thurnheer, R., & Brenner, H. R. (2011). Neuregulin/ErbB regulate neuromuscular junction development by phosphorylation of α-dystrobrevin. *Journal of Cell Biology*, *195*(7), 1171–1184. https://doi.org/10.1083/jcb.201107083

Schultz, C. W., Preet, R., Dhir, T., Dixon, D. A., & Brody, J. R. (2020). Understanding and targeting the disease-related RNA binding protein HuR. *Wiley Interdisciplinary Reviews. RNA*, *11*(3), e1581. https://doi.org/10.1002/wrna.1581

Sengupta, S., Jang, B.-C., Wu, M.-T., Paik, J.-H., Furneaux, H., & Hla, T. (2003). The RNA-binding protein HuR regulates the expression of cyclooxygenase-2. *The Journal of Biological Chemistry*, *278*(27), 25227–25233. https://doi.org/10.1074/jbc.M301813200

Sephton, C. F. (2015). The function of RNA-binding proteins at the synapse: Implications for neurodegeneration. *Cellular and Molecular Life Sciences: CMLS*, *72*(19), 3621–3635. https://doi.org/10.1007/s00018-015-1943-x

Shi, D.-L. (2021). RNA-Binding Proteins in the Post-transcriptional Control of Skeletal Muscle Development, Regeneration and Disease. *Frontiers in Cell and Developmental Biology*, *9*, 738978. https://doi.org/10.3389/fcell.2021.738978

Shi, Fu, A. K. Y., & Ip, N. Y. (2012). Molecular mechanisms underlying maturation and maintenance of the vertebrate neuromuscular junction. *Trends in Neurosciences*, *35*(7), 441–453. https://doi.org/10.1016/j.tins.2012.04.005

Shi, H., Boadu, E., Mercan, F., Le, A. M., Flach, R. J. R., Zhang, L., Tyner, K. J., Olwin, B. B., & Bennett, A. M. (2010). MAP kinase phosphatase-1 deficiency impairs skeletal muscle regeneration and exacerbates muscular dystrophy. *The FASEB Journal*, *24*(8), 2985–2997. https://doi.org/10.1096/fj.09-150045

Shiao, T. (2004). Defects in neuromuscular junction structure in dystrophic muscle are corrected by expression of a NOS transgene in dystrophin-deficient muscles, but not in muscles lacking—And 1-syntrophins. *Human Molecular Genetics*, *13*(17), 1873–1884. https://doi.org/10.1093/hmg/ddh204

Sigoillot, S. M., Bourgeois, F., Lambergeon, M., Strochlic, L., & Legay, C. (2010). ColQ controls postsynaptic differentiation at the neuromuscular junction. *Journal of Neuroscience*, *30*(1), 13–23. https://doi.org/10.1523/JNEUROSCI.4374-09.2010

Simone, L. E. (2013). Mechanisms Coordinating ELAV/Hu mRNA Regulons. *Current Opinion in Genetics & Development*, *23*(1), 35–43. https://doi.org/10.1016/j.gde.2012.12.006

Singhal, N. (2011). Role of extracellular matrix proteins and their receptors in the development of the vertebrate neuromuscular junction. *Developmental Neurobiology*, *71*(11), 982–1005. https://doi.org/10.1002/dneu.20953

Slater, C. R. (2017). The Structure of Human Neuromuscular Junctions: Some Unanswered Molecular Questions. *International Journal of Molecular Sciences*, *18*(10), 2183. https://doi.org/10.3390/ijms18102183

Smith, C. L., Mittaud, P., Prescott, E. D., Fuhrer, C., & Burden, S. J. (2001). Src, Fyn, and Yes are not required for neuromuscular synapse formation but are necessary for stabilization of agrin-induced clusters of acetylcholine receptors. *The Journal of Neuroscience: The Official Journal of the Society for Neuroscience*, *21*(9), 3151–3160. https://doi.org/10.1523/JNEUROSCI.21-09-03151.2001

So, E., Mitchell, J. C., Memmi, C., Chennell, G., Vizcay-Barrena, G., Allison, L., Shaw, C. E., & Vance, C. (2018). Mitochondrial abnormalities and disruption of the neuromuscular junction precede the clinical phenotype and motor neuron loss in hFUSWT transgenic mice. *Human Molecular Genetics*, *27*(3), 463–474. https://doi.org/10.1093/hmg/ddx415

Srikantan, S., & Gorospe, M. (2012a). HuR function in disease. *Frontiers in Bioscience (Landmark Edition)*, *17*(1), 189–205. https://doi.org/10.2741/3921

Srikantan, S., Tominaga, K., & Gorospe, M. (2012b). Functional interplay between RNA-binding protein HuR and microRNAs. *Current Protein & Peptide Science*, *13*(4), 372–379. https://doi.org/10.2174/138920312801619394

Sun, C., Serra, C., Lee, G., & Wagner, K. R. (2020). Stem cell-based therapies for Duchenne muscular dystrophy. *Experimental Neurology*, *323*, 113086. https://doi.org/10.1016/j.expneurol.2019.113086

Swanger, S. A. (2011). Making and breaking synapses through local mRNA regulation. *Current Opinion in Genetics & Development*, *21*(4), 414–421. https://doi.org/10.1016/j.gde.2011.04.002

Talbot, J. (2016). Skeletal muscle fiber type: Using insights from muscle developmental biology to dissect targets for susceptibility and resistance to muscle disease. *Wiley*

Interdisciplinary Reviews. Developmental Biology, *5*(4), 518–534. https://doi.org/10.1002/wdev.230

Tasfaout, H., Lionello, V. M., Kretz, C., Koebel, P., Messaddeq, N., Bitz, D., Laporte, J., & Cowling, B. S. (2018). Single Intramuscular Injection of AAV-shRNA Reduces DNM2 and Prevents Myotubular Myopathy in Mice. *Molecular Therapy*, *26*(4), 1082–1092. https://doi.org/10.1016/j.ymthe.2018.02.008

Tenenbaum, S. A., Carson, C. C., Lager, P. J., & Keene, J. D. (2000). Identifying mRNA subsets in messenger ribonucleoprotein complexes by using cDNA arrays. *Proceedings of the National Academy of Sciences of the United States of America*, *97*(26), 14085–14090. https://doi.org/10.1073/pnas.97.26.14085

Tetorou, K., Aghaeipour, A., Singh, S., Morgan, J. E., & Muntoni, F. (2024). The role of dystrophin isoforms and interactors in the brain. *Brain*, *148*(4), 1081–1098. https://doi.org/10.1093/brain/awae384

Tezuka, T., Inoue, A., Hoshi, T., Weatherbee, S. D., Burgess, R. W., Ueta, R., & Yamanashi, Y. (2014). The MuSK activator agrin has a separate role essential for postnatal maintenance of neuromuscular synapses. *Proceedings of the National Academy of Sciences of the United States of America*, *111*(46), 16556–16561. https://doi.org/10.1073/pnas.1408409111

Thelen, M. P., & Kye, M. J. (2020). The Role of RNA Binding Proteins for Local mRNA Translation: Implications in Neurological Disorders. *Frontiers in Molecular Biosciences*, *6*. https://doi.org/10.3389/fmolb.2019.00161

Theroux, M. C., Olivant, A., & Akins, R. E. (2008). C Histomorphology of neuromuscular junction in Duchenne muscular dystrophy. *Paediatric Anaesthesia*, *18*(3), 256–259. https://doi.org/10.1111/j.1460-9592.2008.02411.x

Tian, H., Liu, S., Ren, J., Lee, J. K. W., Wang, R., & Chen, P. (2020). Role of Histone Deacetylases in Skeletal Muscle Physiology and Systemic Energy Homeostasis: Implications for Metabolic Diseases and Therapy. *Frontiers in Physiology*, *11*, 949. https://doi.org/10.3389/fphys.2020.00949

Tinsley, J. M., Fairclough, R. J., Storer, R., Wilkes, F. J., Potter, A. C., Squire, S. E., Powell, D. S., Cozzoli, A., Capogrosso, R. F., Lambert, A., Wilson, F. X., Wren, S. P., De Luca, A., & Davies, K. E. (2011). Daily treatment with SMTC1100, a novel small molecule utrophin upregulator, dramatically reduces the dystrophic symptoms in the mdx mouse. *PloS One*, *6*(5), e19189. https://doi.org/10.1371/journal.pone.0019189

Tintignac, L. A., Brenner, H.-R., & Rüegg, M. A. (2015). Mechanisms Regulating Neuromuscular Junction Development and Function and Causes of Muscle Wasting. *Physiological Reviews*, *95*(3), 809–852. https://doi.org/10.1152/physrev.00033.2014

Trajanovska, S. (2019). Muscle specific kinase protects dystrophic mdx mouse muscles from eccentric contraction-induced loss of force-producing capacity. *The Journal of Physiology*, *597*(18), 4831–4850. https://doi.org/10.1113/JP277839

Tripodi, L., Villa, C., Molinaro, D., Torrente, Y., & Farini, A. (2021). The Immune System in Duchenne Muscular Dystrophy Pathogenesis. *Biomedicines*, *9*(10), 1447. https://doi.org/10.3390/biomedicines9101447

Tulangekar, A. (2021). Inflammation in Duchenne Muscular Dystrophy–Exploring the Role of Neutrophils in Muscle Damage and Regeneration. *Biomedicines*, *9*(10), 1366. https://doi.org/10.3390/biomedicines9101366

Turk, R., Sterrenburg, E., de Meijer, E., van Ommen, G.-J., den Dunnen, J., & 't Hoen, P. (2005). Muscle regeneration in dystrophin-deficient mdx mice studied by gene expression profiling. *BMC Genomics*, *6*, 98. https://doi.org/10.1186/1471-2164-6-98

Tyers, L., Davids, L. M., Wilmshurst, J. M., & Esterhuizen, A. I. (2018). Skin cells for use in an alternate diagnostic method for Duchenne muscular dystrophy. *Neuromuscular Disorders: NMD*, *28*(7), 553–563. https://doi.org/10.1016/j.nmd.2018.05.001

Tyrpak, D. R., Li, Y., Lei, S., & MacKay, J. A. (2020). SIAL: A simple image analysis library for wet-lab scientists. *Journal of Open Source Software*, *5*(56), 2689. https://doi.org/10.21105/joss.02689

Ule, J., Jensen, K. B., Ruggiu, M., Mele, A., Ule, A., & Darnell, R. B. (2003). CLIP identifies Nova-regulated RNA networks in the brain. *Science*, *302*(5648), 1212–1215. https://doi.org/10.1126/science.1090095

Vaillend, C., Aoki, Y., Mercuri, E., Hendriksen, J., Tetorou, K., Goyenvalle, A., & Muntoni, F. (2025). Duchenne muscular dystrophy: Recent insights in brain related comorbidities. *Nature Communications*, *16*(1), 1298. https://doi.org/10.1038/s41467-025-56644-w

Valdez, G., Tapia, J. C., Kang, H., Clemenson, G. D., Gage, F. H., Lichtman, J. W., & Sanes, J. R. (2010). Attenuation of age-related changes in mouse neuromuscular synapses by caloric restriction and exercise. *Proceedings of the National Academy of Sciences of the United States of America*, *107*(33), 14863–14868. https://doi.org/10.1073/pnas.1002220107

Valera, I. C., Wacker, A. L., Hwang, H. S., Holmes, C., Laitano, O., Landstrom, A. P., & Parvatiyar, M. S. (2021). Essential roles of the dystrophin-glycoprotein complex in different cardiac pathologies. *Advances in Medical Sciences*, *66*(1), 52–71. https://doi.org/10.1016/j.advms.2020.12.004

van der Giessen, K. (2007). Involvement of Transportin 2–mediated HuR Import in Muscle Cell Differentiation. *Molecular Biology of the Cell*, *18*(7), 2619–2629. https://doi.org/10.1091/mbc.E07-02-0167

van der Pijl, E. M., van Putten, M., Niks, E. H., Verschuuren, J. J. G. M., Aartsma-Rus, A., & Plomp, J. J. (2016). Characterization of neuromuscular synapse function abnormalities in multiple Duchenne muscular dystrophy mouse models. *The European Journal of Neuroscience*, *43*(12), 1623–1635. https://doi.org/10.1111/ejn.13249

Van Pelt, D. W., Hettinger, Z. R., & Vanderklish, P. W. (2019). RNA-binding proteins: The next step in translating skeletal muscle adaptations? *Journal of Applied Physiology*, *127*(2), 654–660. https://doi.org/10.1152/japplphysiol.00076.2019

Venugopal, V., & Pavlakis, S. (2025). Duchenne Muscular Dystrophy. In *StatPearls*. StatPearls Publishing. http://www.ncbi.nlm.nih.gov/books/NBK482346/

Verhaart, I. E. C., & Aartsma-Rus, A. (2019). Therapeutic developments for Duchenne muscular dystrophy. *Nature Reviews. Neurology*, *15*(7), 373–386. https://doi.org/10.1038/s41582-019-0203-3

Villalta, S. A., Nguyen, H. X., Deng, B., Gotoh, T., & Tidball, J. G. (2009). Shifts in macrophage phenotypes and macrophage competition for arginine metabolism affect the severity of muscle pathology in muscular dystrophy. *Human Molecular Genetics*, *18*(3), 482–496. https://doi.org/10.1093/hmg/ddn376

von Roretz, C., Beauchamp, P., Di Marco, S., & Gallouzi, I.-E. (2011). HuR and myogenesis: Being in the right place at the right time. *Biochimica et Biophysica Acta (BBA) - Molecular Cell Research, Regulation of Signaling and Cellular Fate through Modulation of Nuclear Protein Import*, *1813*(9), 1663–1667. https://doi.org/10.1016/j.bbamcr.2011.01.036

Wang, J., Guo, Y., Chu, H., Guan, Y., Bi, J., & Wang, B. (2013). Multiple Functions of the RNA-Binding Protein HuR in Cancer Progression, Treatment Responses and Prognosis. *International Journal of Molecular Sciences*, *14*(5), 10015–10041. https://doi.org/10.3390/ijms140510015

Wang, W., Yang, X., Kawai, T., de Silanes, I. L., Mazan-Mamczarz, K., Chen, P., Chook, Y. M., Quensel, C., Köhler, M., & Gorospe, M. (2004). AMP-activated Protein Kinase-regulated Phosphorylation and Acetylation of Importin α1: INVOLVEMENT IN THE NUCLEAR IMPORT OF RNA-BINDING PROTEIN HuR*. *Journal of Biological Chemistry*, *279*(46), 48376–48388. https://doi.org/10.1074/jbc.M409014200

Watkins, S. C. (1982). Muscle Fibre Size and Shape in Duchenne Muscular Dystrophy. *Neuropathology and Applied Neurobiology*, *8*(1), 11–17. https://doi.org/10.1111/j.1365-2990.1982.tb00253.x

Webster, C., Silberstein, L., Hays, A. P., & Blau, H. M. (1988). Fast muscle fibers are preferentially affected in Duchenne muscular dystrophy. *Cell*, *52*(4), 503–513. https://doi.org/10.1016/0092-8674(88)90463-1

Wilson, D. G. S., Tinker, A., & Iskratsch, T. (2022). The role of the dystrophin glycoprotein complex in muscle cell mechanotransduction. *Communications Biology*, *5*(1), 1022. https://doi.org/10.1038/s42003-022-03980-y

Wood, S. J., & Slater, C. R. (1997). The contribution of postsynaptic folds to the safety factor for neuromuscular transmission in rat fast- and slow-twitch muscles. *The Journal of Physiology*, *500*(Pt 1), 165–176. https://doi.org/10.1113/jphysiol.1997.sp022007

Wu, H., Kanatous, S. B., Thurmond, F. A., Gallardo, T., Isotani, E., Bassel-Duby, R., & Williams, R. S. (2002). Regulation of mitochondrial biogenesis in skeletal muscle by CaMK. *Science*, *296*(5566), 349–352. https://doi.org/10.1126/science.1071163

Wu, H., Xiong, W. C., & Mei, L. (2010). To build a synapse: Signaling pathways in neuromuscular junction assembly. *Development*, *137*(7), 1017–1033. https://doi.org/10.1242/dev.038711

Wutikeli, H., Xie, T., Xiong, W., & Shen, Y. (2025). ELAV/Hu RNA-binding protein family: Key regulators in neurological disorders, cancer, and other diseases. *RNA Biology*, *22*(1), 1–11. https://doi.org/10.1080/15476286.2025.2471133

Xie, Z., Samuels, B. A., & Tsai, L.-H. (2006). Cyclin-dependent kinase 5 permits efficient cytoskeletal remodeling—A hypothesis on neuronal migration. *Cerebral Cortex*, *16 Suppl 1*, i64-68. https://doi.org/10.1093/cercor/bhj170

Yao, S., Chen, Z., Yu, Y., Zhang, N., Jiang, H., Zhang, G., Zhang, Z., & Zhang, B. (2021). Current Pharmacological Strategies for Duchenne Muscular Dystrophy. *Frontiers in Cell and Developmental Biology*, *9*, 689533. https://doi.org/10.3389/fcell.2021.689533

Zanetti, G., Negro, S., Megighian, A., & Pirazzini, M. (2018). Electrophysiological Recordings of Evoked End-Plate Potential on Murine Neuro-muscular Synapse Preparations. *Bio-Protocol*, *8*(8), e2803. https://doi.org/10.21769/BioProtoc.2803

Zhang, J., Huang, X., Tang, Y., Zhong, X., Wang, J., Wei, M., Han, X., Ke, Y., & Ba, X. (2025). HuB serves as the central hub for connecting HuR-related mRNAs with translation

machinery in inflammation. *Communications Biology*, *9*(1), 3. https://doi.org/10.1038/s42003-025-09228-9

Zhang, K., Bai, L., Xu, W., & Shen, C. (2021). Human neuromuscular junction three-dimensional organoid models and the insight in motor disorders. *Journal of Molecular Cell Biology*, *13*(11), 767–773. https://doi.org/10.1093/jmcb/mjab046

Zhang, Y., Li, H., Min, Y.-L., Sanchez-Ortiz, E., Huang, J., Mireault, A. A., Shelton, J. M., Kim, J., Mammen, P. P. A., Bassel-Duby, R., & Olson, E. N. (2020). Enhanced CRISPR-Cas9 correction of Duchenne muscular dystrophy in mice by a self-complementary AAV delivery system. *Science Advances*, *6*(8), eaay6812. https://doi.org/10.1126/sciadv.aay6812

Zhou, H., Jarujaron, S., Gurley, E. C., Chen, L., Ding, H., Studer, E., Pandak, W. M., Hu, W., Zou, T., Wang, J.-Y., & Hylemon, P. B. (2007). HIV protease inhibitors increase TNF-alpha and IL-6 expression in macrophages: Involvement of the RNA-binding protein HuR. *Atherosclerosis*, *195*(1), e134-143. https://doi.org/10.1016/j.atherosclerosis.2007.04.008

Zincarelli, C., Soltys, S., Rengo, G., & Rabinowitz, J. E. (2008). Analysis of AAV Serotypes 1–9 Mediated Gene Expression and Tropism in Mice After Systemic Injection. *Molecular Therapy*, *16*(6), 1073–1080. https://doi.org/10.1038/mt.2008.76

Zoltowska, K., Webster, R., Finlayson, S., Maxwell, S., Cossins, J., Müller, J., Lochmüller, H., & Beeson, D. (2013). Mutations in GFPT1 that underlie limb-girdle congenital myasthenic syndrome result in reduced cell-surface expression of muscle AChR. *Human Molecular Genetics*, *22*(14), 2905–2913. https://doi.org/10.1093/hmg/ddt145

Zong, Y., Zhang, B., Gu, S., Lee, K., Zhou, J., Yao, G., Figueiredo, D., Perry, K., Mei, L., & Jin, R. (2012). Structural basis of agrin-LRP4-MuSK signaling. *Genes & Development*, *26*(3), 247–258. https://doi.org/10.1101/gad.180885.111